SUPPORTING INFORMATION

Structural and Functional Analysis of the Allosteric Inhibition of IRE1α with ATP-Competitive Kinase Ligands

Hannah C. Feldman,* Michael Tong,* Likun Wang, Rosa Meza-Acevedo, Theodore A. Gobillot, Ivan Lebedev, Micah J. Gliedt, Sanjay B. Hari, Arinjay K. Mitra, Bradley J. Backes, Feroz R. Papa, Markus A. Seeliger,^ and Dustin J. Maly^

^Correspondence should be addressed to: DJM (Tel: 206-543-1653. Fax 206-685 7002. E-mail: maly@chem.washington.edu) or MAS (Tel: 631-444-3558. Fax:631-444-9749. E-mail: markus.seeliger@stonybrook.edu)

CONTENTS

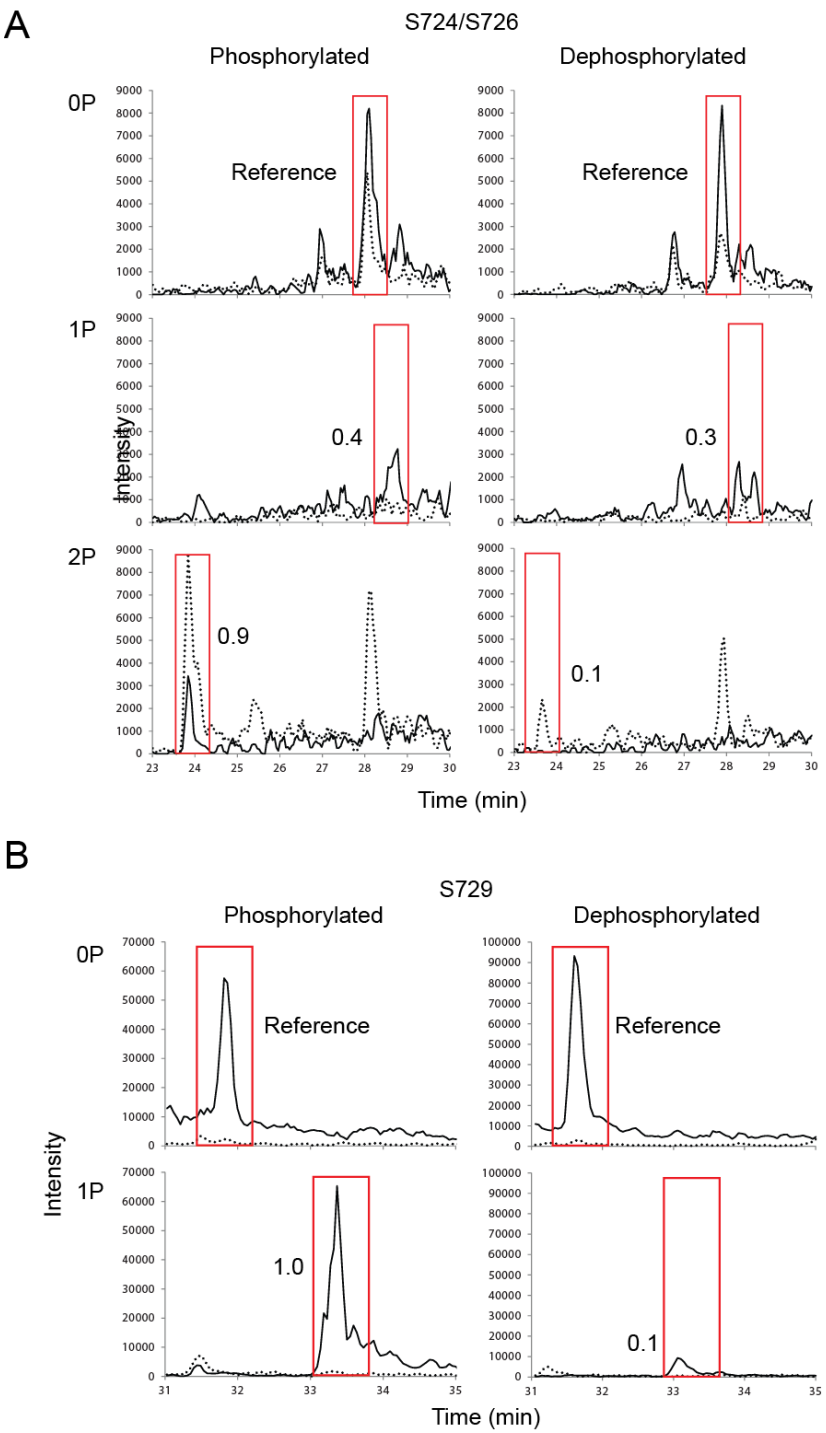

Figure S1. **Phosphorylation sites of IRE1α determined through mass spectrometry.** IRE1α expressed and purified from baculovirus-infected insect cells is phosphorylated at Ser724, Ser726, and Ser729. Extracted ion chromatographs from LC/MS analyses of tryptic peptides of Ire1α expressed and purified from baculovirus-infected insect cells either alone or treated with lambda phosphatase. Tryptic peptides analyzed were (A) LAVGRHSFSRR (phosphorylated Ser724 and Ser726 underlined) and (B) SGVPGTEGWIAPEMLSEDCK (phosphorylated Ser729 underlined). Quantitated peak areas in red boxes are relative to those of unphosphorylated peptide for each sample.

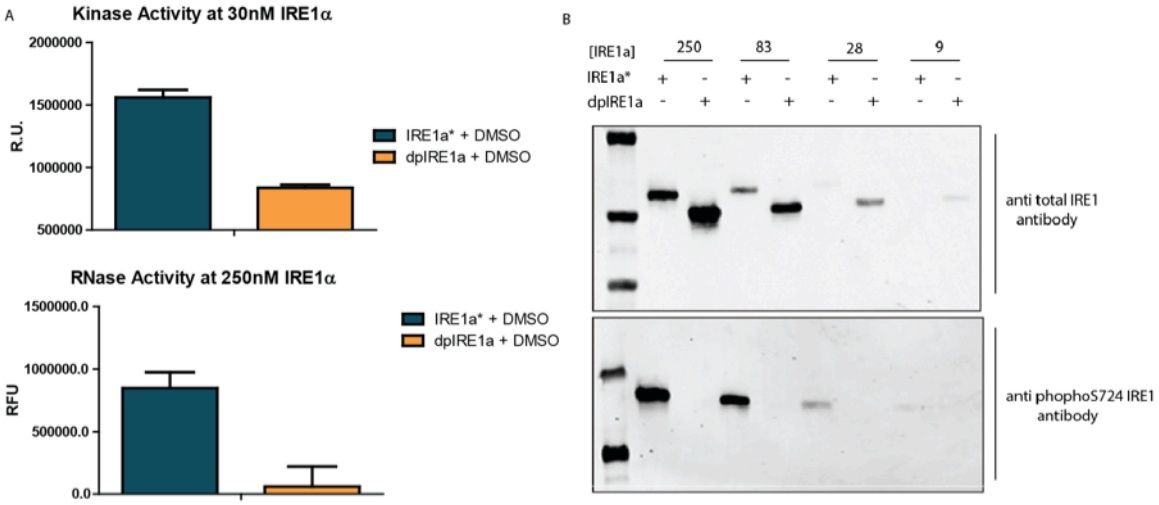

Figure S2. Comparison of IRE1α* and dP-IRE1α* activity. (A) Comparative activity of IRE1α* and dP-IRE1α in the kinase phosphorylation assay at 30nM enzyme. Values are reported as radioactive counts/units (mean ± S.E.M; n=3). Comparative activity of IRE1α* and dP-IRE1α* in the RNase activity assay at 250nM enzyme. Values are reported as fluorescent units (mean ± S.E.M; n=3) (B) Western blot analysis of IRE1α* and dP-IRE1α* at four dilutions using a total and phosphospecific IRE1α primary antibody.

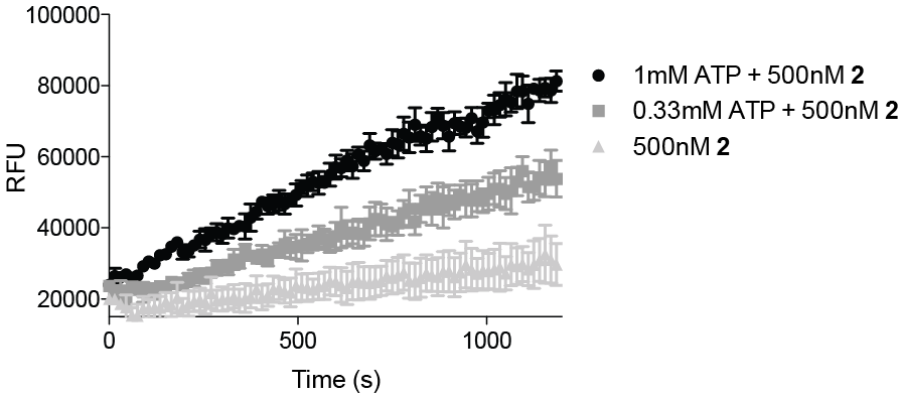

Figure S3. ATP competitively activates IRE1α in the presence of a KIRA. IRE1α* was incubated with an inhibitor concentration of KIRA **2** that inhibits >95% of IRE1α*'s RNase activity in the absence or presence (0.5 or 1 mM) of ATP. The RNase activity of IRE1α* under these conditions was determined by monitoring fluorescence over time.

Figure Ref.	PDB	Protein	Inhibitor	Lys-Glu Salt Bridge Distance (Å)
A	4E93	c-FES	TAE684	2.8
B	2W1I	JAK2	AT9283	3.1
C	2JKK	FAK	TAE226	2.8
D	1UKI	JNK1	SP600125	2.9
E	2YDK	CHK1	AZD7762	2.4
F	4MKC	ALK	LDK378	2.9
G	4JI9	JAK2	TG101209	2.6
H	4QMT	MST3	Hesperadin	2.8

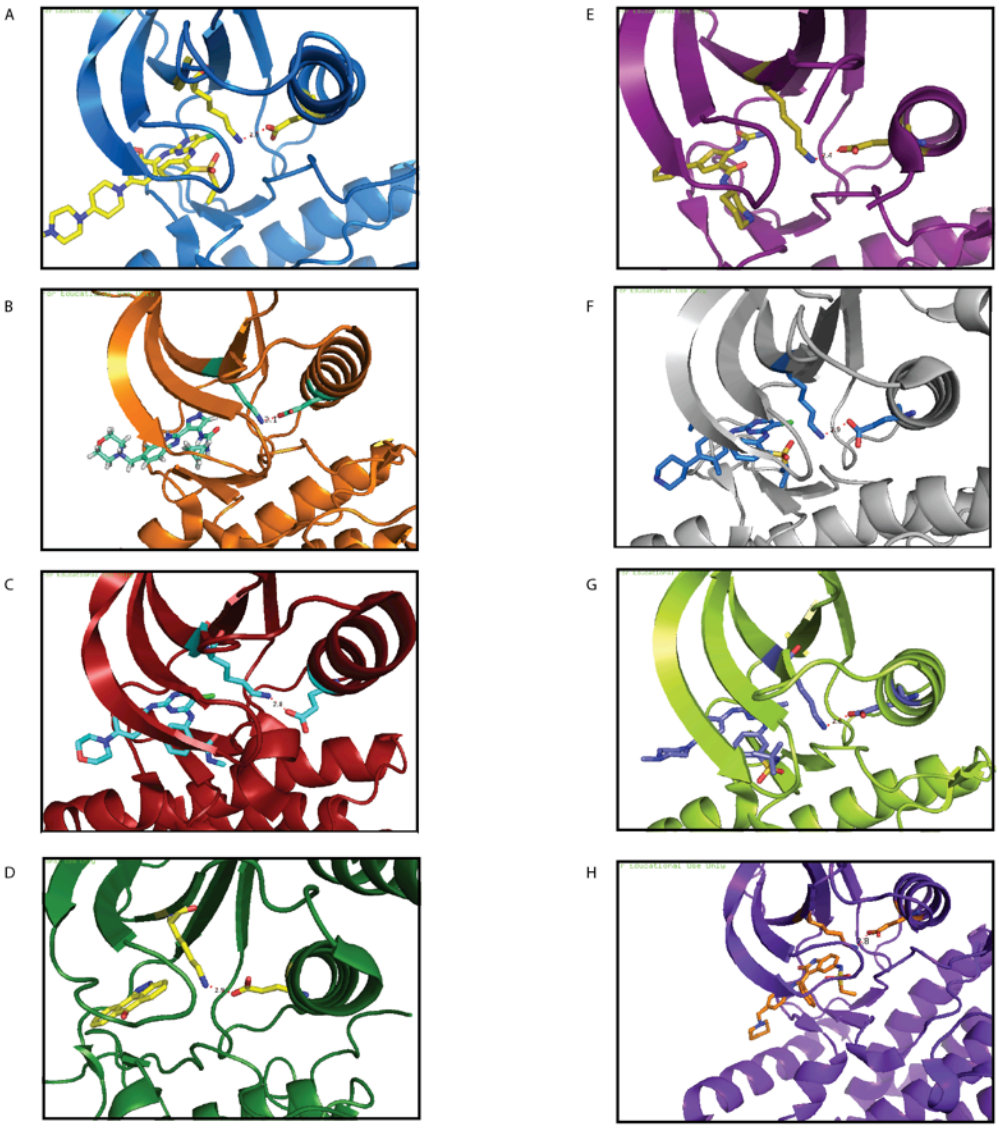

Figure S4. Crystal structures of IRE1α activators bound to various kinase targets. Catalytic lysine-glutatmate (on hlix-αC) interactions. The lysine-glutamate salt bridge is depicted as a stick representation and highlighted in a contrasting color. The length of the salt bridge (Angstroms) is listed in the table above.

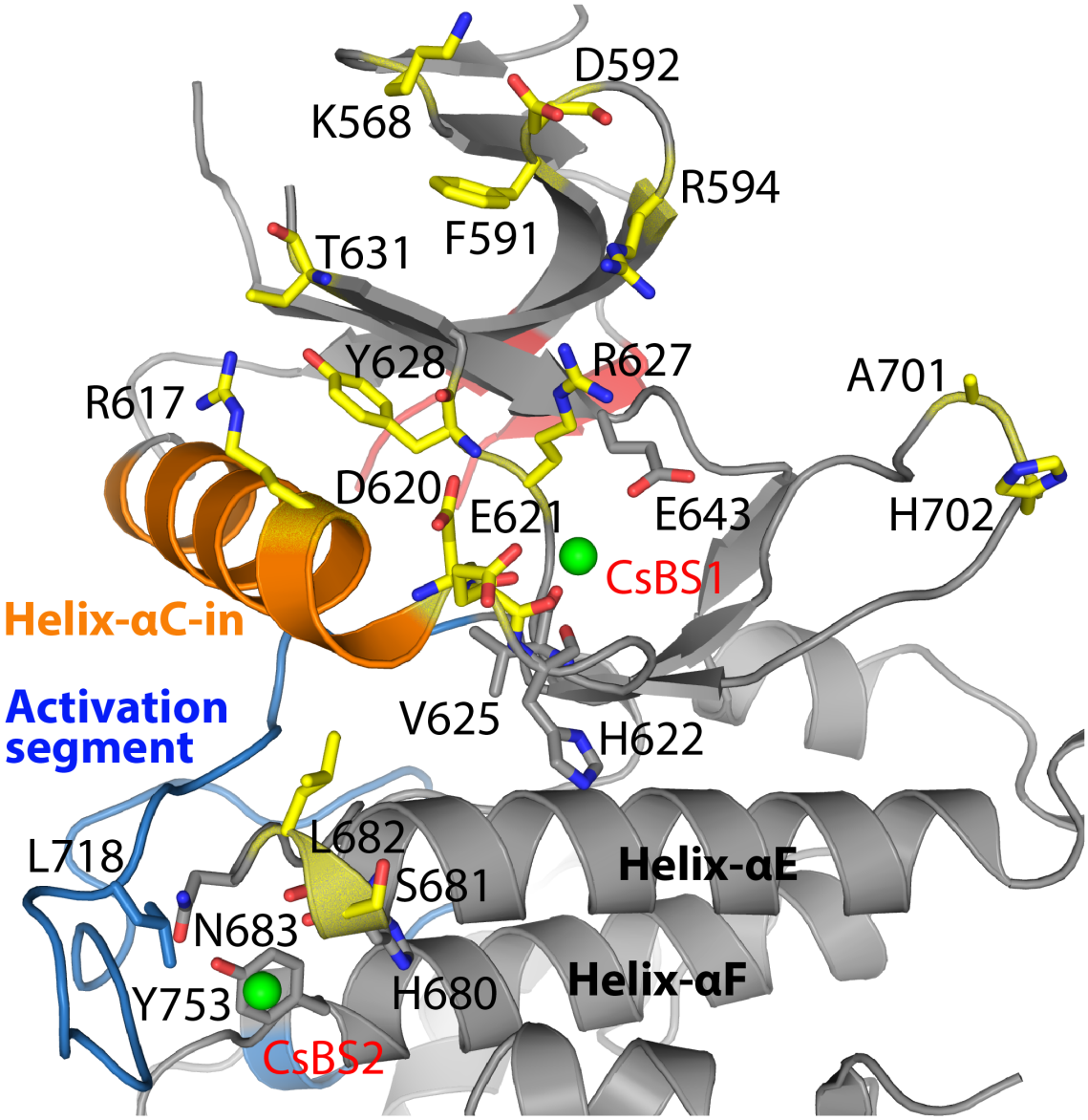

Figure S5. The dP-IRE1α* structure presents two unique Cs^+ binding sites. Cs^+ binding site 1 (CsBS1), resides near the C-terminus of helix-αC, and is defined by the backbone carbonyls of D620, E621, H622, V625, and the E643 side chain. Cs^+ binding site 2 (CsBS2), is defined by the side chains of N683, Y753, and the backbone carbonyl of H680. Cs^+ occupancy of CsB1 appears to stabilize the active conformation of helix-αC, whilst at CsB2 it stabilizes the interaction between Y753 of helix-αE and L718 from the activation segment. Dimer interface residues in the kinase domain of dP-IRE1α*, are represented as sticks highlighted in yellow.

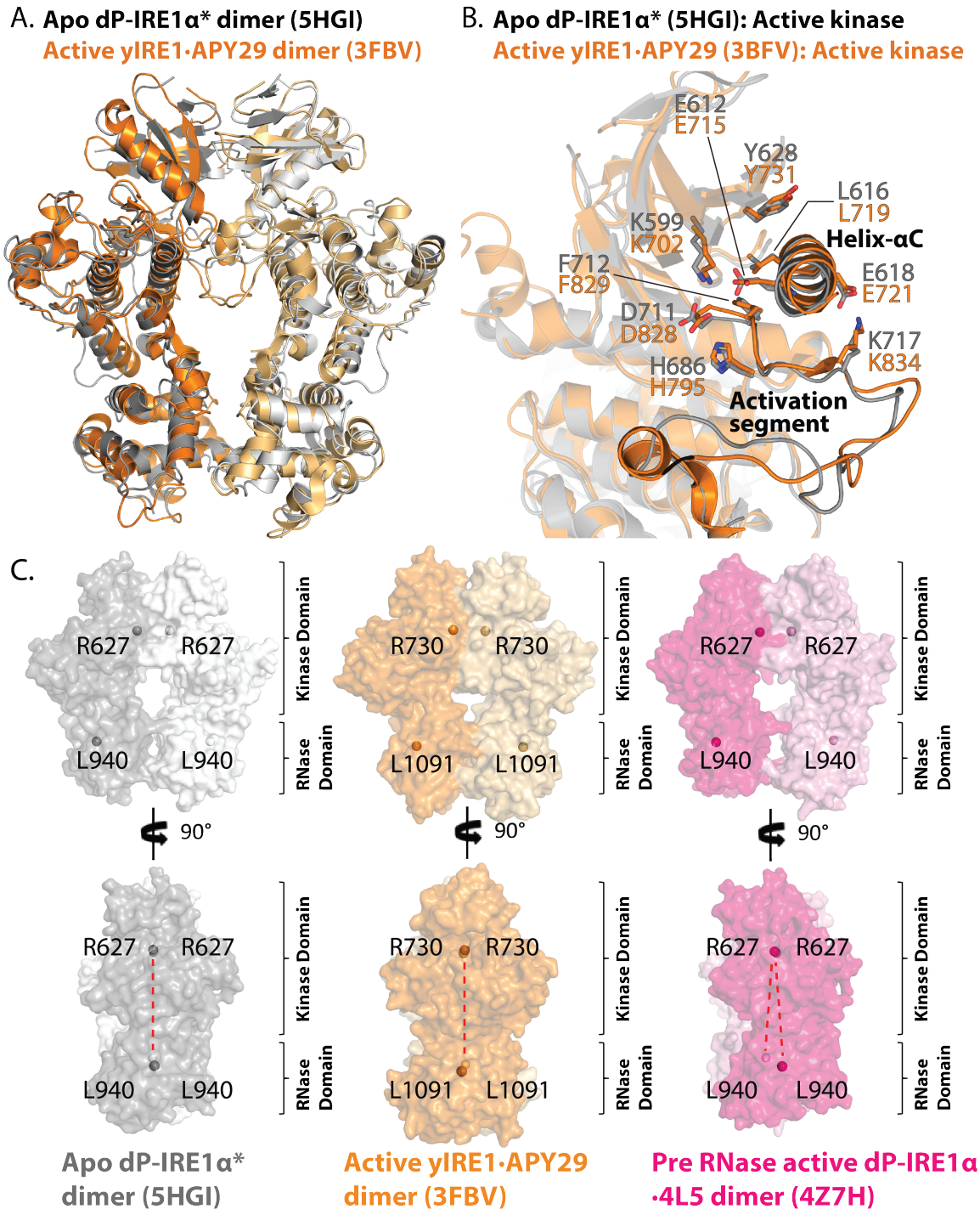

Figure S6. dP-IRE1α* adopts an RNase active back-to-back dimer similar to active yIRE1. **(A)** Structural alignment of the dP-IRE1α* dimer with the phosphorylated active yIRE1 dimer (PDB: 3FBV). Both dimers are similar in overall structure and conformation (RMSD 1.64 Å). **(B)** Hallmarks of the active protein kinase conformation including the activation segment active conformation are conserved between dP-IRE1α* and active yIRE1 (PDB: 3FBV) despite differences in phosphorylation status. The mammalian and yeast conserved salt bridge between

the Glu and Lys residues that couples helix-αC and the activation segment is also shown. **(C)** The dP-IRE1α* dimer (grey, white) is in an RNase active state comparable to the active yIRE1 dimer (PDB: 3FBV, orange, light orange). In contrast, the pre-active human IRE1α dimer (PDB: 4Z7H, pink, light pink) presents protomers that are mis-aligned and not parallel, consequently the RNase domains are disengaged and likely inactive. Here, the alignment of conserved IRE1 residues: Arg627 (*Arg730*), and Leu940 (*Leu1091*) reflects the alignment of the protomers.

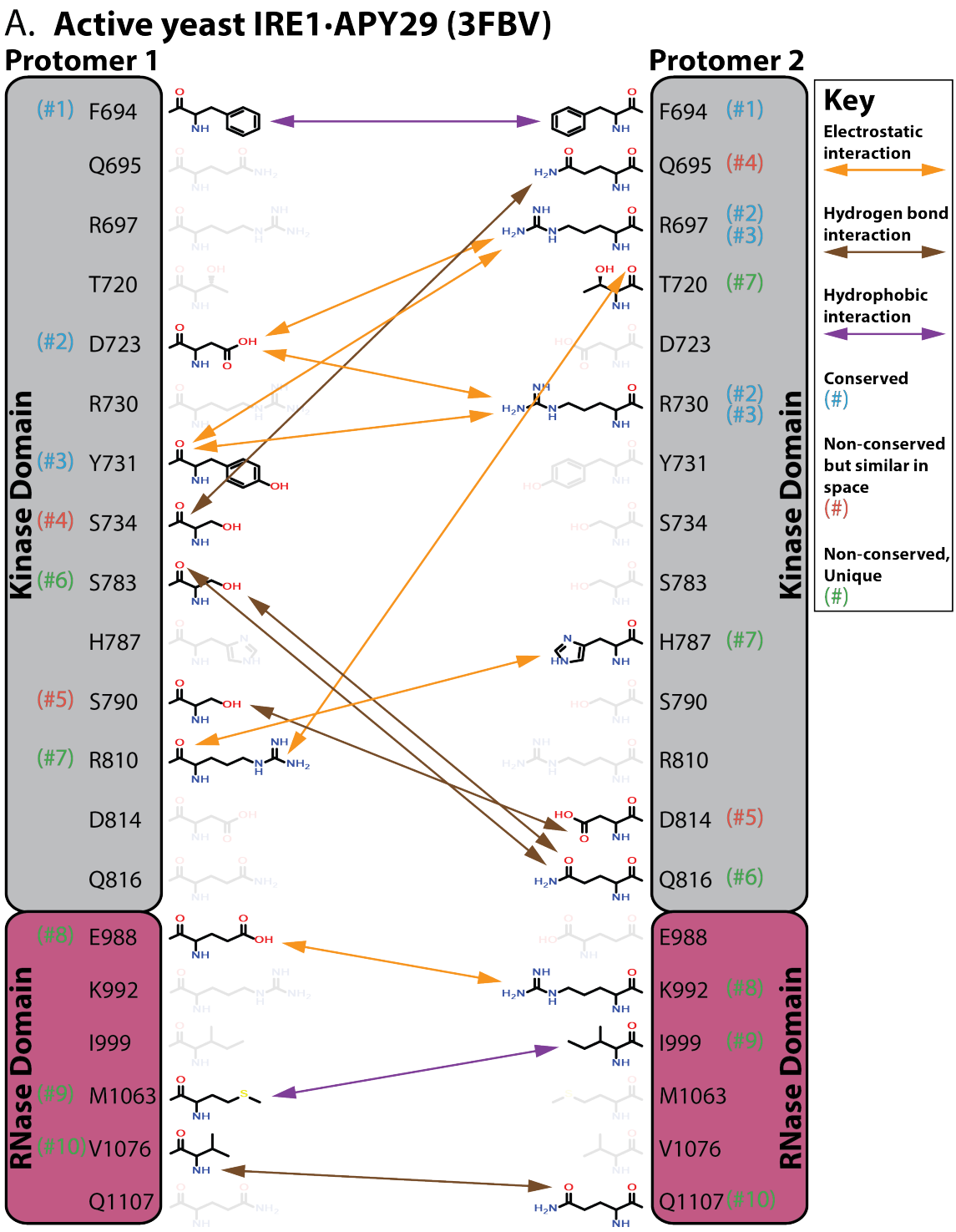

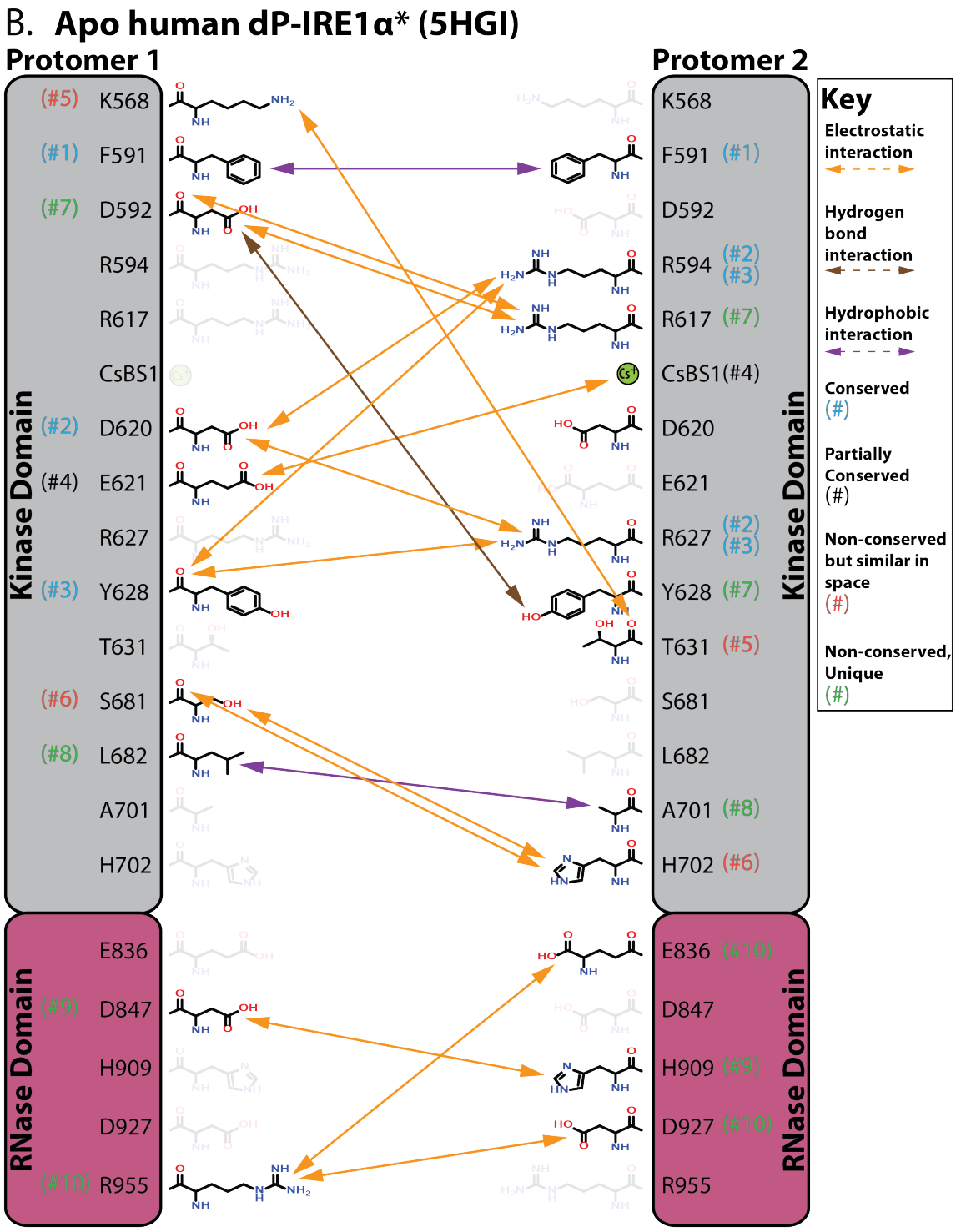

Figure S7. Structural comparison of the back-to-back dimer interface interactions in dP-IRE1α* and active yIRE1. (A and B) Schematic illustrations of the amino acid interactions found at the back-to-back dimer interface of active yIRE1 (PDB: 3FBV), and dP-IRE1α* (PDB: 5HGI). In active yIRE1, seven sets of interactions are mediated by the kinase domain and three by the RNase. Whereas in dP-IRE1α*, eight sets of interactions are mediated by the kinase domain and two by the RNase domain. Three dimer interactions are conserved between dP-

IRE1α* and active yIRE1. The remaining interactions are either partially conserved, not conserved but similar in space, or unique. Listed next to the residue or CsBS1(Cs^+ binding site 1) is the number of the interaction denoted by: (# number), with the color corresponding to the degree of similarity for the interaction found in dP-IRE1α* compared to active yIRE1 (blue is conserved, black is partially conserved, orange is non-conserved but similar in space, and green is unique). The general nature of each interaction is defined in terms of: electrostatic (orange arrow), hydrogen bond (brown arrow), and hydrophobic (purple arrow). For clarity only one set of dimer interactions mediated by protomer A to protomer B is shown, hence some residues appear opaque. Refer to **Table S3** for complementary information.

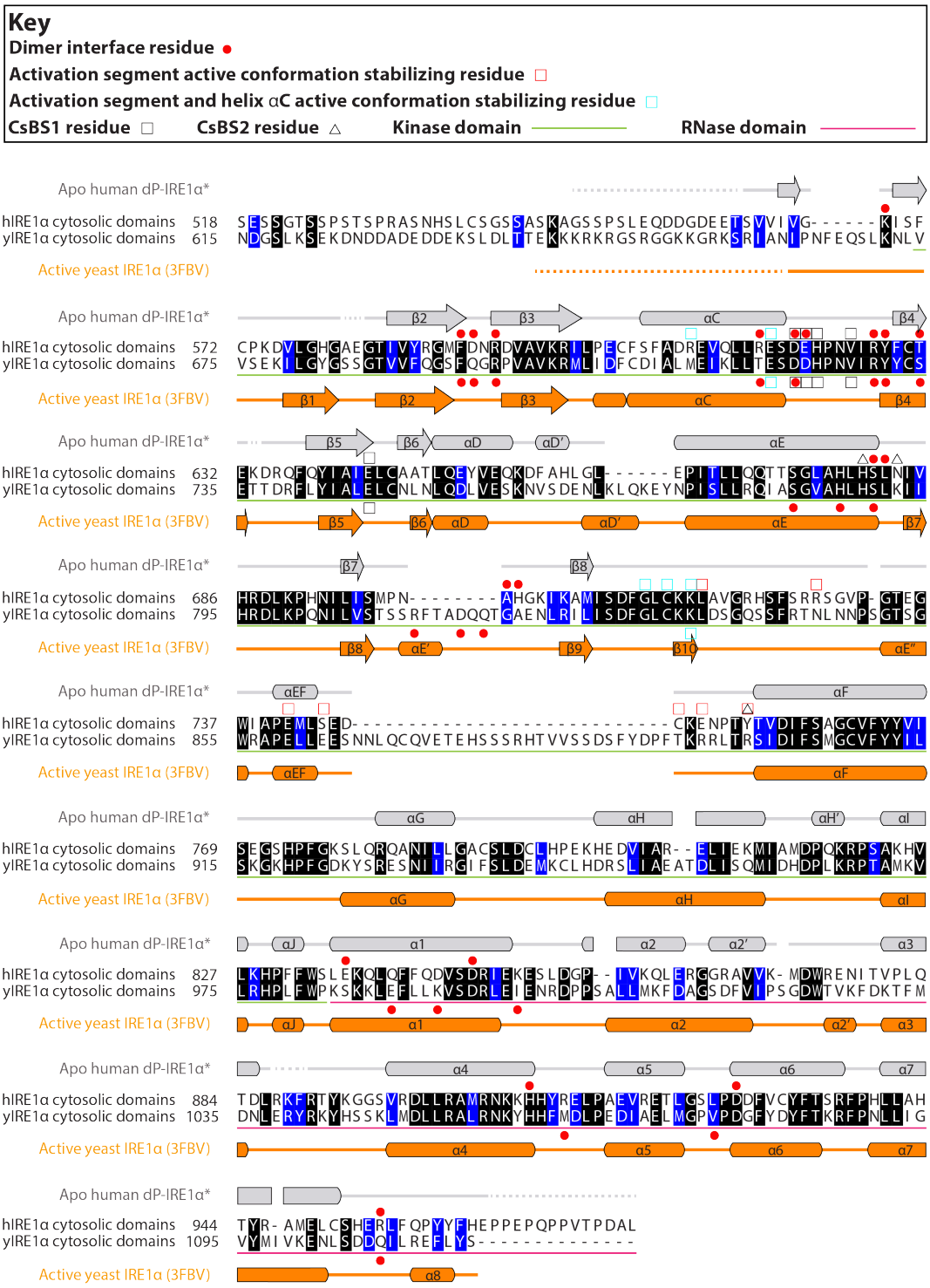

Figure S8. Sequence alignment of human IRE1α and yIRE1 cytosolic domains with secondary structure and key amino acid interaction annotations. (A) clustalw sequence alignment of the human and yIRE1 over a portion of their cytosolic domains is shown. Residues highlighted in black = conserved, blue = similar, white = different. The sequence alignment is annotated with secondary structure elements that are defined by taking the consensus secondary structure from Pymol and dssp. Breaks in the secondary structure correspond to residue insertions in the sequence alignment, whilst dashed lines denote disorder. The protein kinase and RNase

domains are underlined in green and pink respectively. Residues implicated in dimerization, activation segment and helix-αC coupling, *apo* human dP-IRE1α* activation segment stabilization, CsBS1 and CsBS2 are also denoted by their corresponding symbols explained by the key. In the RNase domain, the region spanning helix-α3 and the α3-α4 loop corresponds to the catalytic helix loop element (HLE).

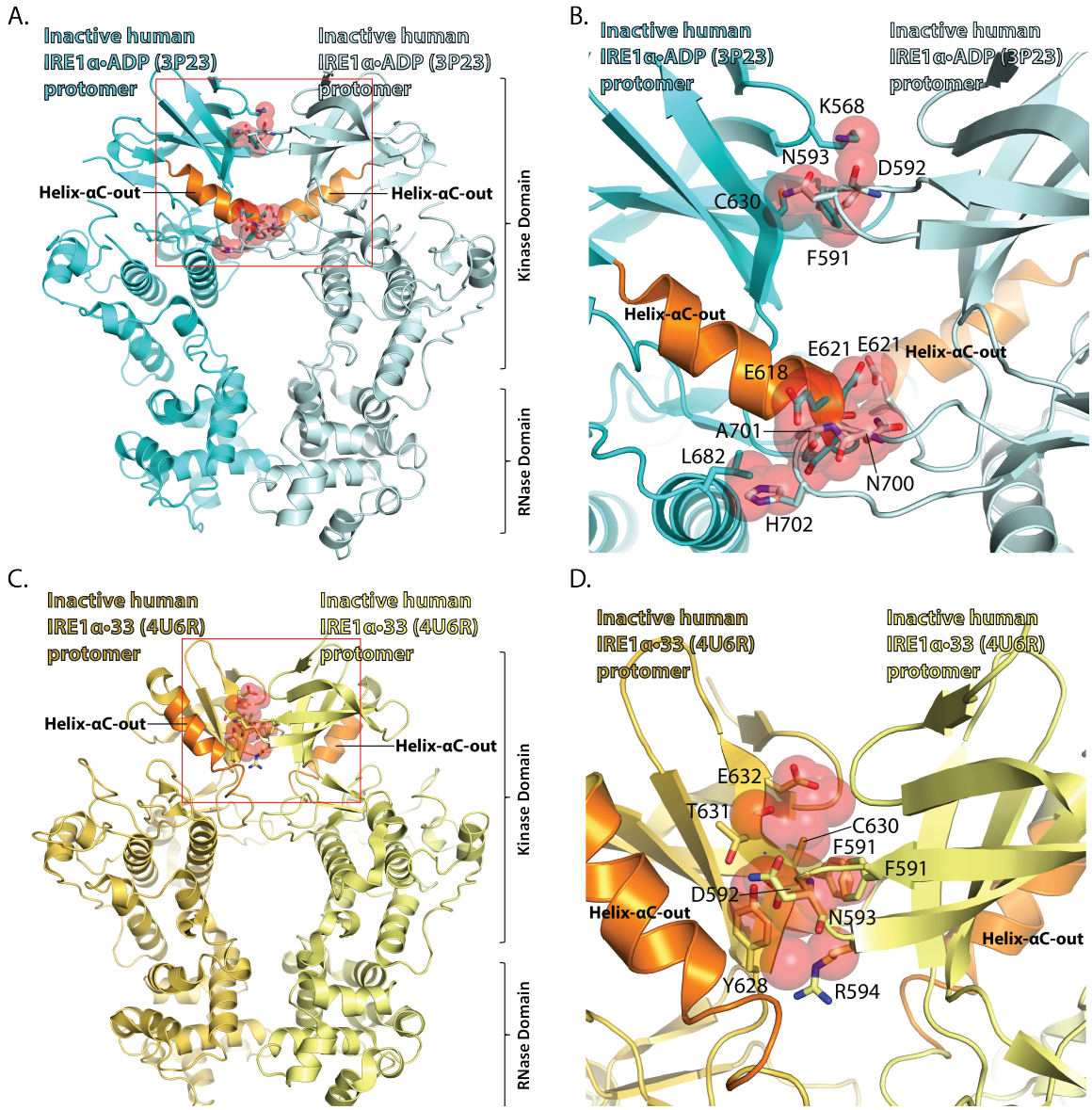

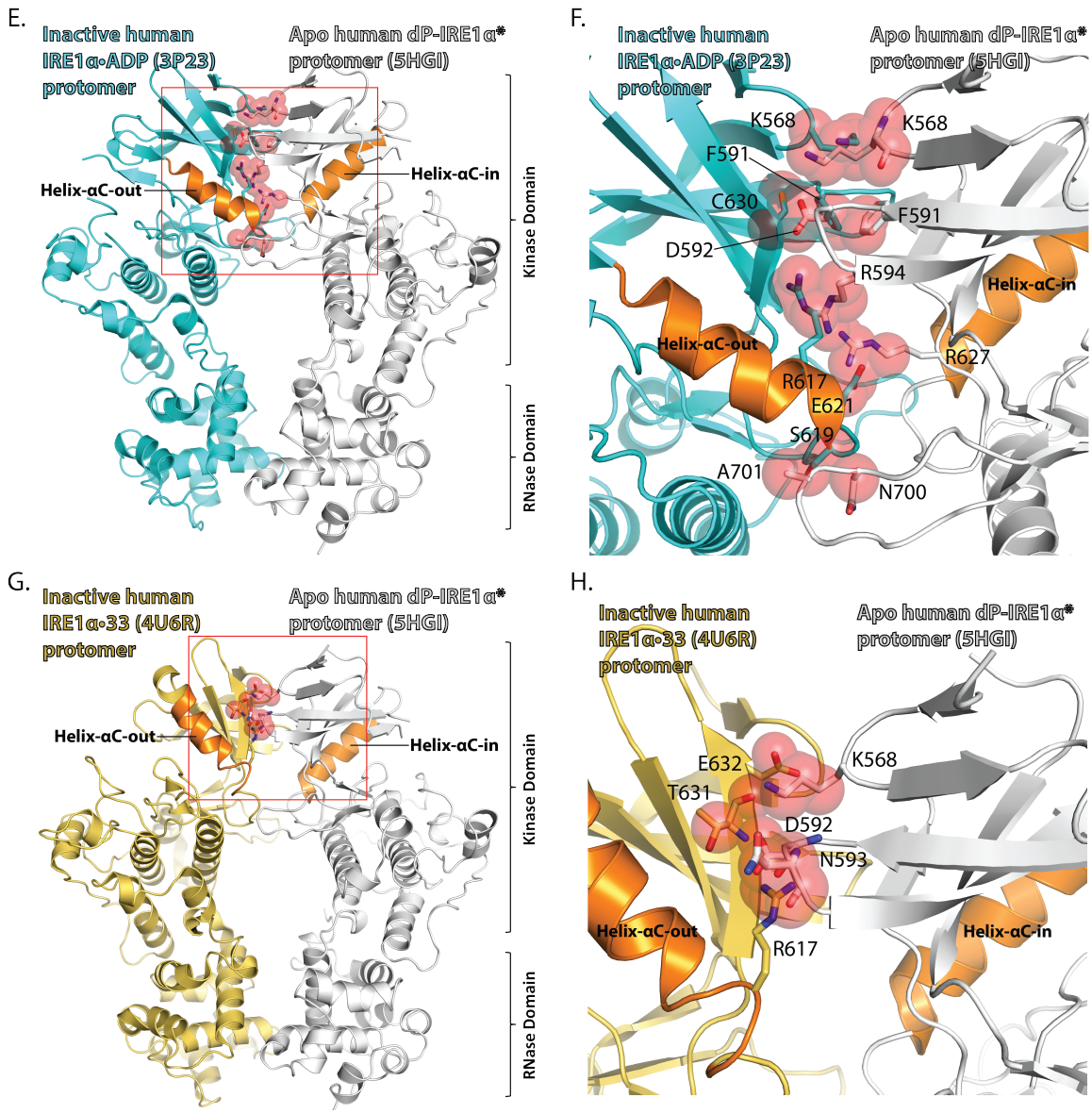

Figure S9. Helix-αC-out is not conducive to forming the IRE1α RNase active back-to-back dimer. (A) Superimposition of two inactive IRE1α·ADP protomers (PDB: 3P23) onto the protomers of our RNase active dP-IRE1α* (PDB: 5HGI). **(B)** A zoomed in view of the incompatible IRE1α·ADP back-to-back dimer model with steric clashed residues indicated. **(C)** Superimposition of two inactive IRE1α·**33** protomers (PDB: 4U6R) onto our RNase active dP-IRE1α* back-to-back dimer also produces an incompatible back-to-back dimer model because of steric clashes resulting from the helix-αC-out conformation. **(D)** A zoomed in view of the incompatible IRE1α·**33** back-to-back dimer model with steric clashed residues indicated. **(E, G)** Similarly, an incompatible dimer results when superimposing onto our RNase active dP-IRE1α* back-to-back dimer, one active dP-IRE1α* protomer in combination with one inactive IRE1α·ADP protomer, or one inactive IRE1α·**33** protomer. Here, the hetero combination of one protomer with helix-αC-in, and the other with helix-αC-out, also creates steric clashes. **Figure S8F** and **S8H** represent zoomed in views of **Figure S8E** and **S8G** respectively. Red spheres = steric clashes, inactive IRE1α·ADP protomer = cyan, inactive IRE1α·**33** protomer = yellow, active *apo* dP-IRE1α* protomer = gray, helix-αC = orange. ADP and **33** have been omitted for clarity.

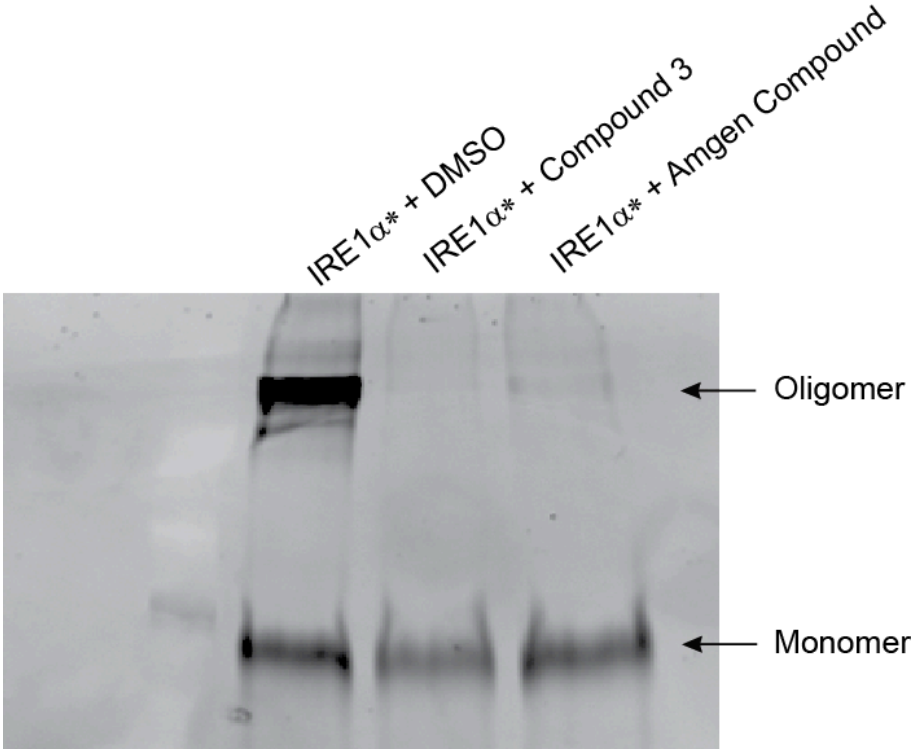

Figure S10. Crosslinking gel of IRE1α* treated with Compound 3 and Amgen Compound 33. SDS-PAGE gel of IRE1α* after incubation with DMSO, Compound **3** (100 μM), or Amgen compound **33** (100 μM) and treated with chemical crosslinker disuccinimidyl suberate (DSS; 250 μM). The gel was visualized via SYPRO-Ruby Red Staining.

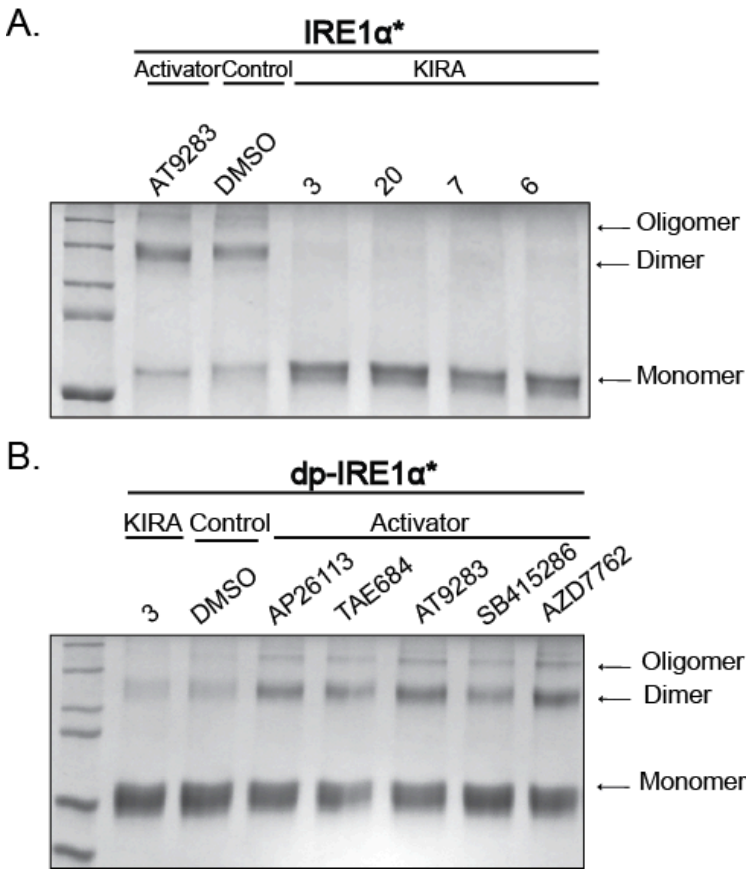

Figure S11. Crosslinking gels of inhibitor treated IRE1α* and dP-IRE1α* (A). SDS-PAGE gel of IRE1α* (15 μM) after incubation with DMSO or KIRA (100 μM) and treated with chemical crosslinker disuccinimidyl suberate (DSS; 250 μM). (B). SDS-PAGE gel of dpIRE1α (15 μM) after incubation with DMSO or inhibitor (100 μM) and treatment with chemical crosslinker disuccinimidyl suberate (DSS; 250 μM).

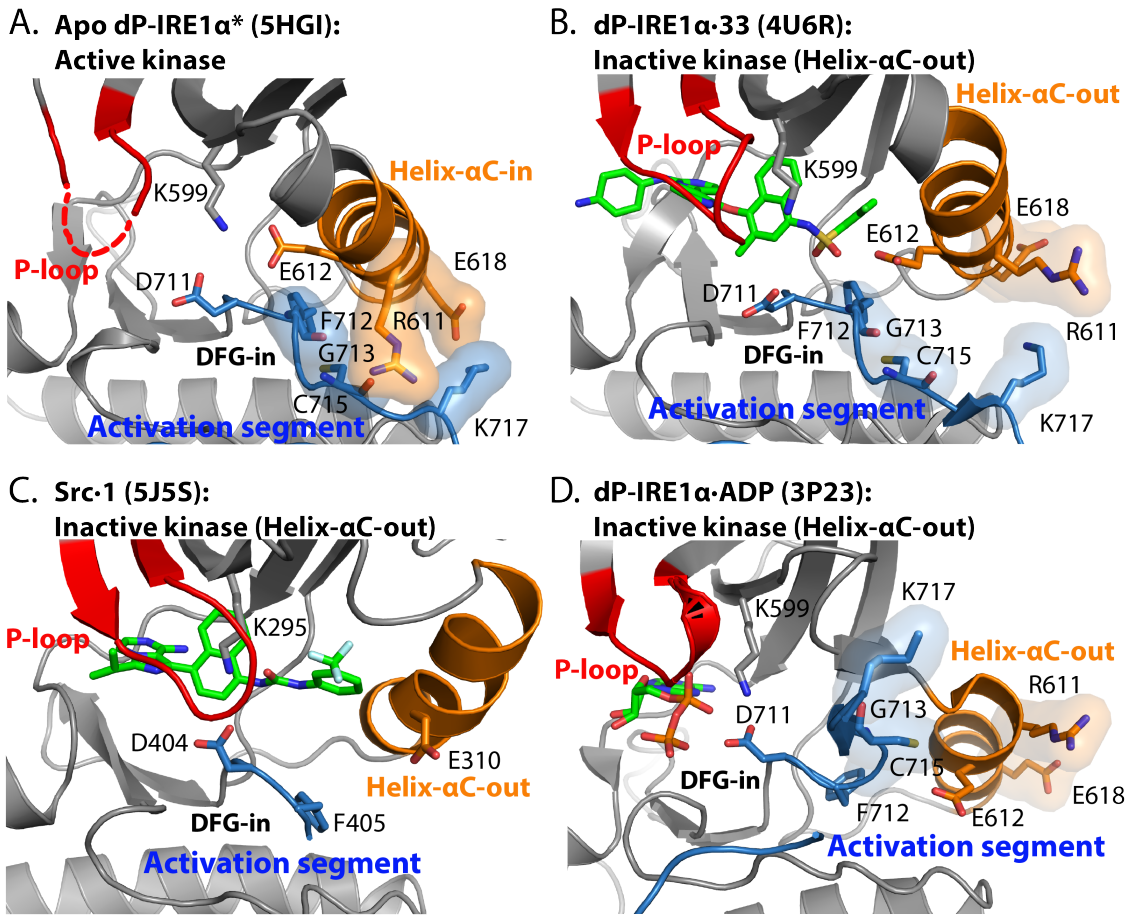

Figure S12. KIRA compounds 1 and 33 produce similar binding modes that stabilize the helix-αC-out kinase inactive conformation.(A) The *apo* dP-IRE1α* kinase domain (PDB: 5HGI) presents an active conformation with coupling between the activation segment and helix-αC. **(B)** dP-IRE1α bound to an Amgen KIRA (compound **33**) (PDB: 4U6R), and **(C)** Src bound to **1 (PDB: 5J5S)**, both present KIRAs bound to kinase active sites with similar binding modes, which stabilize the inactive kinase conformation characterized by the DFG-in and helix-αC-out conformation. **(B)** In the dP-IRE1α·**33** structure, the direct displacement and outward rotation of helix-αC produces steric clashes that are incompatible with the RNase active back-to-back dimer. Since compound **1** produces a similar binding mode to **33**–in Src–it is likely that the mechanism of IRE1α RNase inactivation by **1** also involves direct displacement of helix-αC. **(D)** dP-IRE1α bound to ADP presents an inactive kinase conformation like the dP-IRE1α·**33** structure, adopting a helix-αC-out conformation but with a larger displacement of this structural element.

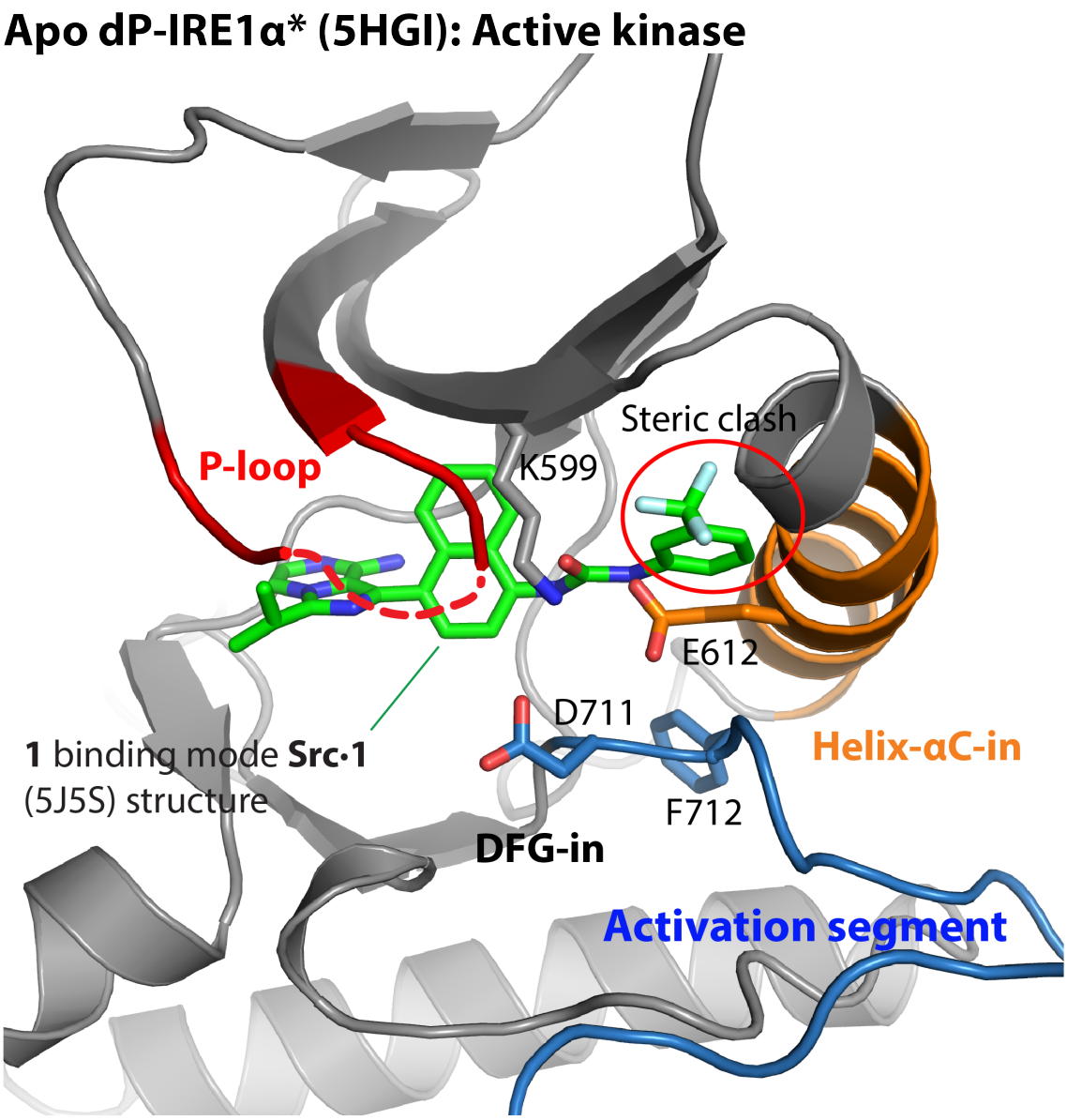

Figure S13. The binding mode of 1 in Src is incompatible with the *apo* dP-IRE1α * active kinase conformation. In complex with **1**, Src is stabilized in the helix-αC-out conformation (PDB: 5SJS). Superimposition of the binding mode of **1** (green) from the Src·**1** crystal structure onto the *apo* dP-IRE1α* ATP-binding site (PDB: 5HGI), produces a steric clash between the R_3 moiety of **1** and the helix-αC-in conformation. **1** was superimposed onto the *apo* dP-IRE1α* ATP-binding site by backbone alignment of the Src·**1** co-crystal structure with the *apo* dP-IRE1α* kinase domain structure.

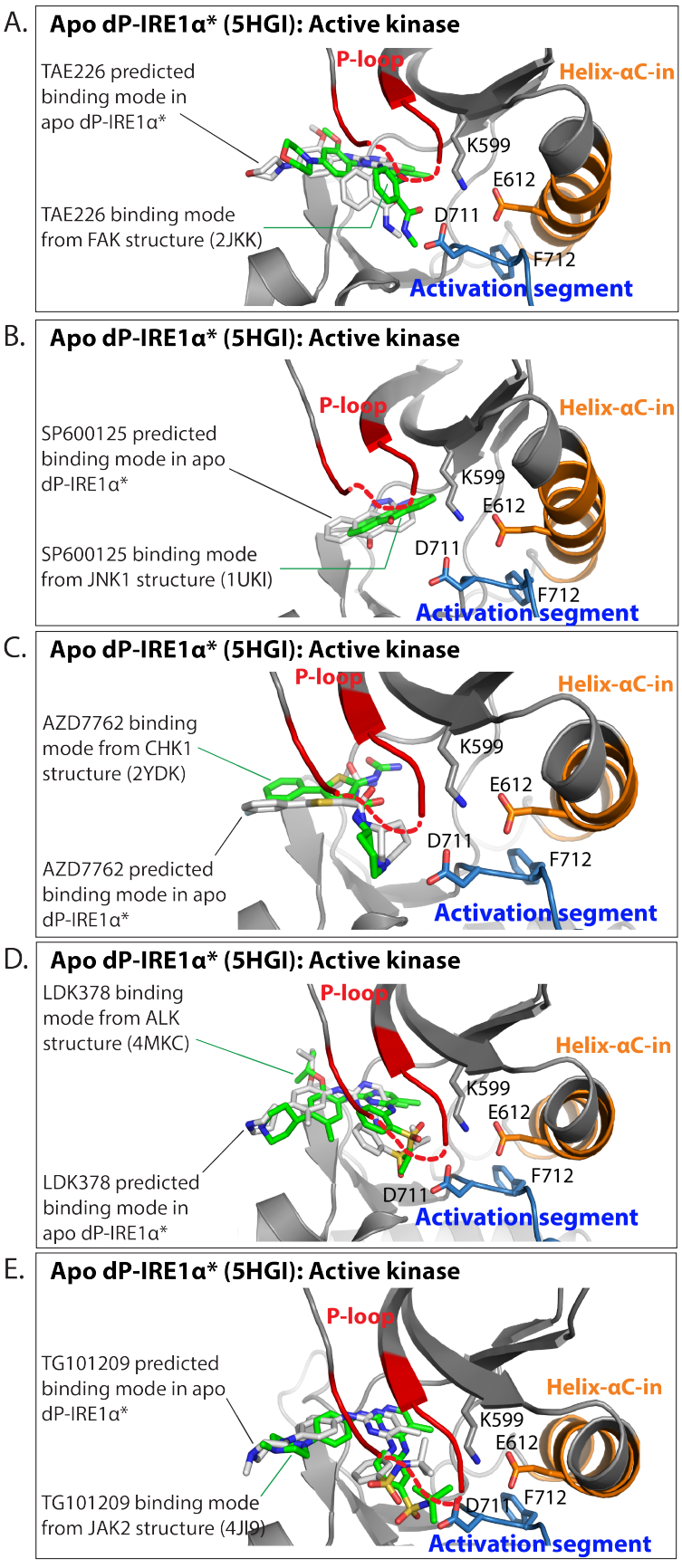
A.
Apo dP-IRE1α* (5HGI): Active kinase
TAE226 predicted binding mode in apo dP-IRE1α*
TAE226 binding mode from FAK structure (2JKK)
P-loop
Helix-αC-in
K599
E612
D711
F712
Activation segment
B.
Apo dP-IRE1α* (5HGI): Active kinase
SP600125 predicted binding mode in apo dP-IRE1α*
SP600125 binding mode from JNK1 structure (1UKI)
P-loop
Helix-αC-in
K599
E612
D711
F712
Activation segment
C.
Apo dP-IRE1α* (5HGI): Active kinase
AZD7762 binding mode from CHK1 structure (2YDK)
AZD7762 predicted binding mode in apo dP-IRE1α*
P-loop
Helix-αC-in
K599
E612
D711
F712
Activation segment
D.
Apo dP-IRE1α* (5HGI): Active kinase
LDK378 binding mode from ALK structure (4MKC)
LDK378 predicted binding mode in apo dP-IRE1α*
P-loop
Helix-αC-in
K599
E612
F712
D711
Activation segment
E.
Apo dP-IRE1α* (5HGI): Active kinase
TG101209 predicted binding mode in apo dP-IRE1α*
TG101209 binding mode from JAK2 structure (4JI9)
P-loop
Helix-αC-in
K599
E612
F712
D711
Activation segment

Figure S14. Computational docking of RNase activators to *apo* dP-IRE1α*. (A-E) IRE1α RNase activators (**Figure 6**) which are known to stabilize an active kinase conformation (**Figure S4**), were docked into the *apo* dP-IRE1α* (PDB: 5HGI) ATP-binding site to try and recapitulate their original binding modes and show compatibility with the *apo* dP-IRE1α* active kinase conformation. Only the predicted binding modes for TAE226, SP600125, AZD7762, LDK378, and TG101209 (grey) from initial docking experiments are shown, because qualitatively these appeared similar to their original binding mode (green). These RNase activators original binding modes were superimposed onto the *apo* dP-IRE1α* kinase ATP-binding site by backbone alignment of the kinase domain RNase activator bound co-crystal structure with the *apo* dP-IRE1α* kinase domain structure.

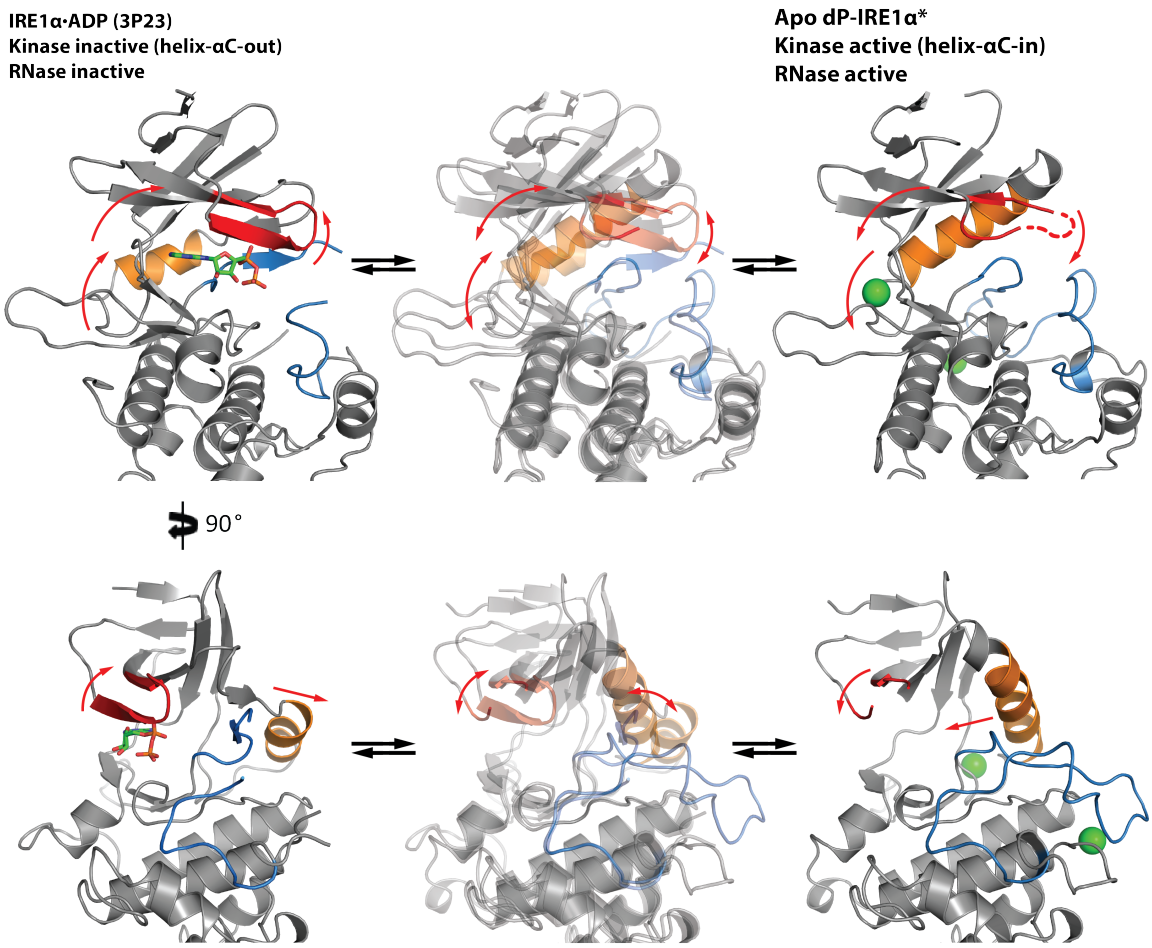

Figure S15. Movement of the IRE1α kinase lobes upon transitioning between inactive and active kinase conformations. Structural alignment of the IRE1α·ADP inactive state (PDB: 3P23) with the *apo* dP-IRE1α* active state (PDB: 5HGI) via the backbone Cα atoms of helix-αE (residues: 663-682) indicates that there are conformational changes in the kinase lobes. The kinase lobes of the active state reflect a more closed conformation with the N-lobe also shifting towards the kinase hinge region. Relative to the active state, the lobes of the inactive state adopt a more open conformation, and the N-lobe is shifted away from the hinge region. To rationalize the mechanism of RNase activators targeting the active kinase conformation, we speculate that they

stabilize this state by promoting and rigidifying the more closed conformation thus restricting helix-αC outward rotation.

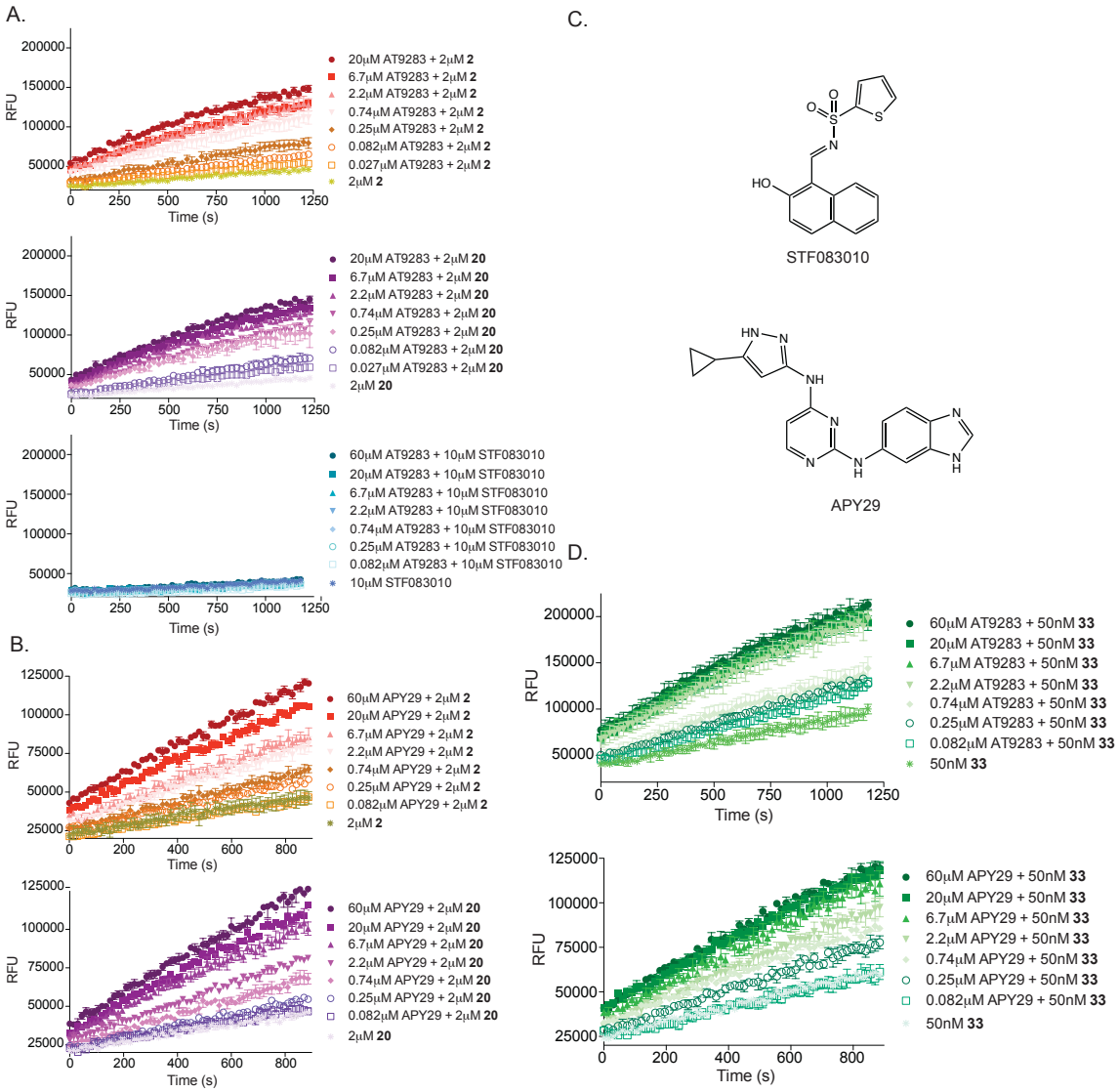

S16. ATP-competitive activators are able to competitively restore IRE1α*'s RNase activity in the presence of an inhibitory concentration of KIRAs but not STF083010. (A) Competitive restoration of IRE1α*'s RNase activity by activator AT9283 in the presence of KIRAs. IRE1α* (15 nM) was incubated with 2 μM **2** *(top),* 2 μM **20** *(middle)*, or 10 μM STF083010 *(bottom)* and variable concentrations of AT9283 at room temperature for 30 minutes. B. Competitive restoration of IRE1α*'s RNase activity by activator APY29 in the presence of KIRAs. IRE1α* (15 nM) was incubated with 2 μM **2** *(top)* or 2 μM **20** *(bottom)* and variable concentrations of APY29 at room temperature for 30 minutes. (**C**) Chemical structures of covalent RNase inhibitor STF083010 *(top)* and ATP-competitive activator APY29 *(bottom)*. (**D**) Competitive restoration of IRE1α*'s RNase activity by activators in the presence of Amgen KIRA **33**. IRE1α* (15 nM) was incubated with 50 nM **33** and variable concentrations of AT9283 (*top*) or APY29 (bottom) at room temperature for 30 minutes.

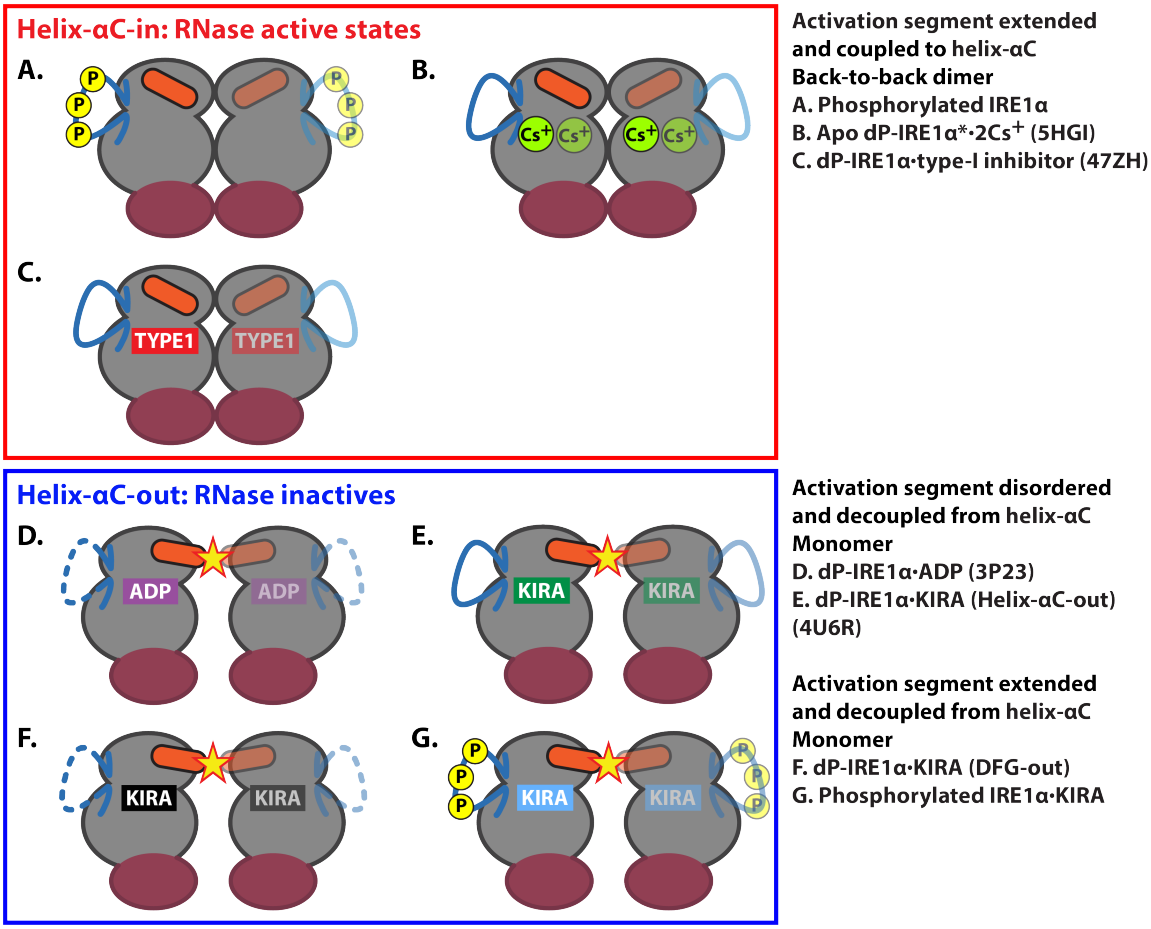

Figure S17. Schematic model summarizing the divergent modulation of IRE1α RNase activity. (**A-G**) IRE1α RNase activity depends on the conformation of helix-αC, because it regulates formation of the RNase active back-to-back dimer. Helix-αC-in, and helix-αC-out, coincides with the RNase active back-to-back dimer (**A-C**), and RNase inactive monomer states (**D-G**), respectively. Helix-αC-in can be stabilized through coupling with an extended activation segment which is stabilized by (**A**) phosphorylation, or (**C**) a type I inhibitor (PDB:4Z7H). (**B**) Helix-αC-in can also be stabilized directly by Cs^+ binding, and through coupling with the extended activation segment that is also stabilized by Cs^+ (PDB: 5HGI). Conversely, helix-αC-out can be stabilized through decoupling of helix-αC froacsm the activation segment. This can occur when bound by (**D**) ADP (PDB: 3P23), (**E, G**) a KIRA that directly displaces helix-αC regardless of the extended activation segment, (PDB: 4U6R), (**F**) a KIRA that indirectly displaces helix-αC by stabilizing the DFG-out conformation and collapsing the activation segment.

	Apo-hIRE1α	SrcKD·**1**
PDB-entry	5HGI	5J5S
Space Group	C 2 2 21	P 1
Unit Cell		
a, b, c (Å) α, β, γ (°)	68.04, 169.20, 104.14 90, 90, 90	42.21, 63.55, 73.66 100.60, 90.61, 90.96
1W1avelength (Å)0	1.00	1.00
Resolution Range (Å)	44.34 - 2.58 (2.676 - 2.584)	36.24 - 2.15 (2.23 - 2.15)
Total Reflections	123661 (11953)	156329 (15774)
Unique Reflections	19194 (1890)	38412 (3996)
Multiplicity	6.4 (6.3)	3.90 (3.90)
Completeness (%)	99.72 (99.68)	94.20 (87.38)
I/σI	20.47 (2.37)	36.44 (9.84)
B-factor	70.04	32.72
R_{merge}	0.05432 (0.8543)	0.27 (0.50)
R-measurement	0.05925	0.31
$CC_{1/2}$	0.999 (0.751)	0.92 (0.70)
CC*	1 (0.926)	0.98 (0.91)
Reflections used for R-free		
R_{work}	0.2385 (0.4574)	0.191 (0.22)
R_{free}	0.2679 (0.4828)	0.22 (0.28)
CC_{work}		
CC_{free}		
Number of non-hydrogen atoms	3010	4412
Macromolecules	2962	4121
Ligands	38	74
Water	10	217
Protein Residues	395	512
RMS (bonds)	0.005	0.003
RMS (angles)	0.76	0.8
Ramachandran favored (%)	95	98
Ramachandran allowed (%)	4.7	
Ramachandran outliers (%)	0.35	0.2
Clashscore	9.62	3.02
Average B-factor	82.51	48.00
Macromolecules	82.61	48.00
Ligands	110.90	56.80
Solvent	78.13	44.20

Table S1. Data collection and refinement statistics. Statistics for the highest-resolution shell are shown in parentheses.

Apo human dP-IRE1α structural feature	Apo human dP-IRE1α* (5HGI)	Active yeast IRE1 (3FBV)	Degree of similarity
Ligand	Apo.	APY29 (type I inhibitor).	Different
P-loop	Incomplete,	Complete.	Different
β4-β5 loop	Incomplete	Fully resolved.	Different
Helix-αC	Helix-αC-In (Active).	Helix-αC-In (Active).	Similar
DFG motif	DFG-Asp-in (Active).	DFG-Asp-in (Active).	Similar
Catalytic Lys and Helix-αC Glu salt bridge	K599:E612. Formed, 3.1, 3.7 Å.	K702:E715. Formed 2.9, 3.5 Å.	Similar
αD-αE	Loop residues: K656-D657, L661-L663. Helix αD' residues: F658-H660.	Loop residues: E757-E764, K770-N773. Helix αD' residues: N765-Q769.	Different
β7-β8 loop	Loop residues: S697-K706.	Loop residues: T807, D814-L822. Helix αE' residues: S808-A813.	Different
Activation segment	Residues: D711-E741. Resolved in an extended conformation.	Residues: D828-E859. Resolved in an extended conformation.	Similar
Activation segment phosphorylation state	Dephosphorylated.	Phosphorylated	Different
Helix-αC and activation loop salt bridge interactions	R611:G713, C715 backbone carbonyl. Formed, 3.6, 2.8, 3.5 Å. E618:K717. Formed, 2.5 Å	R611 equivalent is not conserved E721:K834. Formed, 2.8 Å.	Different Similar
αEF-αF loop	Loop residues: S744-T752.	Loop residues: E863-S864, T893-T898. Wild type loop residues: N865-F892 deleted.	Similar
αG-αH loop	Loop residues: G788-K799. Loop conformation orientated towards C-lobe.	Loop residues: I935-D946. Loop conformation orientated towards N-lobe.	Different
Activation segment stabilizing interactions	Activation segment residue R728 interacts with backbone carbonyls of E741, S744, C747. Hydrophobic interaction between L718 and Y753.	R728 is not conserved . Y753 is not conserved.	Different Different
Cs^+ ion binding site 1	One Cs^+ ion binds near Helix αC C-terminus, coordinated by residues: D620, E621, H622, V625 (backbone carbonyls), E643 (side chain).	Similar residues: D723, D724, H725, V728, and E746, but a coordinated positive ion is absent.	Partially similar
Cs+ ion binding site 2	One Cs^+ ion binds near Helix αF N-terminus, and helix αE C-terminus, coordinated by residue: H680 (backbone carbonyls), N683, and Y753 (side chain).	Not conserved.	Different
Kinase domain C-lobe RNase interface orientation	Orientation conserved and similar to active yeast IRE1 (3FBV).	Orientation conserved and similar to apo human dP-IRE1α*.	Similar
Helix-α2	Helix α2 residues: P857-E863. Loop residues: R864-G865. Helix α2' residues:G866-V870.	Helix α2 residues: S1006-I1020.	Different
α3-α4 loop (part of the catalytic HLE)	R887-F889 are unresolved.	Fully resolved.	Different
Helix α8	No helix, only a loop is present.	Helix α8 residues: R1110-L1113.	Different
Back to back dimer configuration	Protomers align parallel and symmetrically based on alignment of conserved R627 and L940 residues.	Protomers align parallel and symmetrically based on alignment of conserved R730 and L1091 residues.	Similar

Table S2. Structural Comparison of *apo* dP-IRE1α* and yIRE1. A list of the distinct and similar structural features that are found between apo human dP-IRE1α * and yIRE1 structures.

Apo human dP-IRE1α* (5HGI) Kinase domain dimer interface interactions		Nature and distance of the interaction	Active yeast IRE1 (3FBV) Kinase domain dimer interface interactions		Nature and distance of the interaction	Degree of Similarity
Protomer A	**Protomer B**		**Protomer A**	**Protomer B**		
#1. F591 (β2-β3 loop)	#1. F591 (β2-β3 loop)	Hydrophobic interaction (4.2 Å).	#1. F694 (β2-β3 loop)	#1. F694 (β2-β3 loop)	Hydrophobic interaction (4.2 Å).	Conserved
#2. D620 (Helix-αC C-terminus)	#2. R594, R627 (β2-β3 loop, αC-β4 loop)	Electrostatic interaction between D620 and R594 (3.2, 3.8 Å), and R627 (2.7, 3.2 Å) side chains.	#2. D723 (Helix-αC C-terminus)	#2. R697, R730 (β2-β3 loop, αC-β4 loop)	Electrostatic interaction between D723 and R697 (4.1, 4.1 Å), and R730 (2.7, 2.8 Å) side chains.	Conserved
#3. Y628 (αC-β4 loop)	#3. R594, R627 (β2-β3 loop, αC-β4 loop)	Electrostatic/dipole interaction between Y628 backbone carbonyl and R594 (3.6 Å) and R627 (3.5 Å) side chains.	#3. Y731 (β4-strand)	#3. R697, R730 (β2-β3 loop, αC-β4 loop)	Electrostatic/dipole interaction between Y731 backbone carbonyl and R697 (3.3 Å), and R730 (3.3 Å) side chains.	Conserved
#4. E621 (Helix-αC C-terminus)	#4. CsBS1 (Helix-αC and β5-strand C-termini)	Electrostatic interaction between E621 side chain of protomer A and Cs^+ (4.7Å) from CsBS1 in protomer B.	D724 (Helix-αC C-terminus)	CsBS1 (Helix-αC and β5-strand C-termini)	Features similar CsBS1 residues (D723, D724, H725, V728, and E746), but lacks coordination of Cs^+ or similar ion for D724 to engage with.	Partially Conserved
#5. K568 (Precedes β1-strand)	#5. T631 (Precedes β1-strand)	Electrostatic/dipole interaction between K568 side chain and T631 backbone carbonyl (2.4 Å).	#4. S734 (β4-strand)	#4. Q695 (β2-β3 loop)	H-bond/dipole between S734 backbone carbonyl and Q695 side chain (2.9Å).	Non-conserved, but similar in space
#6. S681 (Helix-αE C-terminus)	#6. H702 (β7-β8 loop)	Electrostatic/dipole interaction between S681 backbone carbonyl, side chain, and H702 side chain (4.3, 3.4 Å).	#5. S790, (Helix-αE C-terminus)	#5. D814 (αE'-β9 loop)	H-bond/dipole between S790 and D814 side chains (3.1Å).	Non-conserved, but similar in space
#7. D592 (β2-β3 loop)	#7. R617, Y628 (Helix-αC, αC-β4 loop)	Electrostatic/dipole interaction between D592 backbone carbonyl, side chain, and R617 side chain (2.1, 3.7, 3.0 Å). H-bond/dipole between D592 and Y628 side chains (2.4, 3.5 Å).				Non-conserved, unique
#8. L682 (Helix-αE C-terminus)	#8. A701 (β7-β8 loop)	Hydrophobic interaction between L682 and A701 side chains (3.7 Å).				Non-conserved, unique
			#6. S783 (Helix-αE)	#6. Q816 (αE'-β9 loop)	H- bond/dipole between S783 backbone carbonyl, side chain, and Q816 side chain (3, 3.4Å).	Non-conserved, unique
			#7. R810 (Helix-αE')	#7. T720, H787 (Helices-αC and αE)	Electrostatic/dipole interaction between R810 side chain and T720 backbone carbonyl (4.0, 4.1 Å), R810 backbone carbonyl and H787 side chain (4.3 Å).	Non-conserved, unique
dP-IRE1α* RNase domain dimer interface interactions		**Nature and distance of the interaction**	**Active yIRE1 (3FBV) RNase domain dimer interface interactions**		**Nature and distance of the interaction**	**Similarity**
Protomer A	**Protomer B**		**Protomer A**	**Protomer B**		
#9. D847 (Helix-α1)	#9. H909 (Helix-α4)	Electrostatic/dipole interaction between D847 and H909 side chains (4.0 Å).				Non-conserved, unique

#10. R955 (Helix-α7 C-terminal loop)	#10. E836, D927 (Helices-α1 and α6)	Electrostatic interaction between R955, and E836, D927 side chains (3.5, 3.1, 3.7, 4.0 Å).				Non-conserved, unique
			#8. E988 (Helix-α1)	#8. K992 (Helix-α1)	Electrostatic interaction between E988 and K992 side chains (2.7 Å).	Non-conserved, unique
			#9. M1063 (α4-α5 loop)	#9. I999 (α1- α2 loop)	Hydrophobic interaction between M1063 and I999 side chains (3.8 Å).	Non-conserved, unique
			#10. V1076 (α5-α6 loop)	#10. Q1107 (α7-α8 loop)	H-bond/dipole interaction between V1076 backbone amide and Q1107 side chain (2.9 Å).	Non-conserved, unique

Table S3. A description of the dimer interactions found in the RNase active back-to-back dimer structures of human apo dP-IRE1α* and active yIRE1. The interactions are classified and color coded according to the degree of similarity that the apo human dP-IRE1α* dimer interaction shows with its counterpart in the active yIRE1 dimer. Except for the color white, the numbering (#) and color coding of each interaction is coordinated to match with the interaction number (#) and its color in **Figure S5**, where blue = conserved, red = non-conserved but similar in space, green = non-conserved and unique. Here, white = partially conserved, but in **Figure S5**, this type of interaction is color coded as black.

SYNTHESIS

General Information:
Unless noted, reagents were obtained from commercial sources and used without further purification. ^{1}H NMR spectra were obtained using a Bruker AV-300, AV-301, or 500 instrument at room temperature. Chemical shifts are reported in ppm, and coupling constants are reported in Hertz. Mass spectrometry was performed on a Bruker Esquire Ion Trap MS instrument.

HPLC Preparatory Purification Conditions:
Samples were injected onto a preparatory reverse-phase C18 column (250x21mm) and separated using a Varian Pro-Star 210/325 HPLC instrument over 60 minutes at 8mL/min (Acetonitrile/Water-0.05% TFA gradient: 1% B Phase to 100% B Phase). Purified products were detected using UV absorption at 254nM and 220nM.

HPLC Analytical Conditions:
Samples were injected onto an analytical reverse phase C18 column and separated using a Varian Pro-Star 210 HPLC instrument over 30 minutes at 1mL/min (Acetonitrile/Water-0.05% TFA gradient 1%-100% B Phase). Purity of products was determined using UV absorption at 254nM and 220nM. Purity was determined by integrating the product peak and calculating its purity as a percentage of background subtracted total area.

$$\%\ Purity = \frac{Area\ of\ Compound\ Peak}{(Total\ Area\ of\ Compound\ Chromatogram - Total\ Area\ of\ Background\ Chromatogram)} * 100$$

Analytical chromatograms are shown as first the 220nM channel followed by 254nM channel. Percent purity reported for 220nM channel.

Note: Purity is shown through analytical chromatography or via proton NMR

Synthesis of R1 Derivatives [1]

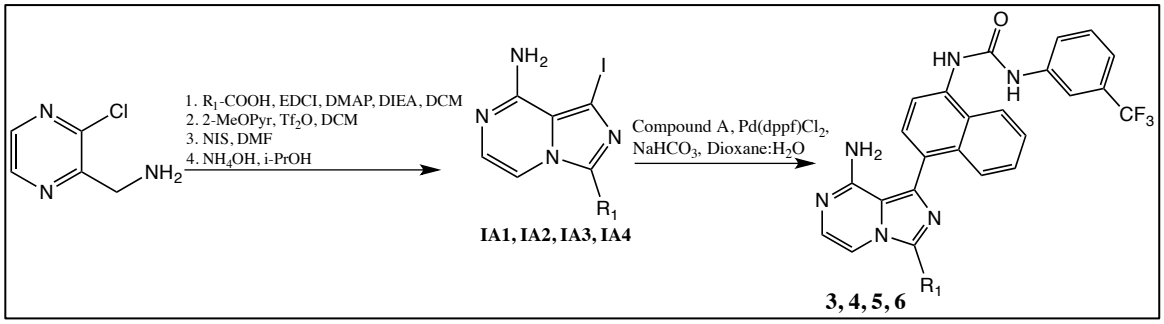

IA1

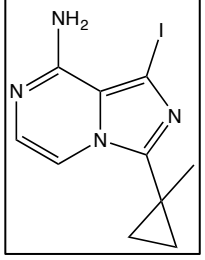

Compound IA1 was synthesized via Scheme 1 and derivatized using commercially available 1-methylcyclopropanecarboxylic acid (CAS: 6914-76-7) ^{1}H NMR (300 MHz, MeOD) δ 7.71 (d, *J* = 5.1 Hz, 1H), 7.03 (d, *J* = 5.1 Hz, 1H), 1.42 (s, 3H), 1.03 (dd, *J* = 11.6, 7.6 Hz, 2H), 1.00 – 0.87 (m, 2H).

IA2

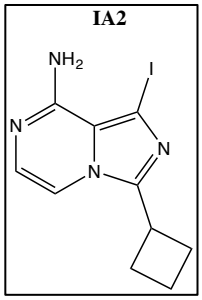

Compound IA2 was synthesized via Scheme 1 and derivatized using commercially available cyclobutancecarboxylic acid (CAS: 3721-95-7) ^{1}H NMR (300 MHz, DMSO) δ 7.47 (d, *J* = 5.0 Hz, 1H), 6.96 (d, *J* = 5.0 Hz, 1H), 6.54 (s, 2H), 3.97 – 3.75 (m, 1H), 2.44 – 2.25 (m, 4H), 2.06 (ddd, *J* = 17.8, 10.7, 8.7 Hz, 1H), 1.98 – 1.81 (m, 1H).

IA3

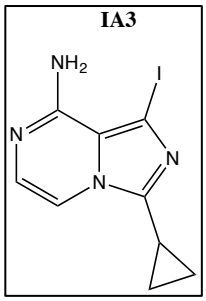

Compound IA3 was synthesized via Scheme 1 and derivatized using cyclopropanecarboxylic acid (CAS: 1759-53-1): ^{1}H NMR (300 MHz, MeOD) δ 7.72 (d, *J* = 5.3 Hz, 1H), 6.98 (d, *J* = 5.3 Hz, 1H), 2.23 – 2.13 (m, 1H), 1.26 – 1.11 (m, 2H), 1.05 (dd, *J* = 12.9, 3.3 Hz, 2H).

IA4

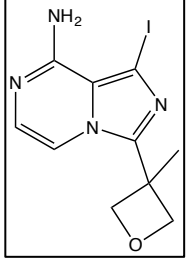

Compound IA4 was synthesized via Scheme 1 and derivatized using commercially available 3-methyl-3-oxetanecarboxylic acid (CAS: 28562-68-7) ^{1}H NMR (300 MHz, MeOD) δ 7.25 (dd, *J* = 5.3, 1.9 Hz, 1H), 6.99 (d, *J* = 5.2 Hz, 1H), 5.17 (dd, *J* = 6.2, 1.9 Hz, 2H), 4.75 (dd, *J* = 6.0, 1.7 Hz, 2H), 1.82 – 1.73 (m, 3H).

Compound A

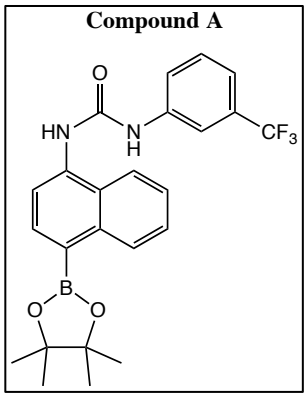

Compound A was synthesized via a previously published procedure. [2]

1: Previously published [2]

2: Previously published [2]

3: Synthesized via Scheme 1 with IA1 and Compound A. ^{1}H NMR (300 MHz, MeOD) δ 8.29 – 8.23 (m, 1H), 8.06 – 7.98 (m, 3H), 7.86 – 7.81 (m, 1H), 7.71 – 7.67 (m, 2H), 7.65 – 7.50 (m, 2H), 7.39 – 7.33 (m, 1H), 7.11 – 7.05 (m, 1H), 1.64 – 1.58 (m, 3H), 1.30 – 1.21 (m, 2H), 1.12 – 1.05 (m, 2H). Chemical Formula: $C_{28}H_{23}F_3N_6$/Exact Mass: 516.19. $[M+H]^+$ detected: 517.3 m/z. Retention Time: 15.099 minutes; Purity: 97.3%

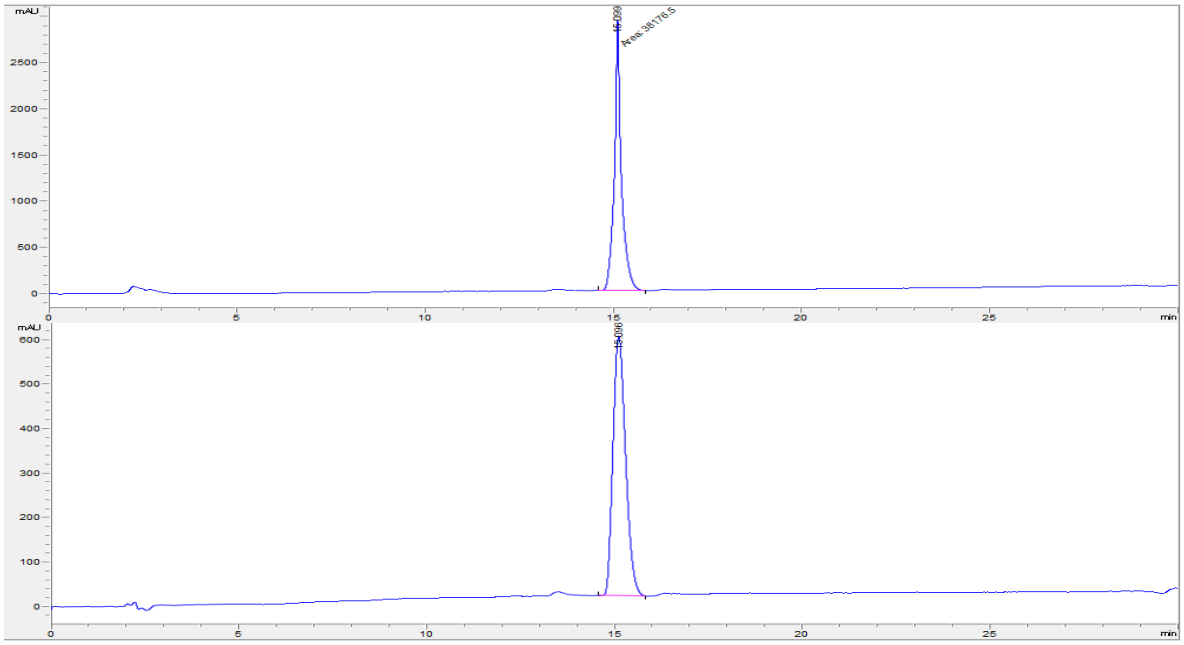

4: Synthesized via Scheme 1 with IA2 and Compound A. ^{1}H NMR (300 MHz, MeOD) δ 8.22 (d, *J* = 8.2 Hz, 1H), 8.05 – 7.97 (m, 2H), 7.77 (d, *J* = 8.4 Hz, 1H), 7.68 (dd, *J* = 14.8, 9.1 Hz, 3H), 7.59 – 7.51 (m, 2H), 7.49 (d, *J* = 5.2 Hz, 1H), 7.34 (d, *J* = 7.5 Hz, 1H), 7.02 (d, *J* = 5.2 Hz, 1H), 4.14 – 4.00 (m, 1H), 2.33 – 2.15 (m, 2H), 2.05 (s, 2H), 1.41 – 1.23 (m, 2H). Chemical Formula: $C_{28}H_{23}F_3N_6O$/Exact Mass: 516.19. $[M+H]^+$ detected: 517.3 m/z. Retention time: 14.792 minutes, purity: >99%

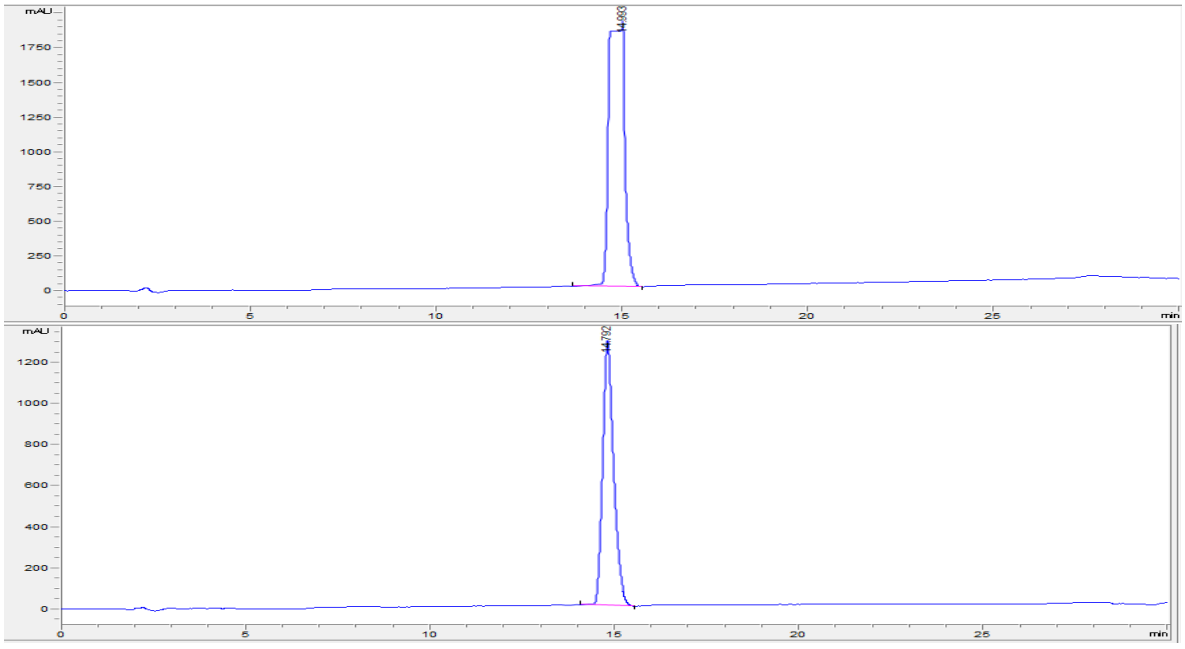

5: Synthesized via Scheme 1 with IA3 and Compound A. ^{1}H NMR (300 MHz, MeOD) δ 8.21 (d, *J* = 8.9 Hz, 34H), 8.01 (d, *J* = 7.7 Hz, 32H), 7.73 (d, *J* = 10.6 Hz, 45H), 7.69 (s, 10H), 7.65 (s, 18H), 7.57 (s, 5H), 7.36 (s, 4H), 7.08 (s, 10H), 2.40 – 2.25 (m, 1H), 1.22 (dd, *J* = 20.7, 11.7 Hz, 7H). Chemical Formula: $C_{27}H_{21}F_3N_6O$/Exact Mass: 502.17. $[M+H]^+$ detected: 503.3 m/z.

Retention time: 15.20 minutes; purity: 99%

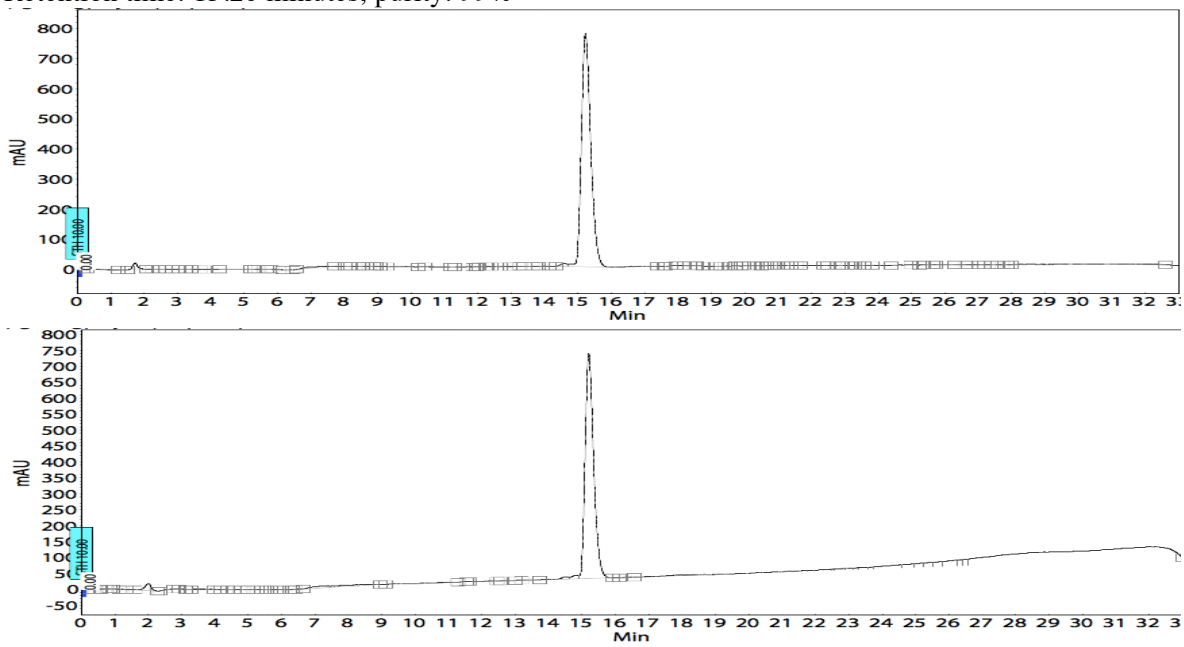

6: Synthesized via Scheme 1 with IA4 and Compound A. ^{1}H NMR (300 MHz, MeOD) δ 8.26 (s, 1H), 7.99 (s, 1H), 7.91 (d, *J* = 8.6 Hz, 1H), 7.73 (d, *J* = 3.1 Hz, 1H), 7.65 – 7.49 (m, 1H), 7.35 (d, *J* = 6.9 Hz, 1H), 7.03 (t, *J* = 3.4 Hz, 1H), 5.33 (s, 1H), 4.86 (d, *J* = 6.1 Hz, 1H), 1.95 (s, 1H). Chemical Formula: $C_{28}H_{23}F_3N_6O_2$/Exact Mass: 532.18. $[M+H]^+$ detected: 533.3 m/z. Retention time: 20.198 minutes; purity: 97%

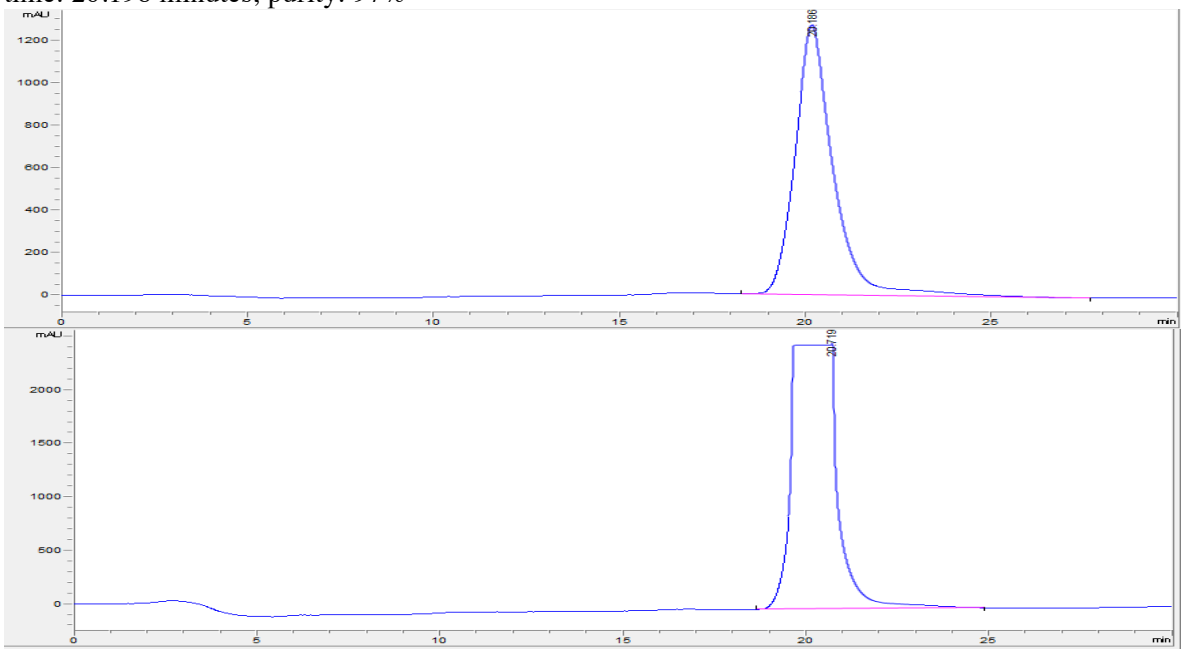

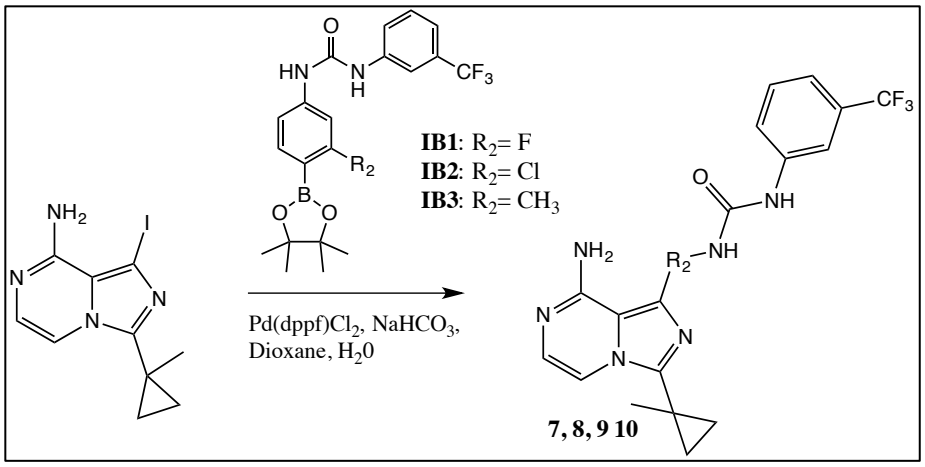

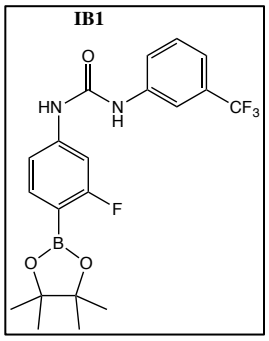

IB1: 4-Amino-2-fluorophenylboronic acid pinacol ester (CAS: 819057-45-9) was dissolved in 0.1M anhydrous THF at 0ºC. 3-(trifluoro)methylphenyl isocyanate was added dropwise to the reaction mixture. The mixture was brought to room temperature and allowed to stir overnight. The mixture was concentrated *in vacuo* and purified on silica. ^{1}H NMR (300 MHz, DMSO) δ 8.01 (s, 1H), 7.54 (dd, *J* = 15.2, 7.3 Hz, 3H), 7.42 (d, *J* = 12.1 Hz, 1H), 7.34 (d, *J* = 7.6 Hz, 1H), 7.18 (dd, *J* = 8.3, 1.9 Hz, 1H), 1.28 (s, 12H).

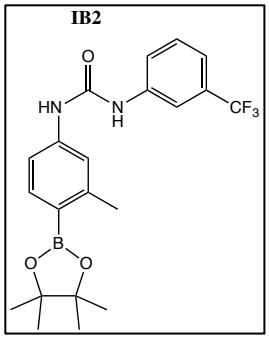

IB2: 4-Amino-2-methylphenylboronic acid, pinacol ester (631911-01-8) was dissolved in 0.1M anhydrous THF at 0ºC. 3-(trifluoro)methylphenyl isocyanate was added dropwise to the reaction mixture. The mixture was brought to room temperature and allowed to stir overnight. The mixture was concentrated *in vacuo* and purified on silica. ^{1}H NMR (300 MHz, DMSO) δ 8.03 (s, 1H), 7.54 (t, *J* = 9.4 Hz, 4H), 7.33 (s, 3H), 2.44 (s, 3H), 1.29 (s, 12H).

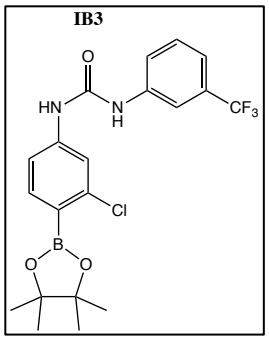

IB3: 4-Amino-2-chlorophenylboronic acid, pinacol ester (CAS: 877160-63-9) was dissolved in 0.1M anhydrous THF at 0ºC. 3-(trifluoro)methylphenyl isocyanate was added dropwise to the reaction mixture. The mixture was brought to room temperature and allowed to stir overnight. The mixture was concentrated *in vacuo* and purified on silica. ^{1}H NMR (300 MHz, DMSO) δ 8.01 (s, 1H), 7.67 (d, J = 1.9 Hz, 1H), 7.64 – 7.51 (m, 5H), 7.31 (d, J = 6.0 Hz, 1H), 1.28 (d, J = 5.2 Hz, 12H).

7: IB1 (2eq.) was dissolved with IA1 (1 eq.) and 0.1M dioxane:water (3:1) was combined with $NaHCO_3$ (3.4 eq.) and Pd(dppf)Cl_2 (0.1 eq.). The vial was sealed and placed in a microwave reactor for 45 minutes at 120ºC. The resulting mixture was washed with DCM:Water, and the organic layers combined. The organic layer was further purified using HPLC in an acetonitrile and water solvent system. ^{1}H NMR (300 MHz, MeOD) δ 7.97 – 7.89 (m, 2H), 7.72 (dd, J = 12.6, 2.1 Hz, 1H), 7.64 (d, J = 8.5 Hz, 1H), 7.55 – 7.47 (m, 2H), 7.36 – 7.30 (m, 2H), 7.04 – 7.01 (m, 1H), 1.51 (s, 3H), 1.16 (t, J = 5.6 Hz, 2H), 1.06 – 1.00 (m, 2H). Chemical Formula: $C_{24}H_{20}F_4N_6O$/Exact Mass: 484.16. Detected $[M+H]^+$= 485.2 m/z. Retention time: 14.738 minutes; purity: 96.8%

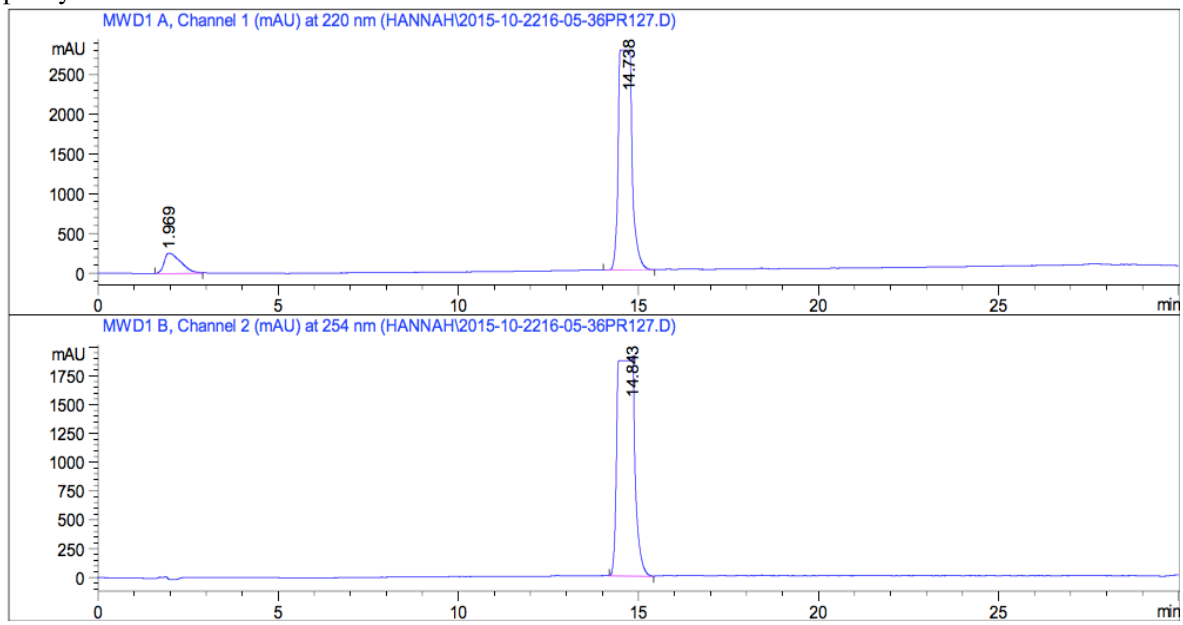

8: IB2 (2eq.) was dissolved with IA1 (1 eq.) and 0.1M dioxane:water (3:1) was combined with $NaHCO_3$ (3.4 eq.) and Pd(dppf)Cl_2 (0.1 eq.). The vial was sealed and placed in a microwave reactor for 45 minutes at 120ºC. The resulting mixture was washed with DCM:Water, and the organic layers combined. The organic layer was further purified using HPLC in an acetonitrile and water solvent system. ^{1}H NMR (300 MHz, MeOD) δ 8.01 – 7.89 (m, 3H), 7.72 – 7.61 (m,

1H), 7.62 – 7.46 (m, 3H), 7.34 (ddt, *J* = 7.8, 1.9, 1.0 Hz, 1H), 7.09 – 7.00 (m, 1H), 4.94 (d, *J* = 20.1 Hz, 13H), 1.53 (s, 3H), 1.23 – 1.12 (m, 2H), 1.04 (dd, *J* = 6.7, 4.6 Hz, 2H). Chemical Formula: $C_{25}H_{23}F_3N_6O$/Exact Mass: 480.19. Detected $[M+H]^+$= 481.3 m/z. Retention time: 14.678 minutes; purity: 95.6%

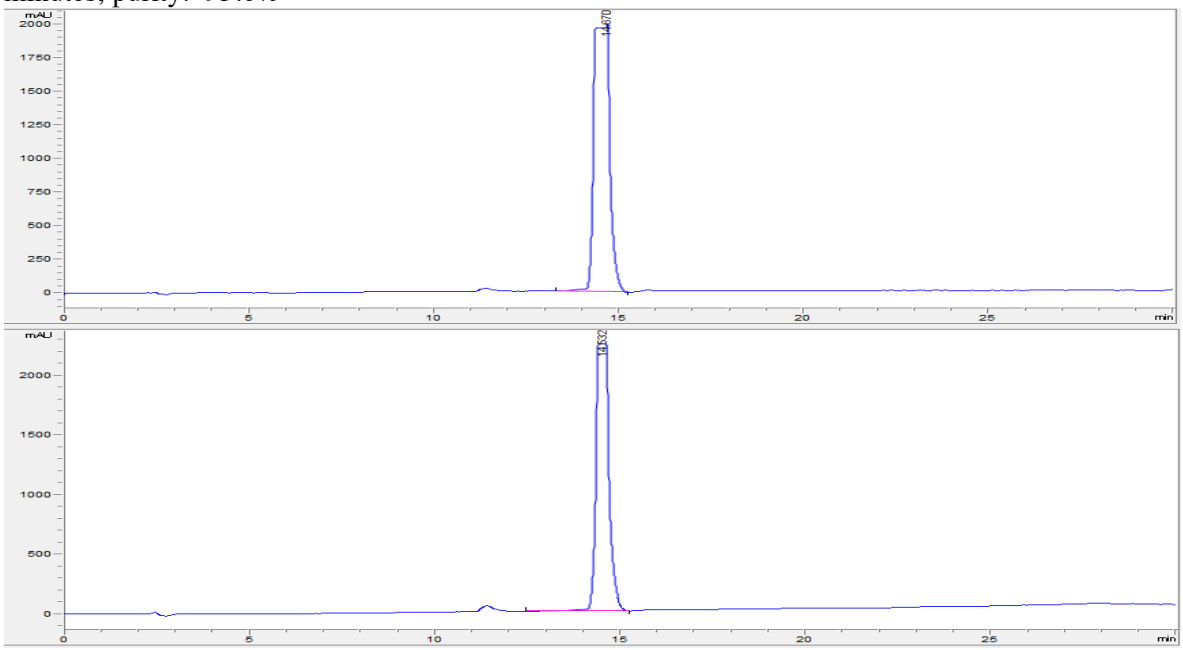

9: IB3 (2eq.) was dissolved with IA1 (1 eq.) and 0.1M dioxane:water (3:1) was combined with $NaHCO_3$ (3.4 eq.) and $Pd(dppf)Cl_2$ (0.1 eq.). The vial was sealed and placed in a microwave reactor for 45 minutes at 120ºC. The resulting mixture was washed with DCM:Water, and the organic layers combined. The organic layer was further purified using HPLC in an acetonitrile and water solvent system. ^{1}H NMR (300 MHz, MeOD) δ 7.93 (dd, *J* = 8.4, 7.6 Hz, 2H), 7.69 – 7.57 (m, 1H), 7.57 – 7.43 (m, 3H), 7.33 (dd, *J* = 8.5, 3.7 Hz, 2H), 7.07 – 6.94 (m, 1H), 1.52 (d, *J* = 0.9 Hz, 3H), 1.19 – 1.06 (m, 2H), 1.02 (q, *J* = 4.2 Hz, 2H). Chemical Formula: $C_{24}H_{20}ClF_3N_6O$/Exact Mass: 500.13. Detected $[M+H]^+$= 501.4 m/z. Retention time: 17.994 minutes, purity: >99%

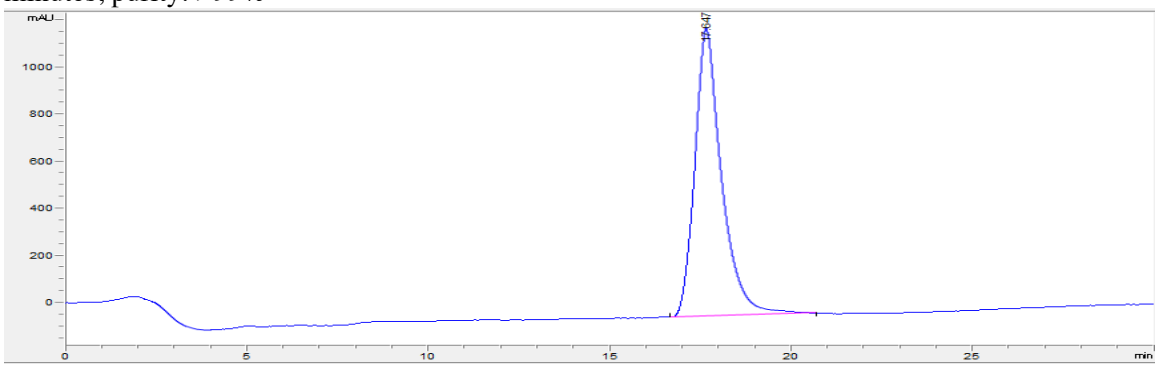

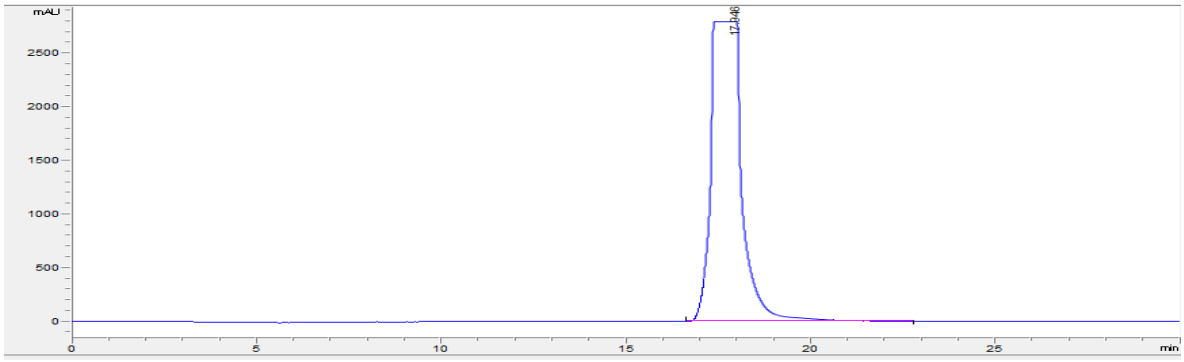

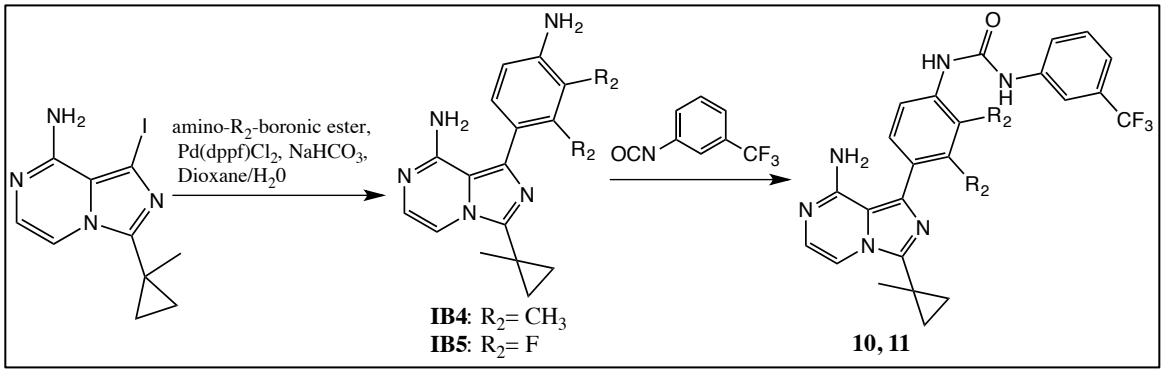

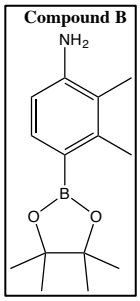

Compound B: 4-bromo-2,3-dimethylbenzenamine (CAS: 22364-25-6) was dissolved in dioxane (0.2M) with Bis(pinacolato)diboron (2eq), K_2CO_3 (4eq), and 1,1'Bis(diphenylphosphino)ferrocene (0.05eq). The reaction was left to stir at 90ºC for 12 hours. Reaction mixture was ran over a celite plug and extracted with DCM and water. The organic layer was concentrated *in vacuo* and purified via flash chromatography (0-30% EtOAc in hexanes) and yielded 70% product. ^{1}H NMR (300 MHz, $CDCl_3$) δ 7.53 (d, J = 8.0 Hz, 1H), 6.60 – 6.55 (m, 1H), 2.53 (s, 3H), 2.10 (s, 3H), 1.35 (s, 12H).

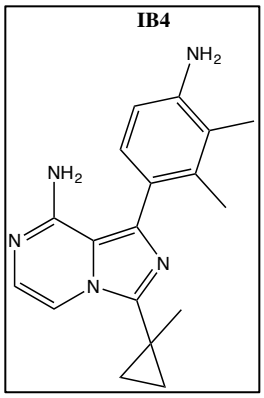

IB4: In a microwave vial, Compound B (1eq.) and IA1 (2 eq.) and 0.1M dioxane:water (3:1) were combined with $NaHCO_3$ (3.4 eq.) and $Pd(dppf)Cl_2$ (0.1 eq.). The vial was sealed and placed in a microwave reactor for 45 minutes at 120ºC. The resulting mixture was washed with DCM:Water, and the organic layers combined. The organic phase was purified via silica chromatography in EtOAc: Hex (0-100%). ^{1}H NMR (300 MHz, $CDCl_3$) δ 7.44 (d, *J* = 4.8 Hz, 1H), 7.02 (d, *J* = 7.9 Hz, 2H), 6.62 (d, *J* = 6.6 Hz, 1H), 3.48 (s, 3H), 2.13 (s, 3H), 1.48 (s, 3H), 1.14 (s, 2H), 0.88 (s, 2H).

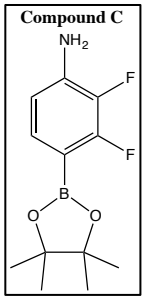

Compound C: Synthesized with the same procedure as compound B using 4-bromo-2,3-difluorobenzenamine (CAS: 112279-72-8) ^{1}H NMR (300 MHz, $CDCl_3$) δ 6.93 – 6.86 (m, 1H), 6.59 (td, *J* = 8.4, 1.5 Hz, 1H), 1.29 (d, *J* = 1.5 Hz, 6H), 1.26 (s, 6H).

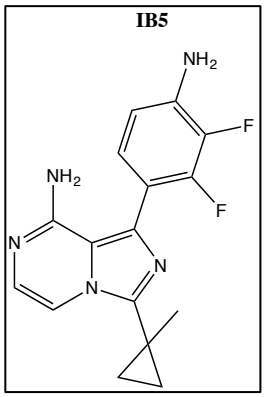

IB5: In a microwave vial, Compound C (1eq.) and IA1 (2 eq.) and 0.1M dioxane:water (3:1) were combined with $NaHCO_3$ (3.4 eq.) and $Pd(dppf)Cl_2$ (0.1 eq.). The vial was sealed and placed in a microwave reactor for 45 minutes at 120ºC. The resulting mixture was washed with DCM:Water, and the organic layers combined. The organic phase was purified via silica chromatography in EtOAc: Hex (0-100%). ^{1}H NMR (300 MHz, MeOD) δ 7.69 (d, *J* = 5.1 Hz, 1H), 7.06 (d, *J* = 5.1

Hz, 1H), 7.03 – 6.95 (m, 1H), 6.74 (td, *J* = 8.4, 1.8 Hz, 1H), 1.48 (s, 3H), 1.10 (t, *J* = 5.3 Hz, 2H), 0.96 (dd, *J* = 6.3, 4.6 Hz, 2H).

10: IB4 dissolved in 0.1M anhydrous THF at 0ºC. 3-(trifluoro)methyl phenyl isocyanate was added dropwise to the reaction mixture. The mixture was brought to room temperature and allowed to stir overnight. The mixture was concentrated *in vacuo*. The concentration mixture was further purified using HPLC in an acetonitrile and water solvent system. ^{1}H NMR (300 MHz, MeOD) δ 7.98 (s, 1H), 7.92 (d, *J* = 6.0 Hz, 1H), 7.63 (d, *J* = 7.1 Hz, 1H), 7.56 – 7.46 (m, 2H), 7.32 (d, *J* = 8.3 Hz, 1H), 7.25 (d, *J* = 8.1 Hz, 1H), 7.03 (d, *J* = 6.0 Hz, 1H), 2.35 (s, 3H), 2.21 (s, 3H), 1.54 (s, 3H), 1.18 (s, 2H), 1.04 (s, 2H). Chemical Formula: $C_{26}H_{25}F_3N_6O$/Exact Mass: 494.20. $[M+H]^+$ detected: 495.4 m/z. Retention Time: 12.465 minutes; purity: >99%

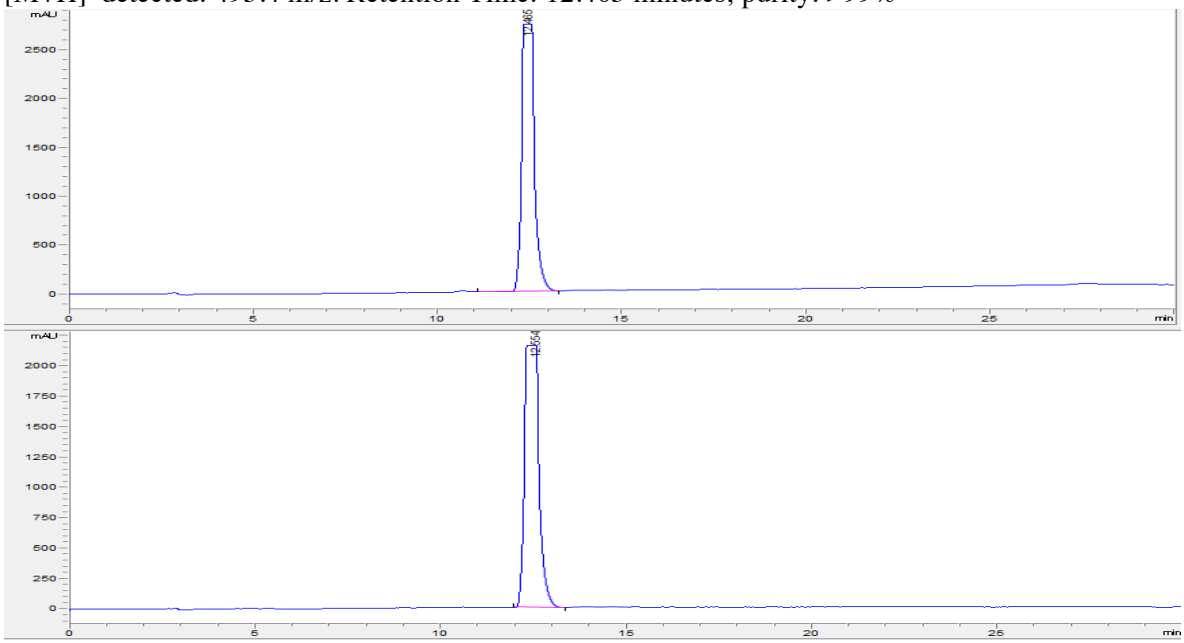

11: IB5 dissolved in 0.1M anhydrous THF at 0ºC. 3-(trifluoro)methyl phenyl isocyanate was added dropwise to the reaction mixture. The mixture was brought to room temperature and allowed to stir overnight. The mixture was concentrated *in vacuo*. The concentration mixture was further purified using HPLC in an acetonitrile and water solvent system. 1H NMR (300 MHz, MeOD) d 7.88 (s, 1H), 7.84 (d, J = 5.9 Hz, 1H), 7.65 (d, J = 12.6 Hz, 1H), 7.57 (d, J = 8.8 Hz, 1H), 7.45 – 7.38 (m, 1H), 7.26 (d, J = 8.2 Hz, 2H), 6.96 (d, J = 5.9 Hz, 1H), 1.46 – 1.43 (m, 3H), 1.12 – 1.07 (m, 2H), 0.96 (t, J = 3.1 Hz, 2H). Chemical Formula: $C_{24}H_{19}F_5N_6O$/Exact Mass: 502.15. $[M+H]^+$ detected: 503.1m/z. Retention Time: 11.831 minutes; purity: 93.5%

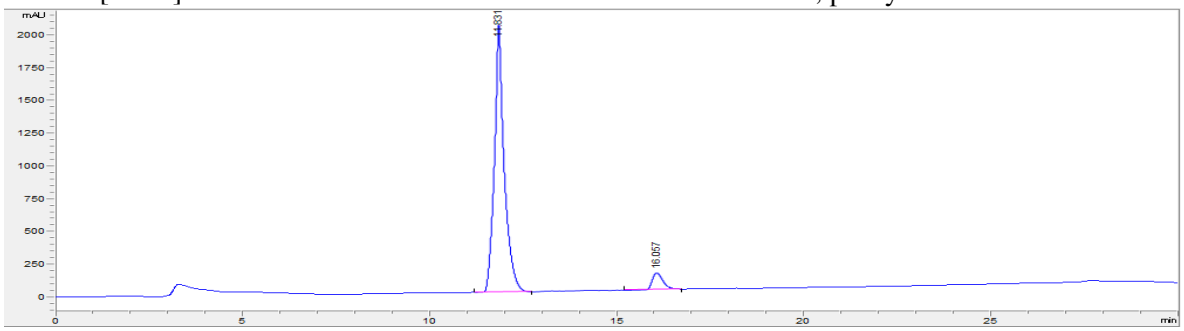

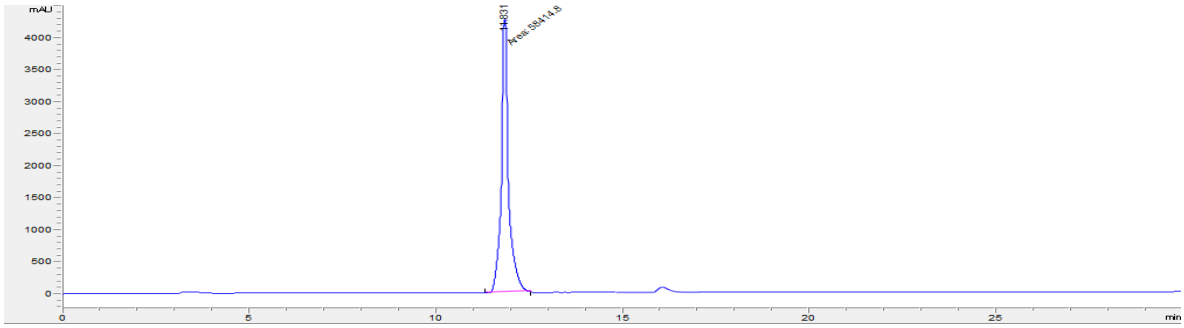

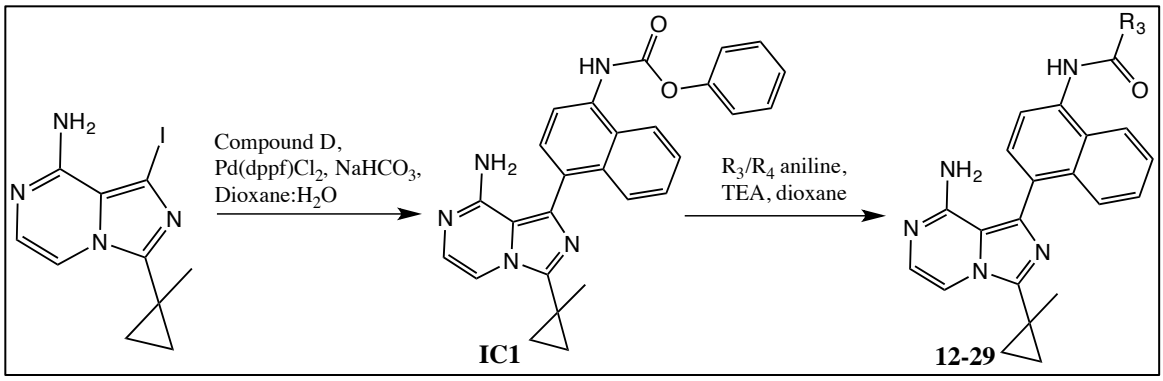

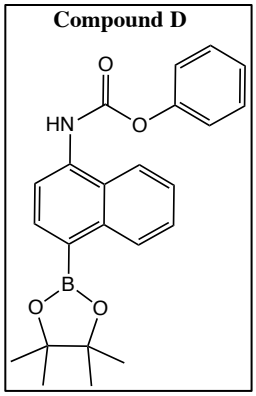

Compound D: 4-(4,4,5,5-tetramethyl-1,3,2-dioxaboroan-2-yl)-1-naphthalenamine (CAS: 1218790-22-7) (1 eq.) was dissolved in 0.1M dioxane with TEA (2.4 eq.) followed with the addition of phenyl chloroformate (CAS: 1885-14-9) (2.4 eq.) added dropwise. The reaction was allowed to stir at room temperature overnight. The resulting micture was extracted with DCM:Water, and the organic layers concentrated *in vacuo*. The concentrated mixture was purified on silica. ^{1}H NMR (300 MHz, $CDCl_3$) δ 8.92 – 8.85 (m, 1H), 8.16 – 8.04 (m, 2H), 8.04 – 7.93 (m, 1H), 7.66 – 7.56 (m, 2H), 7.48 – 7.39 (m, 3H), 7.32 – 7.29 (m, 1H), 7.26 (d, J = 3.4 Hz, 1H), 1.44 (t, J = 0.5 Hz, 12H).

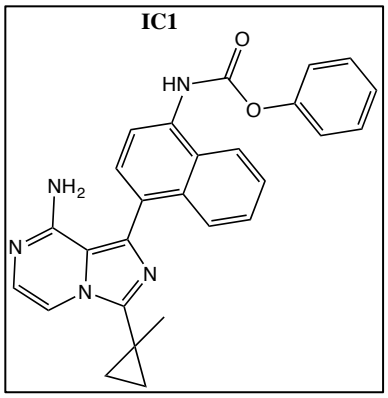

Compound IC1: In a microwave vial, IA1 (1eq.) and Compound D (2 eq.) and 0.1M dioxane:water (3:1) were combined with $NaHCO_3$ (3.4 eq.) and $PdCl_2(dppf)_2$ (0.1 eq.). The vial was sealed and placed in a microwave reactor for 45 minutes at 120ºC. The resulting mixture was washed with DCM:Water, and the organic layers combined. The organic phase was purified via silica chromatography in EtOAc: Hex (0-100%). ^{1}H NMR (300 MHz, $CDCl_3$) δ 8.05 (s, 1H), 7.85 (d, J = 8.3 Hz, 2H), 7.58 (d, J = 5.2 Hz, 1H), 7.47 (dd, J = 15.7, 7.9 Hz, 5H), 7.11 (d, J = 5.1 Hz, 2H), 1.57 (s, 3H), 1.26 (s, 2H), 0.98 (s, 2H).

12: IC1 and aniline (CAS: 62-53-3) (1.7eq.) were dissolved in 0.1M dioxane and TEA (1.7 eq.) and heated at 95ºC for 1.5 hours. The reaction was washed in DCM:Water and the organic layer extracted and concentration. The organic layer was further purified using HPLC in an acetonitrile and water solvent system.^{1}H NMR (300 MHz, Methanol-d_4) δ 8.13 (ddd, J = 8.5, 1.3, 0.7 Hz, 1H), 7.93 – 7.82 (m, 2H), 7.70 (ddd, J = 8.4, 1.4, 0.7 Hz, 1H), 7.63 – 7.42 (m, 4H), 7.21 – 7.07 (m, 2H), 6.95 (d, J = 5.9 Hz, 1H), 6.86 (dt, J = 7.0, 1.9 Hz, 1H), 3.28 – 3.13 (m, 11H), 2.39 (s, 3H), 1.47 (s, 3H), 1.13 (d, J = 3.3 Hz, 2H), 0.95 (d, J = 2.1 Hz, 2H). Chemical Formula: $C_{27}H_{24}N_6O$/Exact Mass: 448.20; $[M+H]^+$ detected = 449.3m/z. Retention time: 12.318 minutes, purity: 97.8%

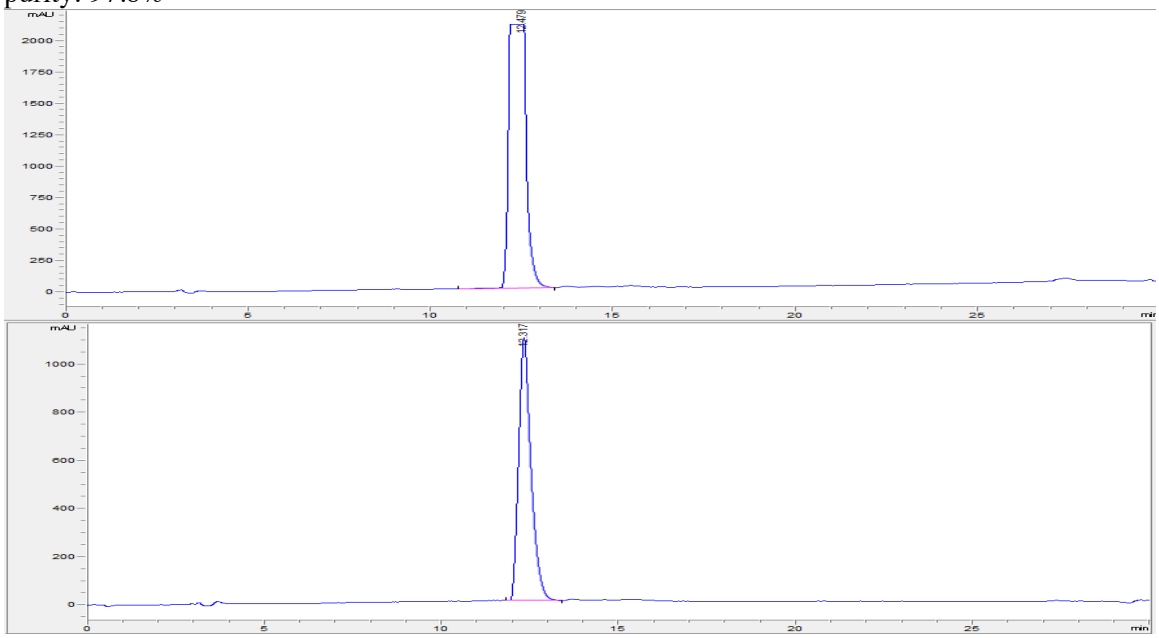

13: IC1 and 3-fluoro benzenamine (CAS: 372-19-0) (1.7eq.) were dissolved in 0.1M dioxane and TEA (1.7 eq.) and heated at 95ºC for 1.5 hours. The reaction was washed in DCM:Water and the organic layer extracted and concentration. The organic layer was further purified using HPLC in an acetonitrile and water solvent system ^{1}H NMR (300 MHz, $CDCl_3$) δ 8.08 – 8.01 (m, 1H), 7.97 – 7.85 (m, 3H), 7.70 (dt, *J* = 7.5, 4.2 Hz, 1H), 7.59 (t, *J* = 4.3 Hz, 1H), 7.49 (d, *J* = 7.8 Hz, 1H), 7.43 (d, *J* = 8.0 Hz, 1H), 7.23 – 7.14 (m, 1H), 6.99 (d, *J* = 8.1 Hz, 1H), 6.88 – 6.84 (m, 1H), 6.72 (dd, *J* = 9.8, 7.5 Hz, 1H), 1.59 (s, 3H), 1.25 (t, *J* = 5.5 Hz, 2H), 1.04 (t, *J* = 5.5 Hz, 2H). Chemical Formula: $C_{27}H_{23}FN_6O$/Exact Mass: 466.19. Detected $[M+H]^+$= 517.3 m/z. Retention Time: 12.475; Purity: 98.3%

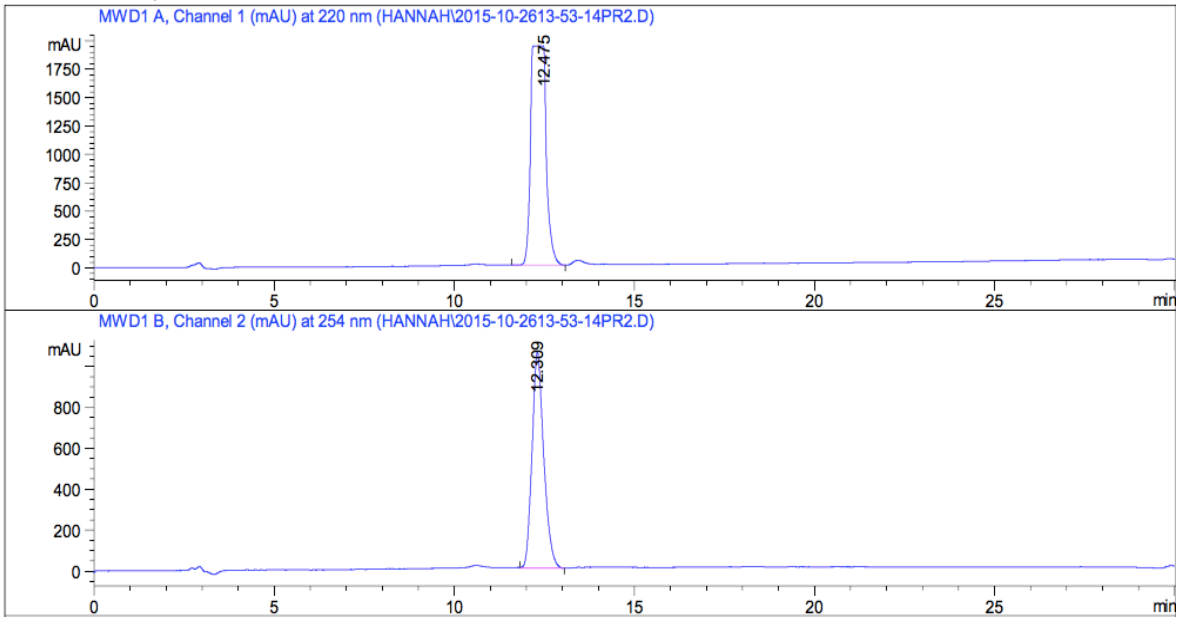

14: IC1 and 3-methyl-benzamine 108-44-1(1.7eq.) were dissolved in 0.1M dioxane and TEA (1.7 eq.) and heated at 95ºC for 1.5 hours. The reaction was washed in DCM:Water and the organic layer extracted and concentration. The organic layer was further purified using HPLC in an acetonitrile and water solvent system. ^{1}H NMR (300 MHz, Chloroform-*d*) δ 8.00 (t, *J* = 6.2 Hz, 1H), 7.83 – 7.66 (m, 1H), 7.63 – 7.45 (m, 2H), 7.33 – 7.14 (m, 3H), 6.92 (dd, *J* = 26.6, 6.4 Hz, 1H), 2.35 (s, 1H), 1.60 (s, 1H), 1.32 – 1.19 (m, 1H), 1.08 – 0.94 (m, 1H). Chemical Formula: $C_{28}H_{26}N_6O$/Exact Mass: 462.22. $[M+H]^+$ detected: 463.3m/z. Retention time: 12.105 minutes; purity: 98.7%

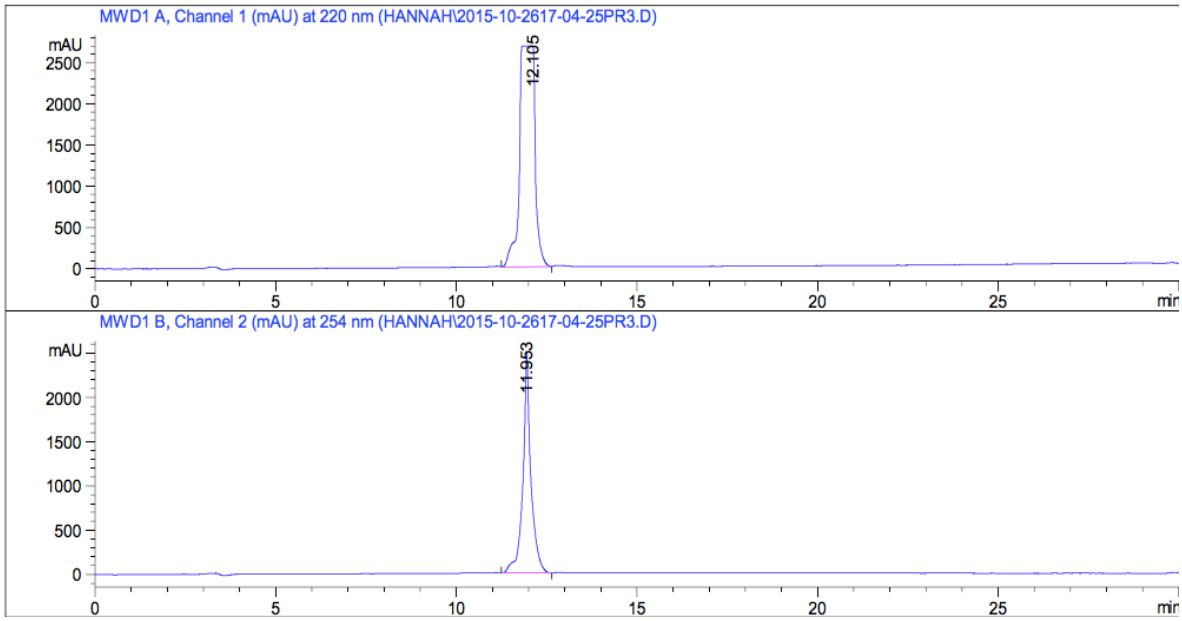

15: IC1 and 3-methoxy aniline (CAS: 536-90-3) (1.7eq.) were dissolved in 0.1M dioxane and TEA (1.7 eq.) and heated at 95ºC for 1.5 hours. The reaction was washed in DCM:Water and the organic layer extracted and concentration. The organic layer was further purified using HPLC in an acetonitrile and water solvent system. ^{1}H NMR (300 MHz, Methanol-d_4) δ 8.17 – 8.08 (m, 1H), 7.92 – 7.83 (m, 2H), 7.74 – 7.67 (m, 1H), 7.62 – 7.45 (m, 3H), 7.19 – 7.08 (m, 2H), 6.95 (d, J = 5.9 Hz, 1H), 6.90 (ddd, J = 8.1, 2.0, 0.9 Hz, 1H), 6.54 (ddd, J = 8.3, 2.5, 0.9 Hz, 1H), 3.70 (s, 3H), 3.31 – 3.17 (m, 18H), 1.47 (s, 3H), 1.13 (d, J = 3.7 Hz, 2H), 1.01 – 0.91 (m, 2H). Chemical Formula: $C_{28}H_{26}N_6O_2$/Exact Mass: 478.21. $[M+H]^+$ detected 479.3m/z. Retention time: 13.462 minutes, purity: 95.6%

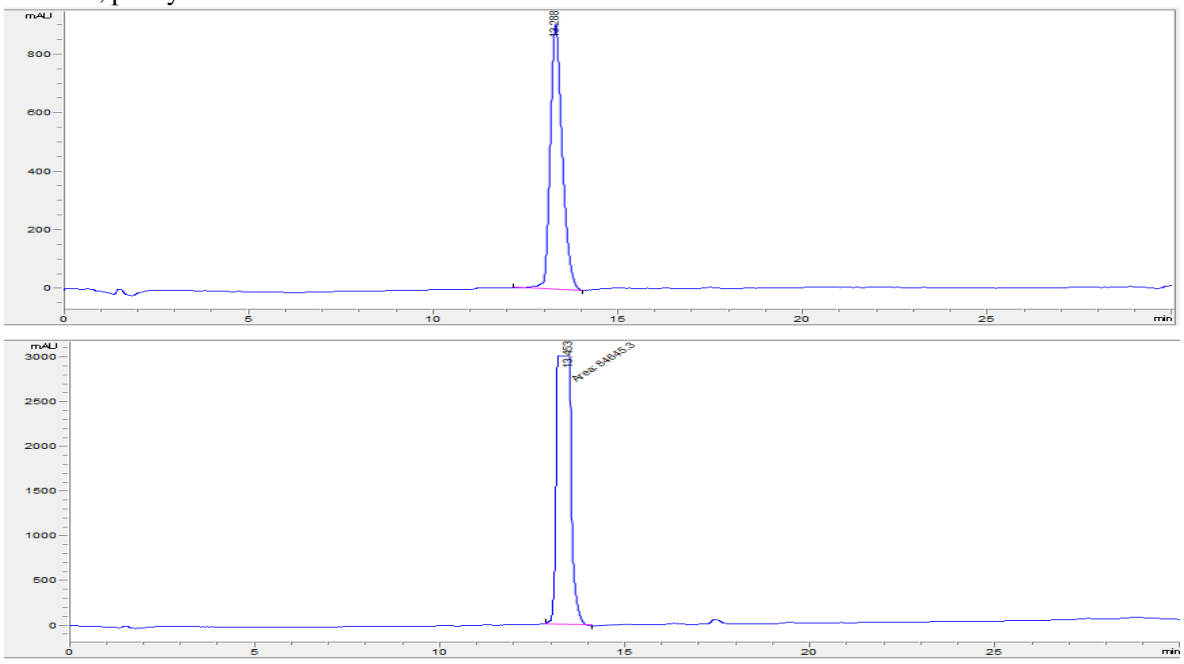

16: IC1 and the 3-(methylthio)-aniline (CAS: 1783-81-9) (1.7eq.) were dissolved in 0.1M dioxane and TEA (1.7 eq.) and heated at 95ºC for 1.5 hours. The reaction was washed in DCM:Water and the organic layer extracted and concentration. The organic layer was further purified using HPLC in an acetonitrile and water solvent system ^{1}H NMR (300 MHz, Methanol-d_4) δ 8.13 (ddd, J = 8.5, 1.3, 0.7 Hz, 1H), 7.93 – 7.82 (m, 2H), 7.70 (ddd, J = 8.4, 1.4, 0.7 Hz, 1H), 7.63 – 7.42 (m, 4H), 7.21 – 7.07 (m, 2H), 6.95 (d, J = 5.9 Hz, 1H), 6.86 (dt, J = 7.0, 1.9 Hz, 1H), 2.39 (s, 3H), 1.47 (s, 3H), 1.13 (d, J = 3.3 Hz, 2H), 0.95 (d, J = 2.1 Hz, 2H). Chemical Formula: $C_{28}H_{26}N_6OS$/Exact Mass: 494.19. Detected $[M+H]^+$= 495.3 m/z. Retention time: 13.546 minutes, purity: 94.9%

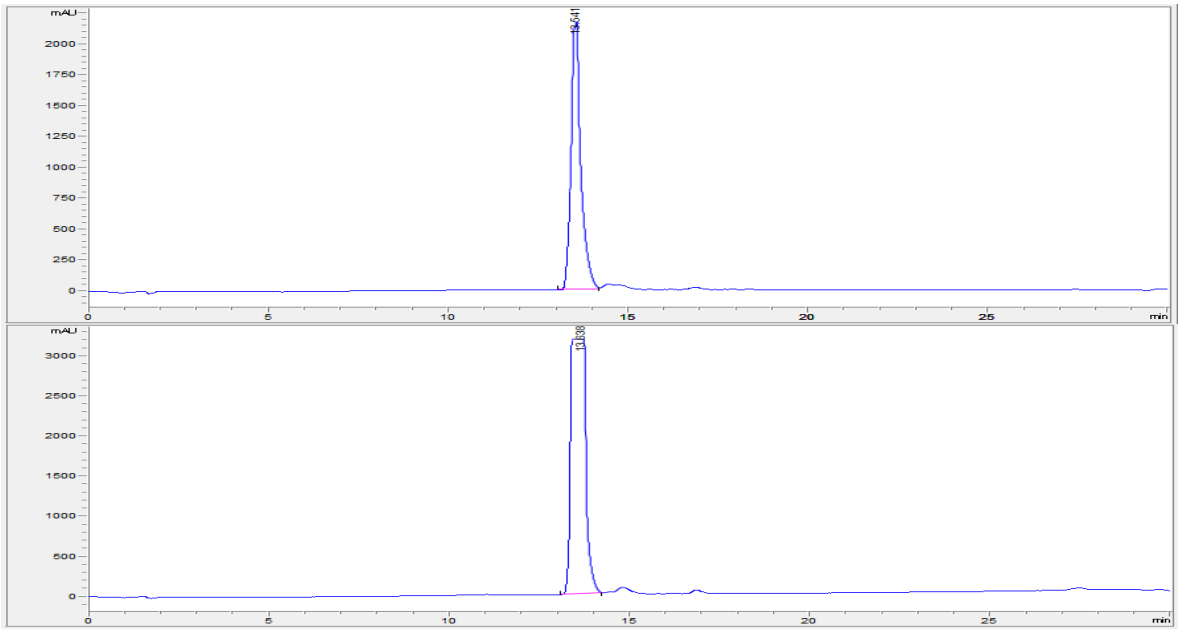

17: IC1 and 3-(methoxy)-5-(trifluoro)methyl aniline)(CAS: 349-55-3) (1.7eq.) were dissolved in 0.1M dioxane and TEA (1.7 eq.) and heated at 95ºC for 1.5 hours. The reaction was washed in DCM:Water and the organic layer extracted and concentration. The organic layer was further purified using HPLC in an acetonitrile and water solvent system. ^{1}H NMR (300 MHz, MeOD) δ 8.24 (d, J = 8.2 Hz, 1H), 7.98 (t, J = 6.8 Hz, 2H), 7.82 (d, J = 7.7 Hz, 1H), 7.75 – 7.54 (m, 3H), 7.44 (d, J = 13.8 Hz, 2H), 7.07 (d, J = 5.9 Hz, 1H), 6.88 (s, 1H), 3.88 (s, 3H), 1.59 (s, 3H), 1.24 (s, 2H), 1.07 (s, 2H). Chemical Formula: $C_{29}H_{25}F_3N_6O_2$/Exact Mass: 546.20. Found mass: $[M+H]^+$ 547.3 m/z. Retention time: 14.732 minutes, purity: 94.7%

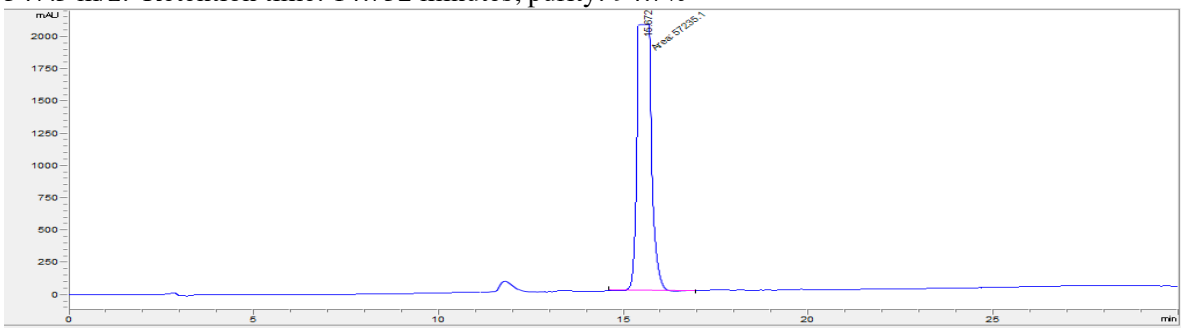

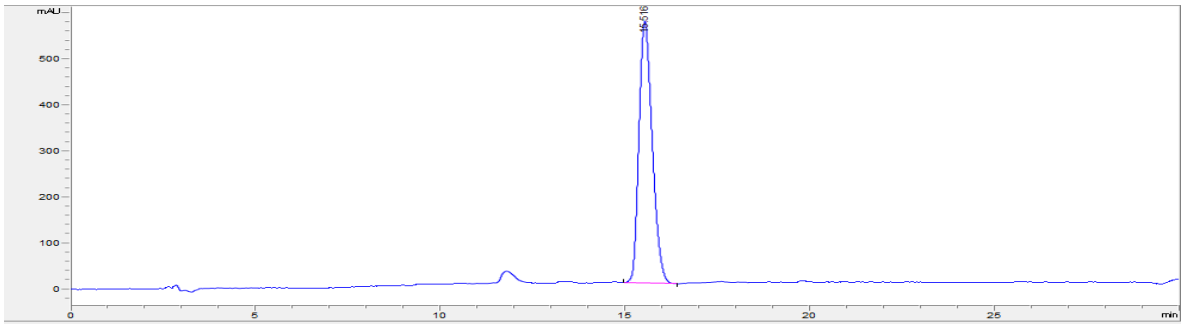

18: IC1 and 3-fluoro-5-(trifluoro)methyl aniline (CAS: 454-67-1) (1.7eq.) were dissolved in 0.1M dioxane and TEA (1.7 eq.) and heated at 95ºC for 1.5 hours. The reaction was washed in DCM:Water and the organic layer extracted and concentration. The organic layer was further purified using HPLC in an acetonitrile and water solvent system. ^{1}H NMR (300 MHz, MeOD) δ 8.26 – 8.20 (m, 1H), 7.98 (dd, *J* = 6.8, 4.0 Hz, 2H), 7.85 – 7.79 (m, 1H), 7.74 – 7.59 (m, 5H), 7.24 – 7.18 (m, 1H), 7.07 (d, *J* = 5.9 Hz, 1H), 1.59 (s, 3H), 1.24 (s, 2H), 1.07 (s, 2H). Chemical Formula: $C_{28}H_{22}F_4N_6O$/Exact Mass: 534.18. Detected $[M+H]^+$=534.3 m/z. Retention time: 13.216 minutes, purity: 96.4%

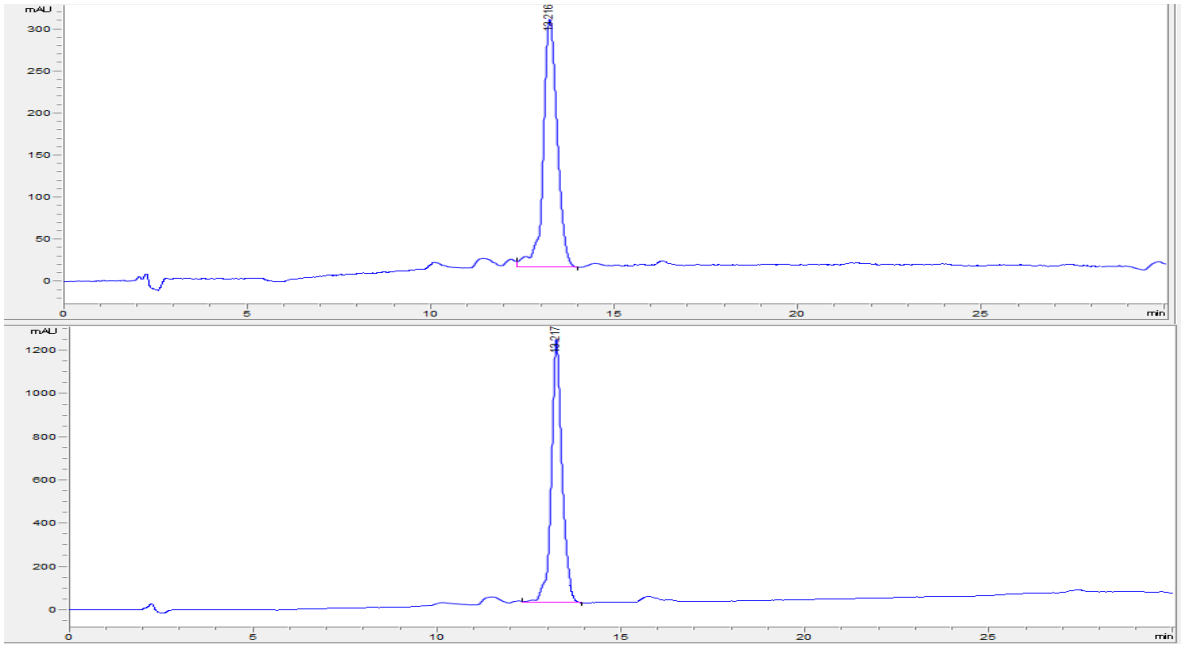

19: IC1 and 2-amino-N-methylbenzenesulfonamide (CAS: 459434-40-3) (1.7eq.) were dissolved in 0.1M dioxane and TEA (1.7 eq.) and heated at 95ºC for 1.5 hours. The reaction was washed in DCM:Water and the organic layer extracted and concentration. The organic layer was further purified using HPLC in an acetonitrile and water solvent system. ^{1}H NMR (300 MHz, MeOD) δ 8.23 (s, 1H), 8.18 (s, 1H), 7.98 (d, *J* = 6.6 Hz, 2H), 7.80 (s, 1H), 7.73 – 7.52 (m, 6H), 7.07 (d, *J* = 5.7 Hz, 1H), 2.58 (s, 3H), 1.59 (s, 3H), 1.24 (s, 2H), 1.07 (s, 2H). Chemical Formula: $C_{28}H_{27}N_7O_3S$/Exact Mass: 541.19. $[M+H]^+$ detected: 542.2 m/z. Retention time: 10.693 minutes; purity: 95.2%

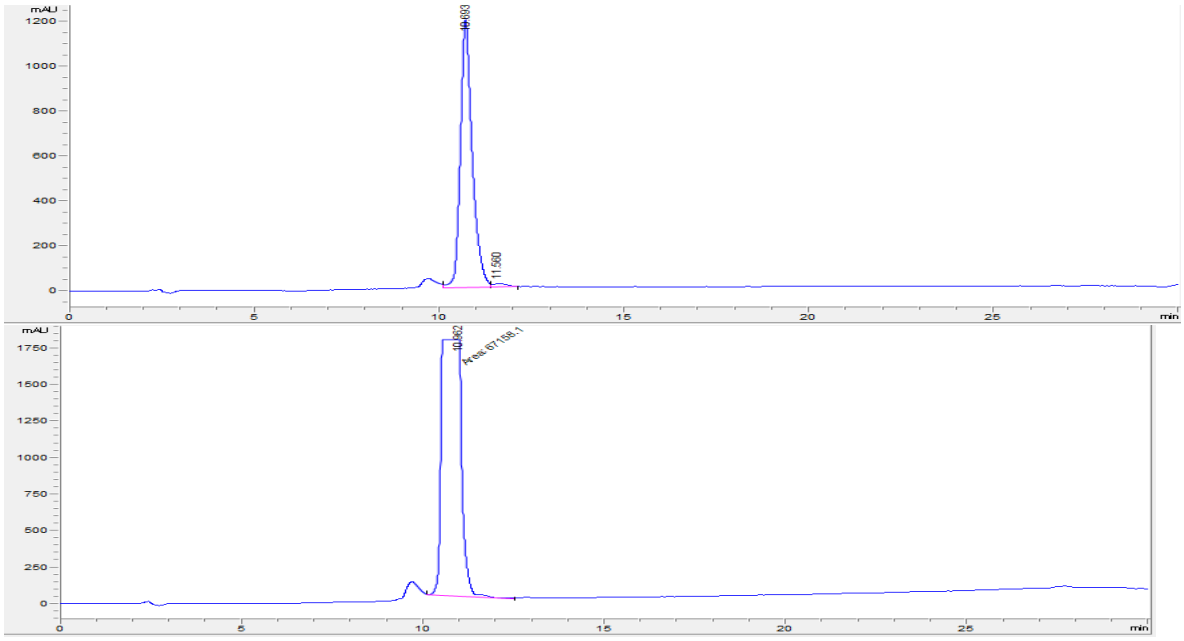

20: IC1 and 4-(4-methylpiperazin-1-ylmethyl)-3-trifluoromethylaniline (1.7eq.) were were dissolved in 0.1M dioxane and TEA (1.7 eq.) and heated at 95ºC for 1.5 hours. The reaction was washed in DCM:Water and the organic layer extracted and concentration. The organic layer was further purified using HPLC in an acetonitrile and water solvent system. ^{1}H NMR (300 MHz, MeOD) δ 8.25 (d, *J* = 7.8 Hz, 1H), 8.01-7.98 (m, 2H), 7.82 (d, *J* = 8.4 Hz, 1H), 7.73 (s, 2H), 7.64 (dd, *J* = 20.5, 7.3 Hz, 3H), 7.51-7.25 (m, 1H), 7.38 (dd, *J* = 4.2, 1.8 Hz, 1H), 7.08 (d, *J* = 5.9 Hz, 1H), 3.76 (s, 2H), 3.48 (s, 4H), 3.09 (s, 4H), 2.93 (s, 3H), 1.59 (s, 3H), 1.24 (s, 2H), 1.06, 2H). Chemical Formula: $C_{34}H_{35}F_3N_8O$/Exact Mass: 628.29. $[M+H]^+$ detected: 629.3 m/z. Retention time: 16.480 minutes, purity: >99%

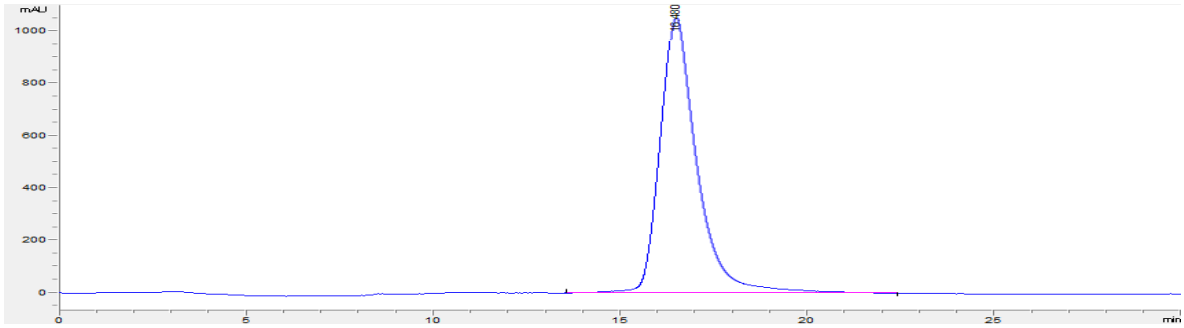

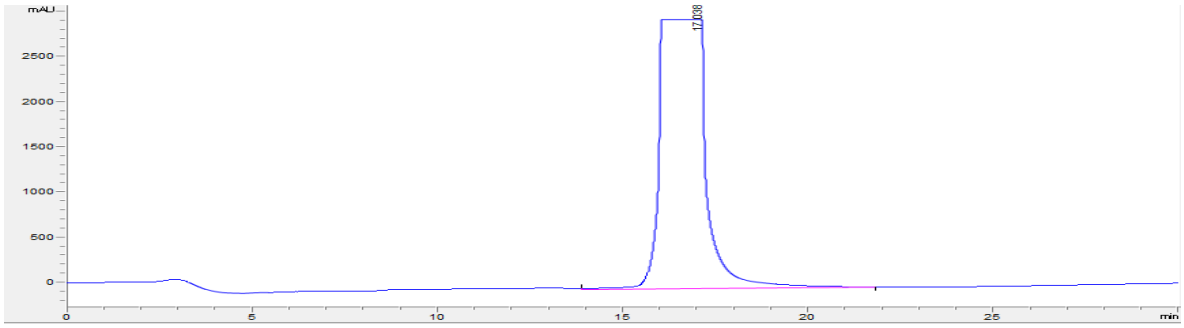

21: IC1 and 4-[(4-methyl-1-piperazinyl)methyl] benzamine (1.7eq.) were dissolved in 0.1M dioxane and TEA (1.7 eq.) and heated at 95ºC for 1.5 hours. The reaction was washed in DCM:Water and the organic layer extracted and concentration. The organic layer was further purified using HPLC in an acetonitrile and water solvent system. ^{1}H NMR (300 MHz, MeOD) δ 7.91 (d, *J* = 5.9 Hz, 1H), 7.73 (d, *J* = 12.6 Hz, 1H), 7.52 (t, *J* = 8.4 Hz, 4H), 7.46 – 7.24 (m, 4H), 7.04 (d, *J* = 5.9 Hz, 1H), 3.76 (s, 2H), 3.27 (s, 4H), 3.07 (d, *J* = 24.0 Hz, 3H), 2.85 (s, 2H), 1.53 (s, 3H), 1.18 (s, 2H), 1.04 (s, 2H). Chemical Formula: $C_{33}H_{36}N_8O$/ Exact Mass: 560.30. $[M+H]^+$ detected: 561.7 m/z. Retention time: 15.478 minutes, purity: 98.3%

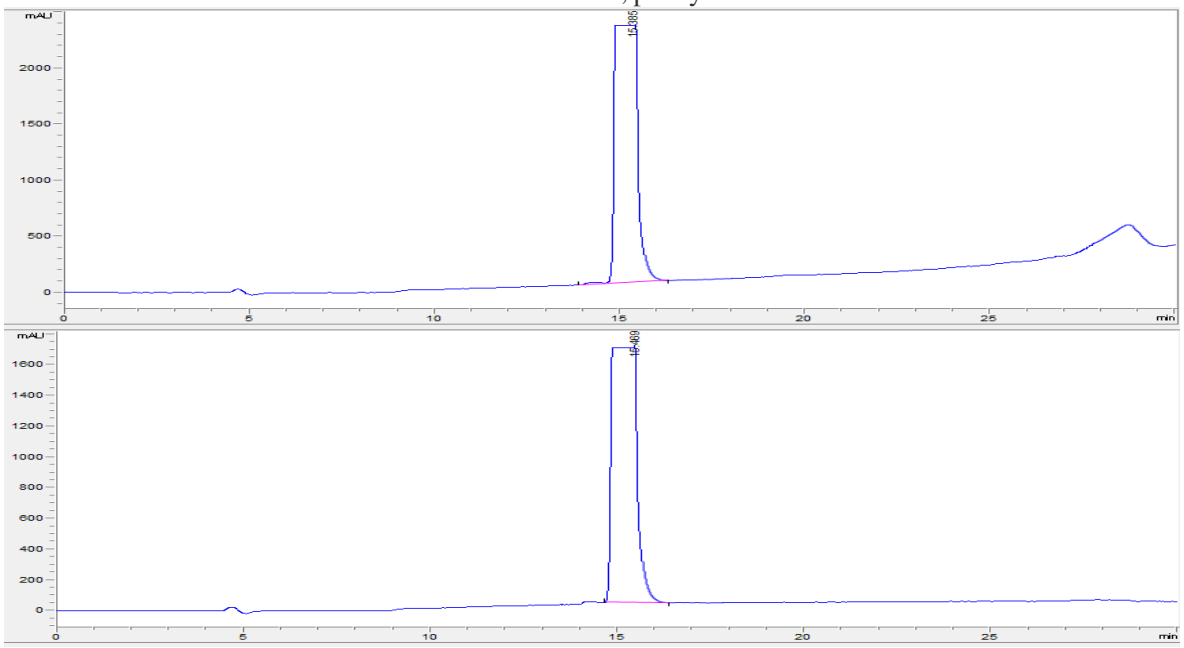

22: IC1 and 5-methyl-1H-pyrzaol-3-amine (CAS: 31230-17-8) (1.7eq.) were dissolved in 0.1M dioxane and TEA (1.7 eq.) and heated at 95ºC for 1.5 hours. The reaction was washed in DCM:Water and the organic layer extracted and concentration. The organic layer was further purified using HPLC in an acetonitrile and water solvent system. ^{1}H NMR (300 MHz, CD_3CN) δ 8.42 (d, *J* = 9.2 Hz, 2H), 7.91 (d, *J* = 8.7 Hz, 1H), 7.78 – 7.66 (m, 2H), 7.59 (s, 2H), 6.91 (d, *J* = 5.7 Hz, 1H), 5.82 (s, 1H), 2.53 (s, 3H), 1.54 (s, 3H), 1.16 (m, 2H), 0.99 (m, 2H). Chemical Formula: $C_{25}H_{24}N_8O$/Exact Mass: 452.21. Retention time: 12.574; Purity: >99%

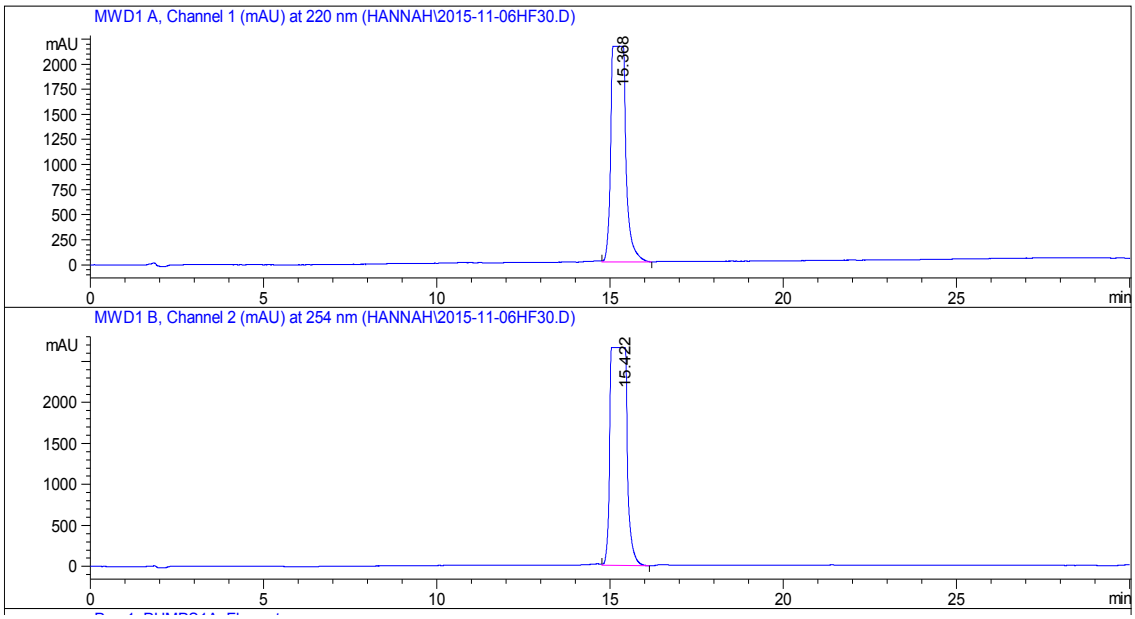

23: IC1 and benzylamine (CAS: 100-46-9) (1.7eq.) were dissolved in 0.1M dioxane and TEA (1.7 eq.) and heated at 95ºC for 1.5 hours. The reaction was washed in DCM:Water and the organic layer extracted and concentration. The organic layer was further purified using HPLC in an acetonitrile and water solvent system. ^{1}H NMR (300 MHz, CD_3CN) δ 8.20 (d, *J* = 8.3 Hz, 1H), 8.13 (d, *J* = 7.8 Hz, 1H), 7.88 (d, *J* = 8.4 Hz, 1H), 7.79 (s, 1H), 7.74 (d, *J* = 5.7 Hz, 1H), 7.63 (d, *J* = 7.2 Hz, 1H), 7.55 (d, *J* = 7.9 Hz, 2H), 7.43 – 7.38 (m, 3H), 7.31 (s, 1H), 6.91 (d, *J* = 6.0 Hz, 1H), 4.47 (d, *J* = 5.9 Hz, 2H), 1.53 (s, 3H), 1.15 (s, 2H), 0.99 (s, 2H). Chemical Formula: $C_{28}H_{26}N_6O$/Exact Mass: 462.22. $[M+H]^+$ detected: 463.3 m/z. Retention time: 12.414 minutes, purity: 96.1%

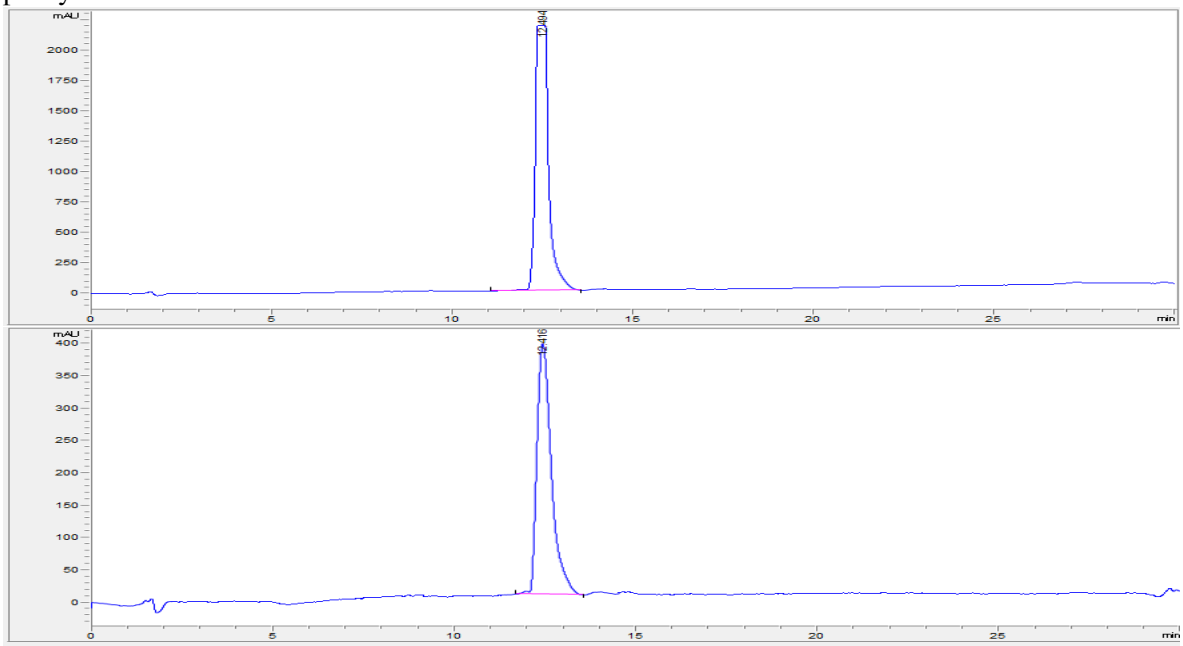

24: IC1 and phenethylamine (CAS: 64-04-0) (1.7eq.) were dissolved in 0.1M dioxane and TEA (1.7 eq.) and heated at 95ºC for 1.5 hours. The reaction was washed in DCM:Water and the

organic layer extracted and concentration. The organic layer was further purified using HPLC in an acetonitrile and water solvent system. ^{1}H NMR (300 MHz, MeOD) δ 8.11 (d, *J* = 8.1 Hz, 1H), 7.97 (d, *J* = 5.9 Hz, 1H), 7.82 (d, *J* = 7.7 Hz, 1H), 7.77 (d, *J* = 7.6 Hz, 1H), 7.67 – 7.53 (m, 4H), 7.36 – 7.29 (m, 4H), 7.06 (d, *J* = 5.9 Hz, 1H), 3.56 (dd, *J* = 7.7, 5.8 Hz, 2H), 2.92 (dd, *J* = 10.8, 3.5 Hz, 2H), 1.62 – 1.54 (m, 3H), 1.23 (d, *J* = 0.9 Hz, 2H), 1.06 (d, *J* = 1.0 Hz, 2H). Chemical Formula: $C_{29}H_{28}N_6O$/Exact Mass: 476.23. $[M+H]^+$ detected: 477.4 m/z. Retention Time: 12.804 minutes, purity: 95.3%

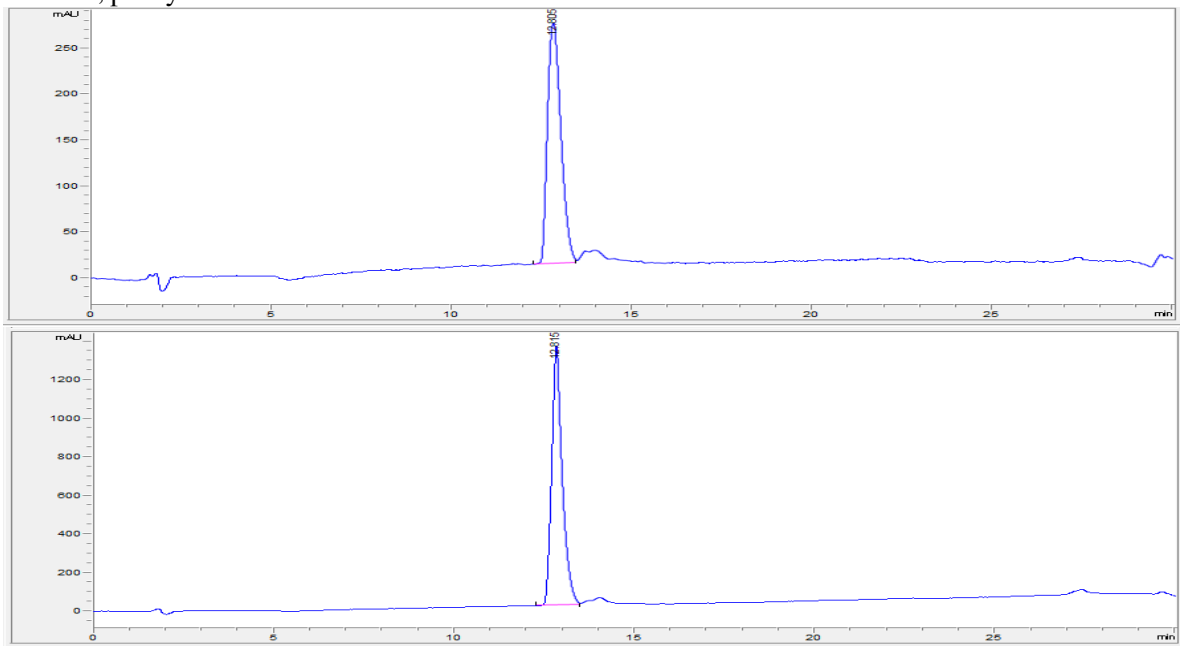

25: IC1 and cyclohexamine (CAS: 108-91-8) (1.7eq.) were dissolved in 0.1M dioxane and TEA (1.7 eq.) and heated at 95ºC for 1.5 hours. The reaction was washed in DCM:Water and the organic layer extracted and concentration. The organic layer was further purified using HPLC in an acetonitrile and water solvent system. ^{1}H NMR (300 MHz, MeOD) δ 8.16 (d, *J* = 8.2 Hz, 1H), 7.98 (d, *J* = 6.1 Hz, 1H), 7.91 (d, *J* = 8.4 Hz, 1H), 7.78 (d, *J* = 8.4 Hz, 1H), 7.62 (d, *J* = 7.6 Hz, 3H), 7.06 (d, *J* = 6.1 Hz, 1H), 3.03 (s, 1H), 1.58 (s, 3H), 1.36 (s, 9H), 1.23 (s, 2H), 1.06 (s, 2H). Chemical Formula: $C_{27}H_{30}N_6O$/Exact Mass: 454.25. $[M+H]^+$ detected: 455.4 m/z. Retention time: 12.976 minutes, purity: >99%

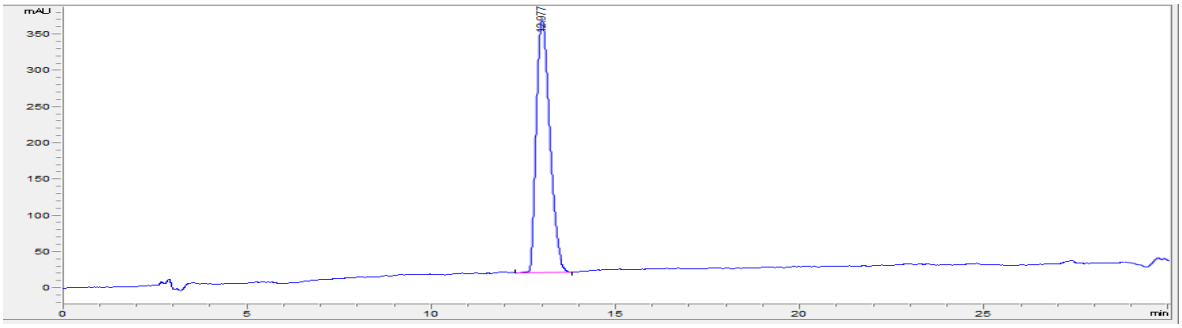

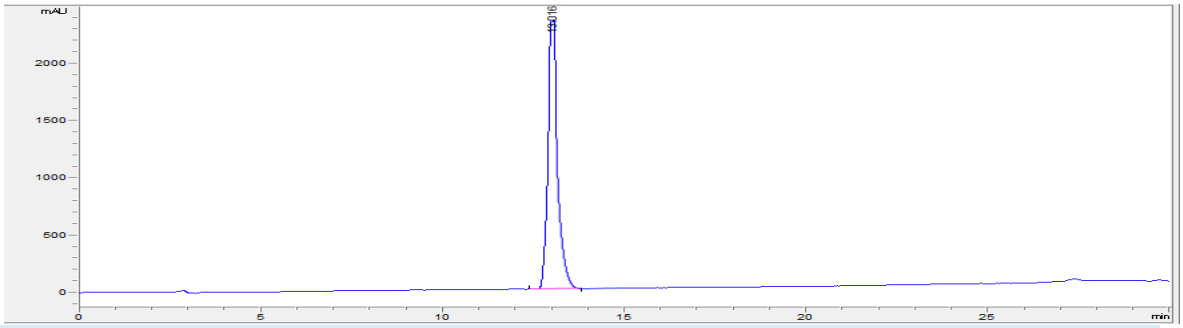

26: IC1 and morpholine (CAS: 110-91-8) (1.7eq.) were dissolved in 0.1M dioxane and TEA (1.7 eq.) and heated at 95ºC for 1.5 hours. The reaction was washed in DCM:Water and the organic layer extracted and concentration. The organic layer was further purified using HPLC in an acetonitrile and water solvent system. ^{1}H NMR (300 MHz, MeOD) δ 8.12 (d, J = 7.5 Hz, 1H), 7.97 - 7.87 (m, 1H), 7.75 (d, J = 7.8 Hz, 1H), 7.69 - 7.38 (m, 4H), 7.07 (d, J = 5.7 Hz, 1H), 3.89 (s, 2H), 3.83 (s, 2H), 3.67 (d, J = 4.9 Hz, 2H), 3.25 (d, J = 5.0 Hz, 2H), 1.57 (d, J = 6.2 Hz, 3H), 1.22 (s, 2H), 1.05 (s, 2H). Chemical Formula: $C_{25}H_{26}N_6O_2$/Exact Mass: 442.21. $[M+H]^+$ detected: 443.3 m/z. Retention time: 10.203 minutes, purity: 94.6%

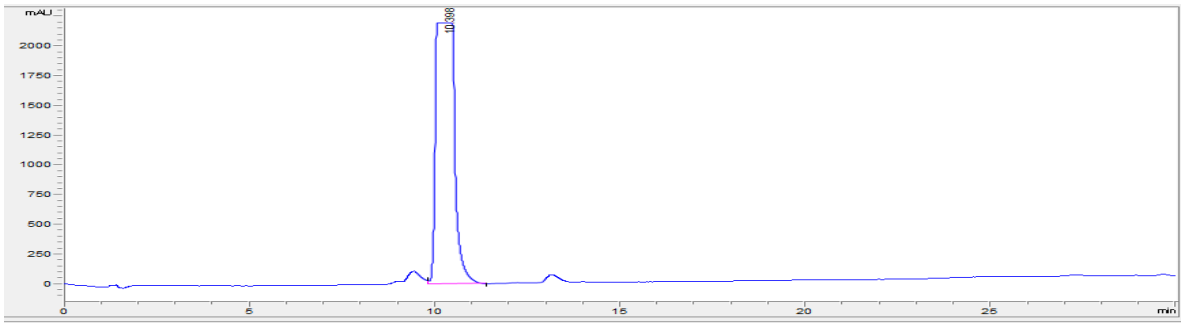

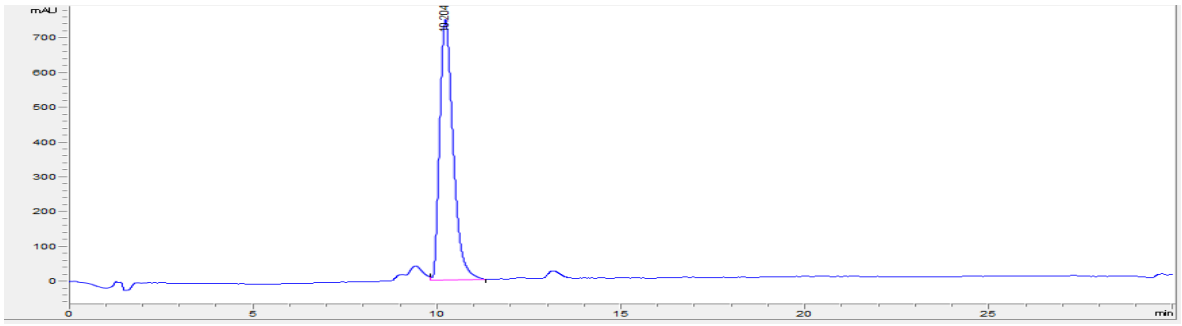

27: IC1 and piperidine (CAS: 110-89-4) (1.7eq.) were dissolved in 0.1M dioxane and TEA (1.7 eq.) and heated at 95ºC for 1.5 hours. The reaction was washed in DCM:Water and the organic layer extracted and concentration. The organic layer was further purified using HPLC in an acetonitrile and water solvent system. ^{1}H NMR (300 MHz, MeOD) δ 8.18 – 8.11 (m, 1H), 7.85 (d, *J* = 5.8 Hz, 1H), 7.61 (s, 1H), 7.49 (s, 2H), 7.40 (d, *J* = 7.5 Hz, 1H), 7.05 (s, 1H), 6.92 (d, *J* = 7.8 Hz, 1H), 3.15 (d, *J* = 5.5 Hz, 4H), 1.81 (s, 5H), 1.55 (s, 3H), 1.21 – 1.17 (m, 2H), 1.02 (s, 2H). Chemical Formula: $C_{26}H_{28}N_6O$/Exact Mass: 440.23. $[M+H]^+$ detected: 441.3 m/z. Retention time: 11.461 minutes, purity: 92.8%

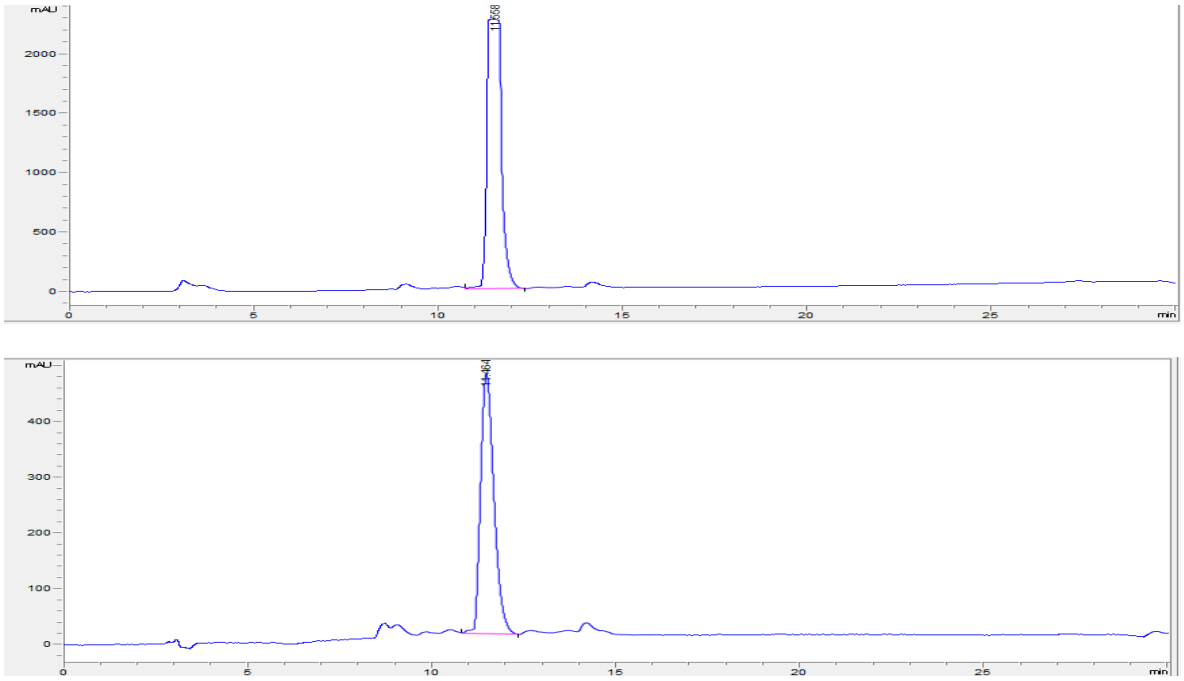

28: IC1 and cyclopropylamine (CAS: 765-30-0) (1.7eq.) were dissolved in 0.1M dioxane and TEA (1.7 eq.) and heated at 95ºC for 1.5 hours. The reaction was washed in DCM:Water and the organic layer extracted and concentration. The organic layer was further purified using HPLC in an acetonitrile and water solvent system. ^{1}H NMR (300 MHz, CD_3CN) δ 8.15 (s, 2H), 7.89 (s, 1H), 7.73 (s, 1H), 7.63 (d, *J* = 7.0 Hz, 2H), 7.54 (s, 2H), 6.92 (s, 1H), 2.71 (s, 1H), 1.53 (s, 3H), 1.15 (s, 2H), 0.99 (s, 2H), 0.81 (s, 2H), 0.62 (s, 2H). Chemical Formula: $C_{24}H_{24}N_6O$/Exact Mass: 412.20. $[M+H]^+$ detected: 413.3 m/z. Retention time: 10.455 minutes, purity: 93.8%

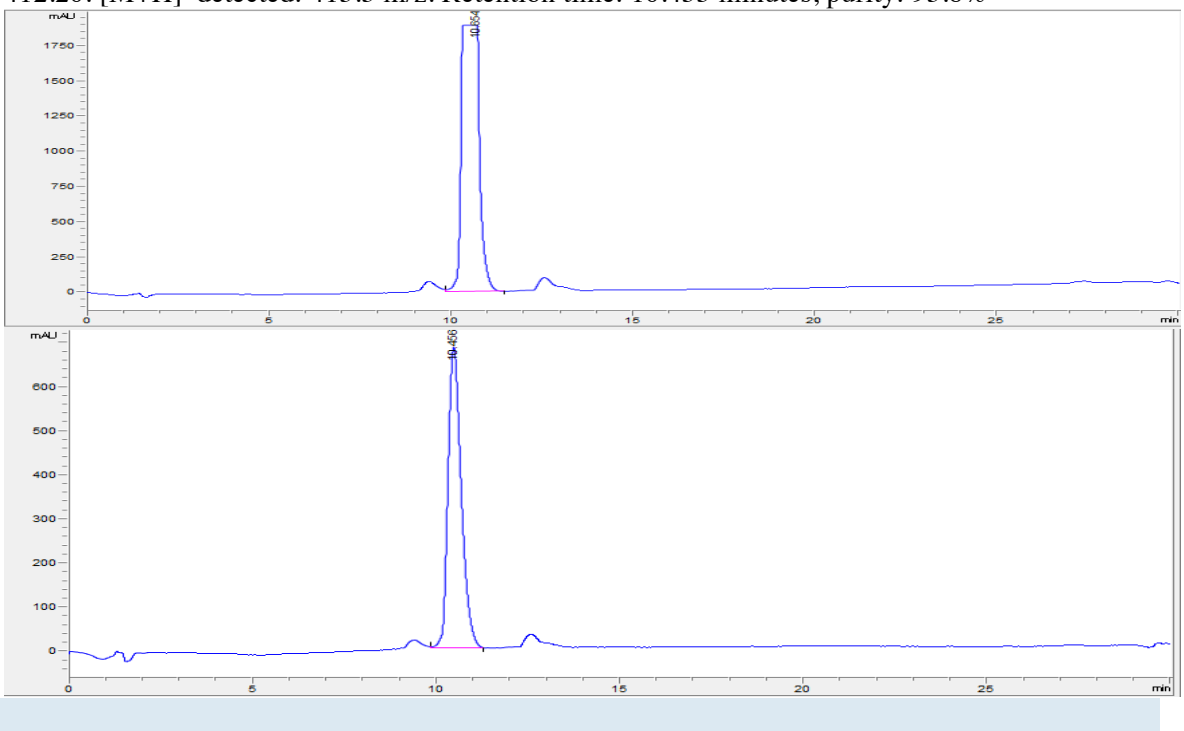

29: IC1 and N-methyl-3-(trifluoromethyl)-benzenamine (CAS:2026-70-2) (1.7eq.) were dissolved in 0.1M dioxane and TEA (1.7 eq.) and heated at 95ºC for 1.5 hours. The reaction was washed in DCM:Water and the organic layer extracted and concentration. The organic layer was further purified using HPLC in an acetonitrile and water solvent system. ^{1}H NMR (300 MHz, MeOD) δ 8.11 (d, J = 8.6 Hz, 1H), 7.98 (d, J = 5.9 Hz, 1H), 7.90 (s, 1H), 7.84 (d, J = 7.7 Hz, 1H), 7.75 (d, J = 9.1 Hz, 2H), 7.72 - 7.61 (m, 4H), 7.61 - 7.56 (m, 1H), 7.06 (d, J = 5.9 Hz, 1H), 3.55 - 3.50 (m, 3H), 1.58 (s, 3H), 1.23 (t, J = 2.7 Hz, 2H), 1.06 (t, J = 2.9 Hz, 2H). Chemical Formula: $C_{29}H_{25}F_3N_6O$/Exact Mass: 530.20. $[M+H]^+$ detected: 531.3 m/z. Retention Time: 14.590; Purity: 92.8%

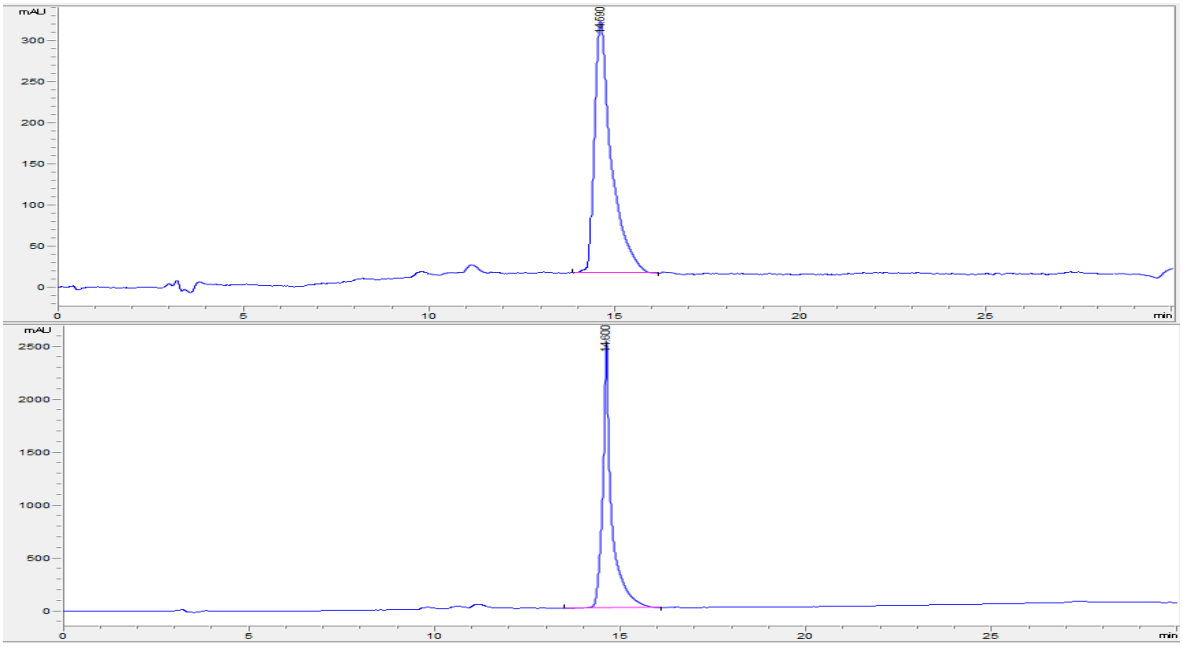

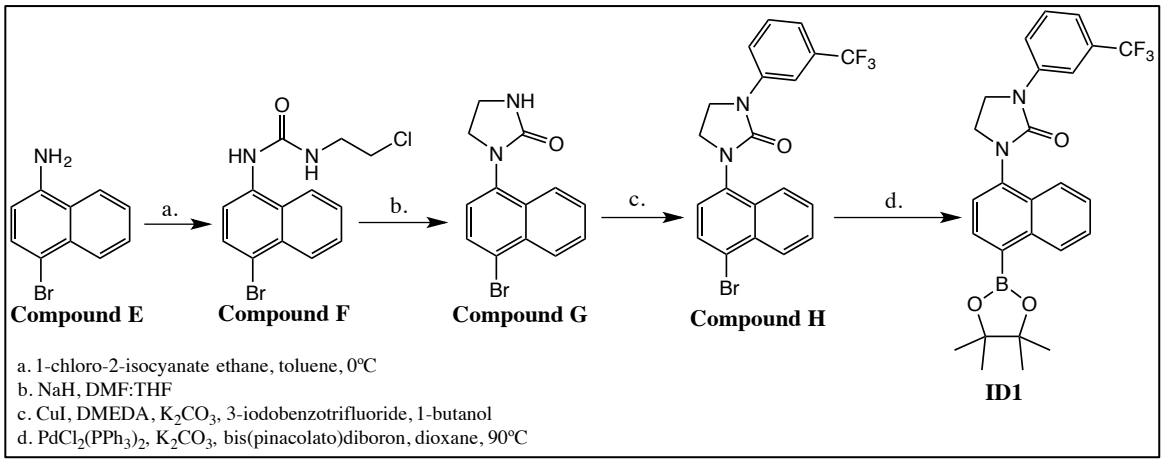

Compound F: Dissolved 1-amino-4-bromonaphthalene (Compound E) (1g, 4.5mmol, 1eq) in anhydrous Toluene (12mL). The reaction was cooled to 0ºC and then 1-chloro-2-isocyanate ethane (0.57g, 5.4mmol, 1.2eq) was dripped into the cooled solution. The reaction was allowed to warm to room temperature and then stirred for 18 hours. The reaction was diluted with ethyl acetate, washed with brine, dried over Na_2SO_4, filtered, and concentrated to yield compound **F**

and taken into the next step without purification. ^{1}H NMR (400MHz, DMSO): d 8.8 (s, 1H), 8.2 (dd, 2H), 8.0 (d, 1H), 7.7 (d, 1H), 7.6 (m, 2H), 7.0 (m, 1H), 3.7 (t, 2H), 3.5 (m, 2H).

Compound G: Sodium Hydride (0.275g, 6.9mmol, 1.5eq) was suspended in THF (17mL) and cooled to 0ºC. Compound F (1.5g, 4.6mmol, 1eq) was dissolved in DMF (17mL) and dripped into the Sodium Hydride suspension. The reaction was stirred at room temperature for 1 hour and then recooled to 0ºC. The reaction was then quenched with methanol. The reaction was diluted with ethyl acetate, washed with brine, dried over Na_2SO_4, filtered, and concentrated to a solid. The solid was purified by column (0% to 100% ethyl acetate/hexane) to yield compound **G** (0.69g, 52% yield). ^{1}H NMR (400MHz, DMSO): d 8.2 (d, 1H), 8.0 (d, 1H), 7.9 (d, 1H), 7.7 (m, 2H), 7.4 (d, 1H), 6.9 (s, 1H), 3.8 (m, 2H), 3.5 (m, 2H).

Compound H: Compound G (0.1g, 0.345mmol, 1eq), 3-Iodobenzotrifluoride (0.075mL, 0.517mmol, 1.5eq), Copper(I) Iodide (7mg, 0.0345mmol, 0.1eq), DMEDA (0.013mL, 0.1035mmol, 0.3eq), and K_2CO_3 (0.143g, 1.034mmol, 3eq) were dissolved in n-butanol (1.4mL). The reaction was heated at 100oC for 2 hours. The reaction was diluted with ethyl acetate, washed with NH_4Cl and brine, dried over Na_2SO_4, filtered, and concentrated to yield crude compound **H** ^{1}H NMR (400MHz, DMSO): d 8.3 (m, 2H), 8.1 (d, 1H), 8.0 (d, 1H), 7.7-7.5 (m, 5H), 7.4 (d, 1H), 4.2 (m, 2H), 4.0 (m, 2H).

ID1: Compound H (0.15g, 0.345mmol, 1eq), Bis(pinacolato) diboron (0.132g, 0.518mmol, 1.5eq), Bis(triphenylphosphine) palladium(II) dichloride (0.012g, 0.017mmol, 0.05eq), and K_2CO_3 (0.191g, 1.382mmol, 4eq) in Dioxane (1.7mL). The reaction was heated at 90ºC for 18 hours. The reaction was diluted with ethyl acetate, washed with brine, dried over Na_2SO_4, filtered, and concentrated to a solid. The solid was purified by column (0% to 35% ethyl acetate/hexane) to IC4 (0.042g, 25% yield). ^{1}H NMR (400MHz, $CDCl_3$): d 8.8 (d, 1H), 8.2 (d. 1H), 7.9 (m, 3H), 7.5 (m, 4H), 7.4 (d, 1H), 4.2 (m, 2H), 4.1 (m, 2H), 1.4 (s, 12H)

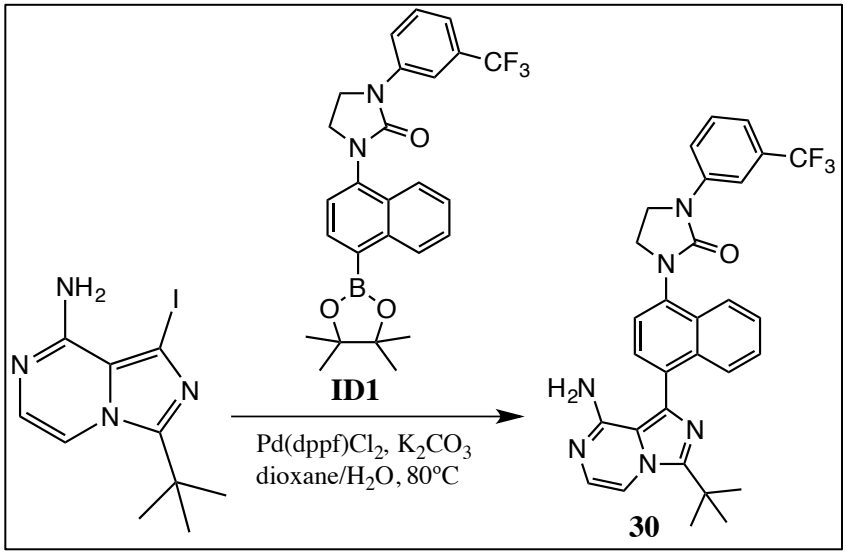

30: Both the water (0.2mL) and dioxane (0.4mL) were degassed with nitrogen for 10 minutes. Then compound **8** (0.04g, 0.083mmol, 1.2eq) was dissolved in the degassed water and dioxane. Next compound **4** (0.022g, 0.070mmol, 1eq), Bis(triphenylphosphine) palladium(II) dichloride (5mg, 0.0070mmol, 0.1eq), and K_2CO_3 (0.021g, 0.153mmol, 2.2eq) were added to the reaction. The reaction was heated at 80ºC for 3 hours. Then the reaction was diluted with ethyl acetate,

washed with brine, dried over Na_2SO_4, filtered, and concentrated to a solid. The solid was purified by column (0% to 10% methanol/DCM) to yield compound **9** (0.028g, 74% yield). ^1H NMR (400MHz, $CDCl_3$): d 8.1-7.8 (m, 3H), 7.6 (m, 2H), 7.55-7.4 (m, 5H), 7.3 (d, 1H), 7.0 (d, 1H), 4.2-3.9 (m, 4H), 1.7 (s, 9H). Chemical Formula: $C_{30}H_{27}F_3N_6O$/Exact Mass: 544.22. $[M+H]^+$ detected: 545.3 m/z.

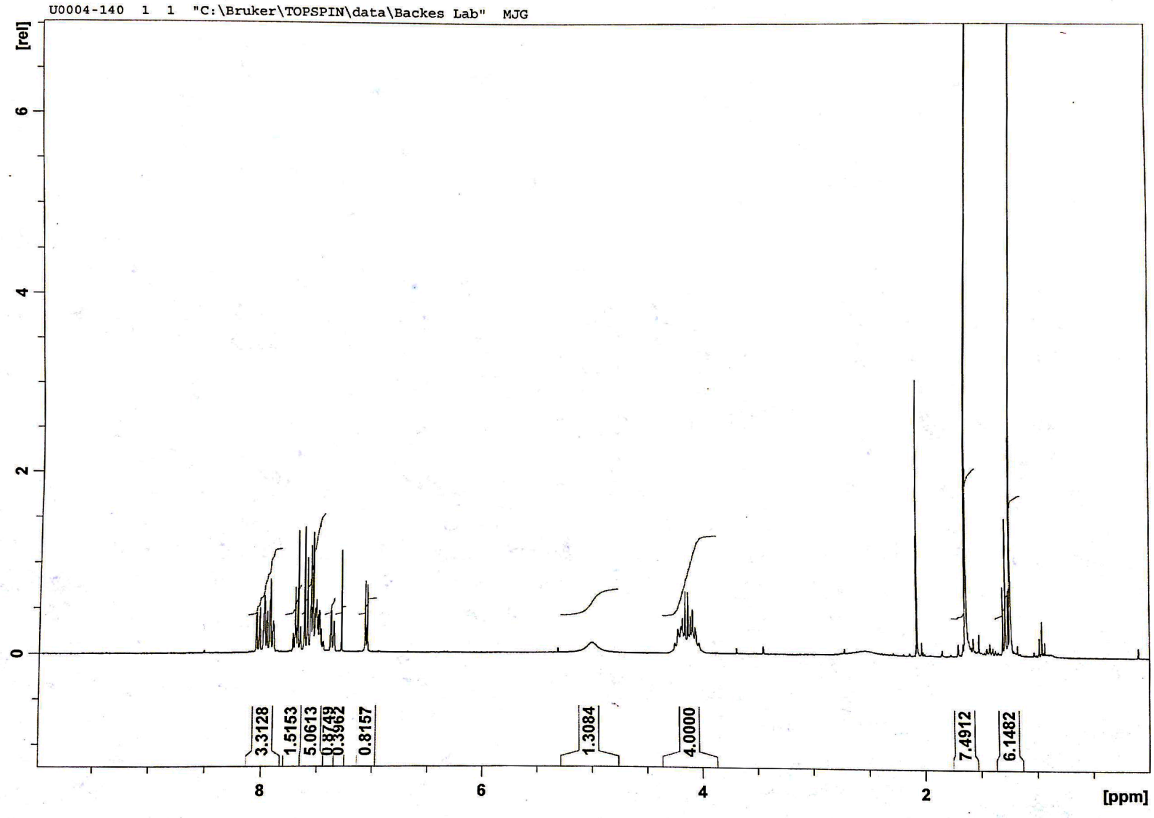

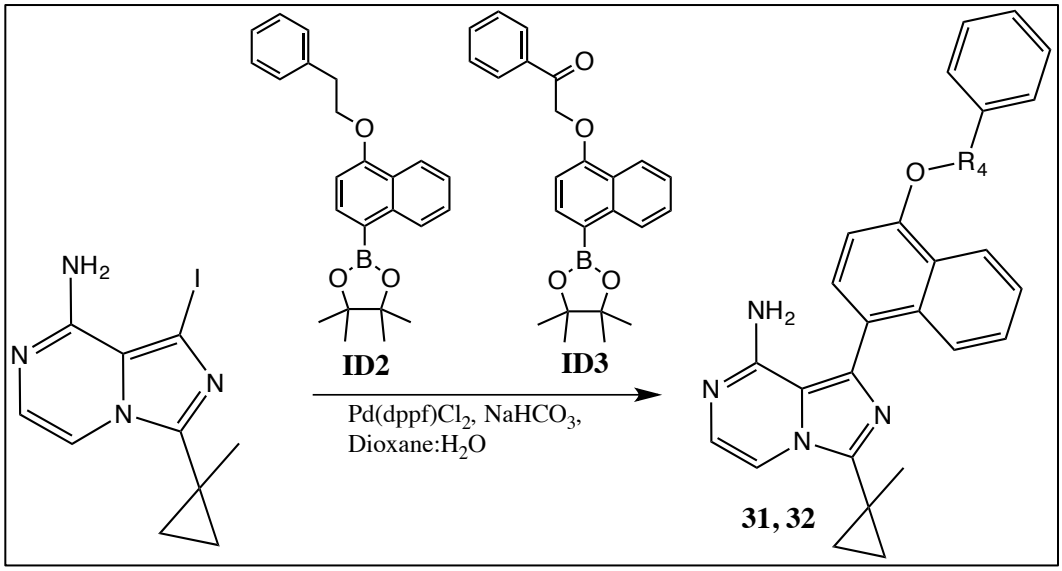

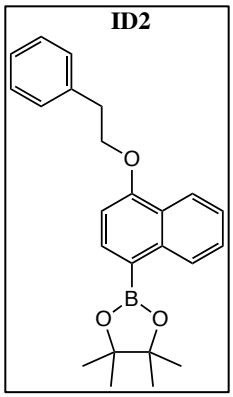

ID2: 4-bromo-1-naphthalenol (1eq.) (CAS: 571-57-3) and (2-bromoethyl)-benzene (CAS:103-63-9) (2eq) were dissolved in DMF with K_2CO_3 (4eq.) and stirred at 75ºC overnight. The resulting mixture was washed with DCM:Water and the organic phase concentrated *in vacuo*. The concentrated mixture was further purified on silica. ^{1}H NMR (300 MHz, $CDCl_3$) δ 8.79 (dd, *J* = 8.4, 0.6 Hz, 1H), 8.41 – 8.26 (m, 1H), 8.05 (d, *J* = 7.8 Hz, 1H), 7.54 (dddd, *J* = 25.6, 8.1, 6.8, 1.4 Hz, 2H), 7.43 – 7.25 (m, 5H), 6.84 (d, *J* = 7.8 Hz, 1H), 4.38 (dt, *J* = 11.6, 5.7 Hz, 2H), 3.29 (t, *J* = 6.9 Hz, 2H), 1.50 – 1.39 (m, 12H).

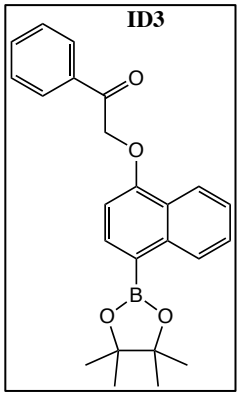

ID3: 4-bromo-1-naphthalenol (1 eq.) (CAS: 571-57-3) and 2-bromo-1-phenyl-ethanone (2 eq.) (CAS: 70-11-1) were dissolved in DMF with K_2CO_3 (4eq.) and stirred at 75ºC overnight. The resulting mixture was washed with DCM:Water and the organic phase concentrated *in vacuo*. The concentrated mixture was further purified on silica. ^{1}H NMR (300 MHz, $CDCl_3$) δ 8.86 – 8.74 (m, 1H), 8.52 – 8.38 (m, 1H), 8.17 – 7.91 (m, 3H), 7.70 – 7.38 (m, 5H), 6.87 – 6.72 (m, 1H), 5.45 (t, *J* = 1.8 Hz, 2H), 1.43 (t, *J* = 1.9 Hz, 12H).

31: ID2 (2eq.) was dissolved with IA1 (1 eq.) and 0.1M dioxane:water (3:1) were combined with $NaHCO_3$ (3.4 eq.) and $PdCl_2(dppf)_2$ (0.1 eq.). The vial was sealed and placed in a microwave reactor for 45 minutes at 120ºC. The resulting mixture was washed with DCM:Water, and the organic layers combined. The organic layer was further purified using HPLC in an acetonitrile and water solvent system. ^{1}H NMR (300 MHz, MeOD) δ 8.59 – 8.49 (m, 1H), 8.20 – 8.11 (m, 2H), 7.97 (d, *J* = 5.9 Hz, 1H), 7.71 (dd, *J* = 7.9, 5.8 Hz, 2H), 7.59 (ddd, *J* = 17.4, 10.5, 7.0 Hz, 6H), 7.04 (t, *J* = 6.7 Hz, 2H), 5.83 (s, 2H), 1.59 (d, *J* = 9.8 Hz, 3H), 1.21 (s, 2H), 1.05 (s, 2H). Chemical Formula: $C_{28}H_{26}N_4O$/Exact Mass: 434.21. $[M+H]^+$ detected: 435.4 m/z. Retention time: 13.773 minutes, purity: 97.9%

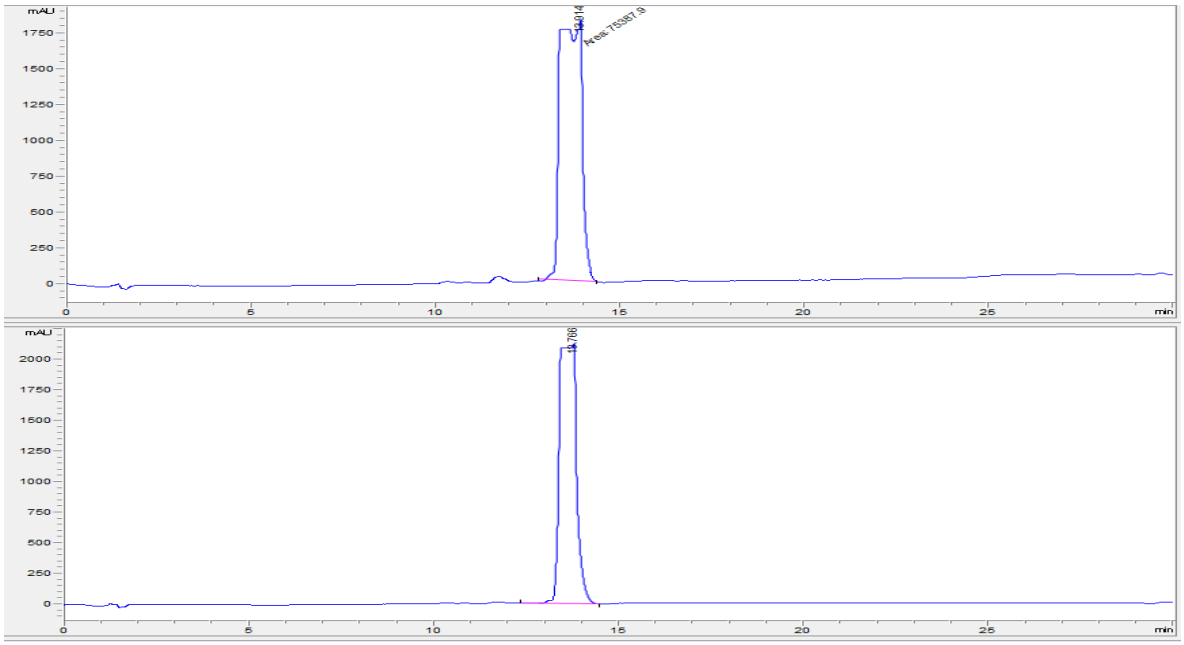

32: ID3 (2eq.) was dissolved with IA1 (1 eq.) and 0.1M dioxane:water (3:1) were combined with $NaHCO_3$ (3.4 eq.) and $PdCl_2(dppf)_2$ (0.1 eq.). The vial was sealed and placed in a microwave reactor for 45 minutes at 120ºC. The resulting mixture was washed with DCM:Water, and the organic layers combined. The organic layer was further purified using HPLC in an acetonitrile and water solvent system. ^{1}H NMR (300 MHz, MeOD) δ 8.37 (d, *J* = 9.6 Hz, 1H), 7.97 (d, *J* = 5.9 Hz, 1H), 7.68 (d, *J* = 9.7 Hz, 1H), 7.56 (dd, *J* = 7.8, 6.0 Hz, 3H), 7.44 (d, *J* = 7.5 Hz, 2H), 7.34 (t, *J* = 7.5 Hz, 2H), 7.25 (d, *J* = 7.5 Hz, 1H), 7.08 (dd, *J* = 16.6, 7.0 Hz, 2H), 4.51 (t, *J* = 6.2 Hz, 2H), 3.29 (s, 2H), 1.57 (s, 3H), 1.21 (s, 2H), 1.05 (s, 2H). Chemical Formula: $C_{28}H_{24}N_4O_2$/Exact Mass: 448.19. $[M+H]^+$ detected: 449.3 m/z. Retention Time: 15.817 minutes; Purity: 97.2%

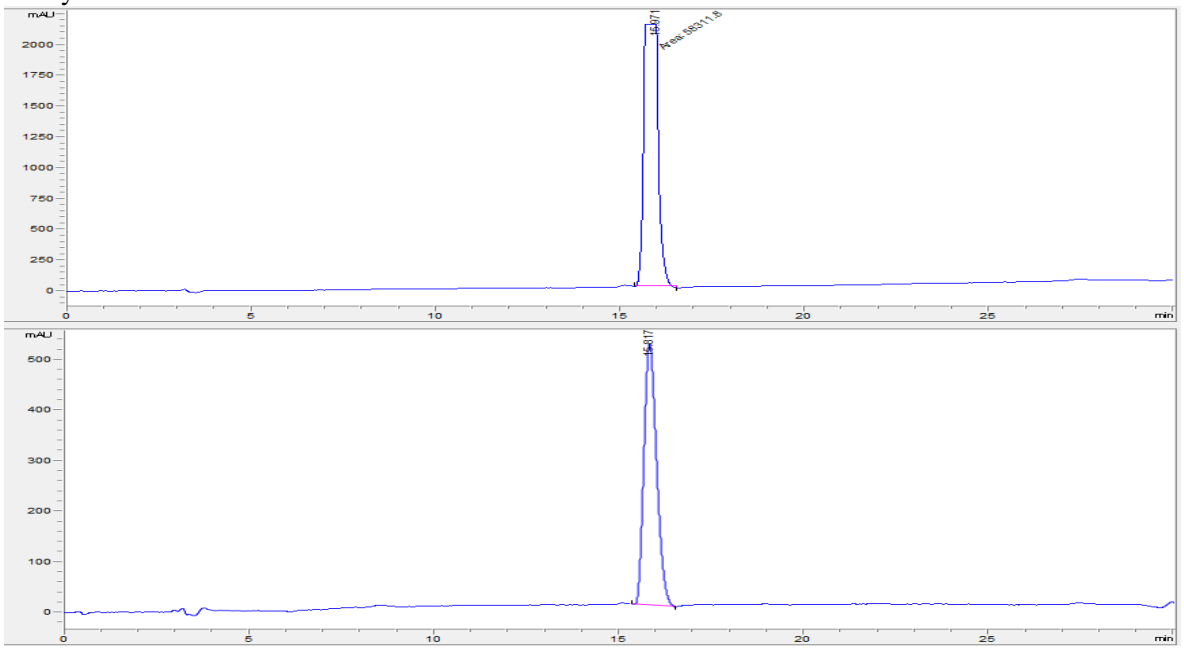

IV. Expression and purification of IRE1α* and dP-IRE1α*.
A construct containing the cytosolic kinase and RNase domains of human IRE1α (residues 547–977, IRE1α*) was expressed in SF9 insect cells by using the Bac-to-Bac baculovirus expression system (Invitrogen) with a His_6 tag at the N terminus and purified with a nickel–nitriloacetic acid (Qiagen) column. To generate dP-IRE1α*, we removed basal phosphorylation sites by incubatingIRE1α* with λ-PPase (New England Biolabs) at a molar ratio of 5:1 (IRE1α*/λ-PPase) in 50 mM HEPES pH 7.5, 100 mM NaCl, 1 mM $MnCl_2$, 2 mM dithiothreitol (DTT) and 0.01% Brij 35 detergent (v/v) for 40 min at 23 °C. Dephosphorylation was verified by immunoblotting with an antibody specific for phosphoIRE1α.

V. Activity Assays

A. Kinase assays.
Inhibitors (initial concentration 10 or 60 μM, three-fold serial dilutions) were incubated with IRE1α* in cleavage buffer (20 mM HEPES at pH 7.5, 0.05% Triton X-100 (v/v), 50 mM potassium chloride, 1 mM magnesium chloride, 1 mM DTT) for 30 min, followed by incubation with 10 μCi [γ-^{32}P] ATP(3,000 Ci mmol^{-1}, PerkinElmer) at 23 °C for 3 hours. Samples were then spotted onto phosphocellulose paper and washed in triplicate with 0.5% phosphoric acid and autoradiographed. The percent inhibition was quantified by setting the background as 0 and standardizing to IRE1α* without compound treatment.

B. *In vitro* RNase assay.
5′-Carboxyfluorescein (FAM)- and 3′-Black Hole Quencher (BHQ)-labeled XBP1 single stem-loop mini-substrate (5′FAM-CUGAGUCCGCAGCACUCAG-3′BHQ) were purchased from Dharmacon. We incubated 0.25 μM IRE1α* or dP-IRE1α* with inhibitors or DMSO for 30 min in assay buffer (20mM Tris at pH7.5, 50mM sodium chloride, 1mM magnesium chloride, 2mM DTT, 0.05% Triton X-100 (v/v)), followed by incubation with 1 μM RNA substrate for 10 min. The reaction was quenched by adding urea to a final concentration of 4 M, and the fluorescence was detected on a SpectraMax M5 microplate reader (Molecular Devices) or a Perkin Elmer 2104 Envision microplate reader with excitation and emission wavelengths of 494 nm and 525 nm, respectively. The fluorescence intensities were normalized by setting the signal for the reaction without IRE1α* to 0.

VI. IRE1α* crosslinking to determine oligomer to monomer ratio.
Concentration of IRE1α* or dpIRE1α at 15uM were incubated with DMSO, KIRA, or Activator for 30 min and then crosslinked by adding 250 μM disuccinimidyl suberate (Pierce) for 1 h at 23 °C in the dark in crosslinking buffer (20mM HEPES at pH 7.5, 50mM sodium chloride). The reaction was quenched by addition of 100 mM Tris-HCl (pH 7.5). The samples were then boiled, resolved on SDS-PAGE and visualized via Coomassie stain via Alpha Innotech FluoroChem FC2 Gel Imager. Quantification of bands was done using ImageQuant.

VII. Cell culture and XBP1 mRNA splicing.
INS-1 cells were grown in RPMI, 10% FBS buffer (v/v), 1 mM sodium pyruvate, 10 mM HEPES, penicillin-streptomycin, 2 mM glutamine and 50 μM β-mercaptoethanol. T-REx 293 IRE1α or IRE1α^{I642A} were grown in DME H-21 with 10% FBS buffer (v/v) and penicillin-streptomycin.

VIII. In Vivo XBP1 splicing assay

After 1 h incubation with compounds, INS-1 cells were treated with 6 nM thapsigargin for 4 h, and T-REx 293 IRE1α-expressing cells were treated with 1 μM Dox for 8 h. The RNA was then extracted using RNeasy Mini Kit (Qiagen) and reverse transcribed using the QuantiTect Reverse Transcription Kit (Qiagen). XBP1 splicing was performed as previously described[7]. Primers used: sense primer rXBP 1.3S (5′- AAACAGAGTAGCAGCACAGACTGC-3′) and antisense primer rXBP 1.2AS (5′- GGATCTCTAAGACTAGAGGCTTGGTG-3′) for the INS-1 cell line and sense primer mXBP1.3S (5′-AAACAGAGTAGCAGCGCAGACTGC-3′) and antisense primer mXBP1.2AS (5′-GGATCTCTAAAACTAGAGGCTTGGTG-3′) for the T-REx 293 cell line. PCR products were resolved on 2.5% (w/v) agarose gels, stained with ethidium bromide and quantified by ImageJ.

IX. Crystallography [4, 5, 6, 7, 8, 9]

dP-IRE1 α*

A. Buffer Composition:

Purified dP-IRE1α* stock protein was stored in a default buffer composed of: 25 mM HEPES pH 7.5, 250 mM NaCl, 5% glycerol, 1 mM DTT, 1 mM EDTA. The dP-IRE1α*·**2** complex was prepared to a final concentration of: 10mg/ml (205 μM) of dP-IRE1α*, and 500 μM of **2**, (Protein to inhibitor ratio of 1:2.4). In order to achieve these final protein concentrations and a final NaCl concentration of approximately 90 mM, the dP-IRE1α* stock protein was diluted with dilution buffer (25 mM HEPES pH7.5, 10 mM DTT, 1 mM EDTA) The final buffer composition of the dP-IRE1α*·**2** complex was: 25 mM HEPES pH 7.5, 90 mM NaCl, 10 mM DTT, 1 mM EDTA, 1.8% glycerol, 5% DMSO, 500 μM **2**.

B. Protein-inhibitor Complex Formation:

The dP-IRE1α*·**2** complex was prepared on ice according to the following steps: (i) Pipette the inhibitor. (ii) Pipette the dilution buffer to the inhibitor and add the appropriate amount of DMSO to maintain DMSO at 5% in the final protein inhibitor complex. Pipette further to mix the inhibitor and buffer mixture. (iii) Add the inhibitor buffer mixture to the protein with further mixing by pipetting to make the final protein□inhibitor complex. (iv) Spin down the protein□inhibitor complex mixture at 14K RPM for 5 minutes at 4 °C. Post spin precipitation was visible, which in hindsight of determining the apo dP-IRE1α* crystal structure, suggests that this was likely compound **2**. (v) Use the supernatant to set up crystallization via the hanging drop method.

C. Crystallization Buffer and Procedure:

The crystallization buffer condition was: 25 mM Bis-Tris Propane pH 9, 39% PEG 200, 250 mM CsCl, 10% glycerol, at 4°C, with a final concentration of 143 mM B-Me added into the reservoir mother liquor after setting up the protein-inhibitor complex drop and crystallization drop mixture. The protein□inhibitor complex drop and crystallization drop mixture were setup in a 1 μL:1 μL ratio using the liquid bridge method. Crystals appeared and continued to grow from overnight to a few days, forming long thick blades, and three dimensional hexagons. They were harvested and immersed in the crystallization buffer for cryoprotection because of the high percentage of PEG200.

D. X-ray Diffraction Data Collection and Processing

X-ray diffraction data was collected at 100 K, with a wavelength of 1.0 Å, using the beamline X25 at the National Synchrotron Light source (Brookhaven National Laboratories). Data were processed using XDS and aimless implemented in the autoProc pipeline. The structure was determined by molecular replacement using the IRE1α kinase domain (minus helix-αC residues: 609-620, and activation segment residues: 711-741), and the RNase domain from the PDB entry:3P23 as a search model in PHASER. The structure was built using COOT and refined with PHENIX. The Cs^+ ions were identified and built using the anomalous scattering map.

Src

A. Buffer Composition:

Purified Src stock protein was stored in a default buffer composed of: 20 mM Tris pH 8.0, 25 0mM NaCl, 5% glycerol, 1 mM DTT. The Src·**1** complex was prepared to a final concentration of: 4.68 mg/ml (78.2 μM) of Src, and 250 μM of **1**, (Protein to inhibitor ratio of 1:3.2). In order to achieve these final protein concentrations, the Src stock protein was diluted with dilution buffer (20 mM Tris pH 8.0). The final buffer composition of the Src·GP146 complex was: 20 mM Tris pH 8.0, 83.3 mM NaCl, 1.67 mM Glycerol, 0.33 mM DTT, 5% DMSO, 250 μM GP146.

B. Protein-Inhibitor Complex Formation:

The Src·**1** complex was prepared on ice according to the following steps: (i) Pipette the inhibitor. (ii) Pipette the dilution buffer to the inhibitor and add the appropriate amount of DMSO to maintain DMSO at 5% in the final protein·inhibitor complex as well as glycerol to maintain 20 % in the final mixture. Pipette further to mix the inhibitor and buffer mixture. (iii) Add the inhibitor buffer mixture to the protein with further mixing by pipetting to form the final protein·inhibitor complex. (iv) Set up crystallization via the hanging drop method.

C. Crystallization Buffer and Procedure:

The crystallization buffer condition was: 100 mM BIS-Tris pH 6.0, 7% PEG5000MME, 1.5% Tacsimate pH 6.0, at 16°C. The protein·inhibitor complex drop and crystallization drop mixture were setup in a 1 μL:1 μL ratio using by pipetting the drops on top of each other. Crystals appeared and continued to grow from overnight to a few days, forming relatively small monoclinic plates. They were harvested and immersed in the crystallization buffer containing glycerol for cryoprotection because of the high percentage of glycerol content.

D. X-ray Diffraction Data Collection and Processing

X-ray diffraction data was collected at 100 K, with a wavelength of 1.0 Å, using the beamline X29 at the National Synchrotron Light source (Brookhaven National Laboratories). Data were processed using HKL2000 and Xtriage in Phenix. The structure was determined by molecular replacement using the Src kinase domain (minus helix-αC residues: 298-317, and minus activation segment residues: 400-407, and 421-425) from the PDB entry: 2OIQ as a search model in PHASER. The structure was built using COOT and refined with PHENIX.

XI. Computational Docking and structural analysis

Docking experiments were performed using Autodock tools, Autogrid, Autodock4, and Autodock vina. The grid box was defined to span the kinase active site. The genetic algorithm was used in the docking parameter file with 250,000 evaluations per run for all the ligands, apart from TAE684, where 2,5000,000 evaluations were run was applied. 10-50 dockings were run per docking experiment. Pymol was used for structural analysis and generation of structure figures.

X. Phosphomapping

Ire1α (75 pmol) expressed from baculovirus was incubated either alone or with 400 U lambda phosphatase (NEB) and 1 mM MnCl2 for 1 h at room temperature. Samples were then precipitated with 0.02% sodium deoxycholate and 10% trichloroacetic acid on ice for 10 min. Mixtures were centrifuged at 4 °C for 15 min, and the pellets were washed once with cold acetone. After centrifugation, the pellets were resuspended in 30 μL 200 mM Tris (pH 8.0), 8 M urea, and 2.4 mM iodoacetamide, and incubated in the dark for 30 min. Solutions were then diluted with 210 μL 200 mM Tris (pH 8.0), 5.7 mM CaCl2, and 1 μg/μL porcine trypsin (TPCK treated, Sigma), and incubated at 37 °C overnight. Samples (0.3 pmol) were injected onto a Thermo Scientific Dionex Acclaim Pepmap100 NanoLC capillary column (C18, 150 mm length, I.D. 75 μm, 3 μm particle size) connected inline to a Finnigan LTQ mass spectrometer. Peptides of interest were identified by MS/MS data (Thermo), and corresponding XIC peaks were integrated.

References:

1. Van Voorhis, W. C. V. et al. Compositions and methods for treating toxoplasmosis. cryptosporidiosis and other apicomplexan protozoan related diseases. PCT Int. Appl., WO/2011/094628 (2011).
2. Wang, Likun, et al. "Divergent allosteric control of the IRE1α endoribonuclease using kinase inhibitors." *Nature chemical biology* 8.12 (2012): 982-989.
3. Harrington, Paul E., et al. "Unfolded Protein Response in Cancer: IRE1α Inhibition by Selective Kinase Ligands Does Not Impair Tumor Cell Viability."*ACS medicinal chemistry letters* 6.1 (2014): 68-72.
4. Kabsch,W. (2010) Xds. Acta Crystallogr. Sect. D, Biol. Crystallogr., 66, 125–132.
5. Evans,P.R. and Murshudov,G.N. (2013) How good are my data and what is the resolution? Acta Crystallogr. Sect. D, Biol. Crystallogr., 69, 1204–1214.
6. Vonrhein,C., Flensburg,C., Keller,P., Sharff,A., Smart,O., Paciorek,W.,Womack,T. and Bricogne,G. (2011) Data processing and analysis with the autoPROC toolbox. Acta Crystallogr. Sect. D, Biol. Crystallogr., 67, 293–302.
7. McCoy, A.J., Grosse-Kunstleve, R.W., Storoni, L.C. & Read, R.J. Likelihood-enhanced fast translation functions. Acta Crystallogr. D Biol. Crystallogr. 61, 458–464 (2005).
8. Adams, P.D. et al. PHENIX: building new software for automated crystallographic structure determination. Acta Crystallogr. D Biol. Crystallogr. 58, 1948–1954 (2002).
9. Emsley, P. & Cowtan, K. Coot: model-building tools for molecular graphics. Acta Crystallogr. D Biol. Crystallogr. 60, 2126–2132 (2004).